PHOTOINDUCED PROCESSES STUDIED IN CONVENTIONAL SOLVENTS, ROOM TEMPERATURE IONIC LIQUIDS AND PROTEINS

A Thesis
Submitted for the Degree of
DOCTOR OF PHILOSOPHY

by

Bhaswati Bhattacharya

School of Chemistry
University of Hyderabad
Hyderabad 500 046
INDIA

December 2008

To
My Family

“If we knew what it was we were doing, it would not be called research, would it?"

-Albert Einstein

Contents

STATEMENT

I hereby declare that the matter embodied in the thesis entitled ***"Photoinduced Processes Studied in Conventional Solvents, Room Temperature Ionic Liquids and Proteins"*** is the result of investigations carried out by me in the School of Chemistry, University of Hyderabad, Hyderabad, India under the supervision of **Prof. Anunay Samanta**.

In keeping with the general practice of reporting scientific investigations, due acknowledgements have been made wherever the work described is based on the findings of other investigators. Any omission or error that might have crept in is regretted.

December 2008 **Bhaswati Bhattacharya**

SCHOOL OF CHEMISTRY
UNIVERSITY OF HYDERABAD
HYDERABAD-500 046, INDIA

Phone: +91-40-2313 4813 (O)
+91-40-2313 0715 (R)
Fax: +91 40 2550 1532
Email: assc@uohyd.ernet.in
anunay_s@yahoo.com

Anunay Samanta
Professor

CERTIFICATE

Certified that the work embodied in the thesis entitled ***"Photoinduced Processes Studied in Conventional Solvents, Room Temperature Ionic Liquids and Proteins"*** has been carried out by **Ms. Bhaswati Bhattacharya** under my supervision and that the same has not been submitted elsewhere for any degree.

Anunay Samanta
(Thesis Supervisor)

Dean
School of Chemistry
University of Hyderabad

Acknowledgement

It gives me immense pleasure to express my profound gratitude and deep respect to Prof. Anunay Samanta, my research supervisor, for his constant cooperation, encouragement and kind guidance. He has been quite helpful to me in both academic and personal fronts.

My sincere respect is due to Dr. Lalitha Guruprasad for her helpful guidance and encouragement. It has been my privilege to work with her in one of the project.

I would like to thank the former and present Deans, School of Chemistry, for providing infrastructure and research facilities and all the faculty members of the school for their cooperation during my stay in the campus.

I value my association with my lab seniors: Sandip, Tamal, Prasun, Moloy and Aniruddha from whom I have learned many valuable aspects of research. I would like to specially thank Sandip and Aniruddha for giving me useful research tips, while my heartly thanks to Moloy for helping me to overcome all the depressing experiences I went through during my research tenure. I acknowledge my junior friends Ravi, Dinesh, Santhosh and Sanghamitra for maintaining friendly and cooperative atmosphere in the lab. I am really lucky to have them as my juniors.

I also thank all non-teaching staff for their timely help, Mr. Shetty in particular.

I am thankful to all my colleagues in the School of Chemistry for helping and supporting me in various issues.

I would also like to express my sincere thanks to all my dadas with whom I have some wonderful memories and they are the people who made my stay possible in Hyderabad during those initial years. The senior dadas who still matter are Dinuda, Binoyda, Sandy, Abhikda, Sunirbanda, Archanda, Subhashda, Manabda, Saikatda, Bishuda, Moloyda and Jethu. Prashant is beyond any sense of gratitude as he is the person who reintroduced self-esteem in me and supported me through thick and thin in these five years period.

I cherished the close association of Podu, Ghona, Bipul, Tapta, Sandip, Tanmoy, Arindam, Ghanta, Pati, Sanjib, Ranjit and Naba. They were more of friends than my juniors and would like to thank them for giving eternal names like 'pishi' and 'jaali' to me. I equally loved the company of fresh batch of juniors which include Susruta, Rishi, Dinesh, Palash, Tridib, Sudhangshu, Sandip, Mehboob, Anup, Nayan, Supratim and Tanmay. I am also thankful to Tejender and Yasser for nice company. A note of thanks also goes to Shatabdi di, Kedarda, Rahulda, Masumda, Bidhan, Suman, Utpalda, Jayashree, Padmaja, Balaraman, Biju, Rajesh, Arun, Murli, Narahari, Rajeshwar, Satpal, Srinivas, Raji, Saritha, Bhargavi, Monima and Moushumi for their friendly behavior. I never felt alone in the hostel due to the lovely company of Joya, Vasudhara, Rumpa, Anindita, Tulika and Sanghamitra. We were like a family and shared a feeling of a home away from home. I must not forget Susmita, Somdatta, Papri, Vaswati, Meghna, Gitasri, Madhumita, Paromita, Sharmistha, Anindita, Sriparna di and Suparna. It was lovely to interact with juniors like Suman, Tunghadri, Chandrani, Tanveer, Krishnendu and Nirabhra. It is difficult to forget the wonderful memories of Saraswati Pujo, Bengali Freshers' and Picnic in the HCU campus as we celebrated those occasions with high passion and lots of enthusiasm. I would like to specially thank Joya, Vasudhara and Tapta for taking great pains in organizing cultural programmes for these occasions.

I want to pay deep gratitude from the bottom of my heart to CKP who is a friend, philosopher and guide to me since my college days and I consider myself enough fortunate that I could maintain the relationship with him till today. I would also like to thank Sujoy Chakraborty for his efficient teaching and kindness. I still value the friendship of Abantika, Sujata, Somasri, Srirupa, Sutapa, Rajarshi, Mithun, Sudipta, Madhuri, Nital, Rupashree and Doyel made during college days.

My sincere gratitude to Krishna Miss for introducing me to the fascinating world of chemistry. I am also grateful to my other teachers like Pervez Sir, Bapi Sir, Korean George, Rubi Miss, Tuli Miss, Bandana Miss, Tapati Miss and Jaya Miss for the valuable teaching and guidance during the school days. I value the association of all my school buddies but the space is too small to accommodate all

their names. I would also like to thank my friends Pompa, Debi, Tina, Tinnidi, Bibidi, Piu and Shobhona with whom I grew up. I should mention about Chhotomama, Mami, Tushi and Subratada who are always there for supporting me. I should thank Manjeer and Urna for their caring attitude towards me.

This thesis would have not been possible without the sefless love and support of Ma, Baba, Didi, Bhaiya, Sabyada, Praggya and Prashant. I value the blessings of Thakuma, Dadu and Dida.

Financial assistance from CSIR, New Delhi is greatly acknowledged.

Bhaswati

List of Publications

1. "Fluorescence response of mono- and tetra-azacrown derivatives of 4-aminophthalimide with and without some transition and post transition metal ions." N. B. Sankaran, P. K. Mandal, **B. Bhattacharya** and A. Samanta *J. Mater. Chem.* **2005**, *15*, 2854.
2. "Ratiometric fluorescence signaling of fluoride ions by an amidophthalimide derivative." M. Sarkar, Y. Raghavendra, **B. Bhattacharya,** K. Ravi Kumar and A. Samanta *J. Chem. Sci.* **2007,** *119*, 91.
3. "Laser flash photolysis study of aminophthalimide derivatives: Elucidation of nonradiative deactivation route." **B. Bhattacharya** and A. Samanta *Chem. Phys. Lett.* **2007,** *442*, 316.
4. "Polarity dependence of the radiative and nonradiative rates of flavone derivatives comprising structurally similar amino moieties: Change in the nature of the emitting state." M. Sarkar, K. Ravi Kumar, **B. Bhattacharya** and A. Samanta *J. Phys. Chem. A* **2008**, *112*, 3302.
5. "Excited-state proton-transfer dynamics of 7-Hydroxyquinoline in room temperature ionic liquids." **B. Bhattacharya** and A. Samanta *J. Phys. Chem. B* **2008**, 112, 10101.
6. "Interaction of bovine serum albumin with dipolar molecules: fluorescence and molecular docking studies." **B. Bhattacharya,** S. Nakka, L. Guruprasad and A. Samanta *J. Phys. Chem. B* (*in press*).
7. "Photoinduced electron transfer in 1,8-naphthalimide derivatives." **B. Bhattacharya** and A. Samanta (*in preparation*)

Conference Presentations

1. Nonradiative Deactivation Route of the Fluorescent State of 4-aminophthalimide Derivatives. **Bhaswati Bhattacharya** and Anunay Samanta. – 4th Annual In-house Symposium of School of Chemistry, ChemFest 2007, organized by School of Chemistry, University of Hyderabad, Hyderabad, India, Mar. 2007 (Poster Presentation).
2. Unusual Anisotropy Behavior of EDA Probes in Bovine Serum Albumin. **Bhaswati Bhattacharya** and Anunay Samanta. – Trombay Symposium on Radiation and Photochemistry, 2008, organized by BARC, YASHADA, Pune, India, Jan. 2008 (Poster Presentation).

Thesis Layout

The thesis has been divided into seven chapters. ***Chapter 1*** provides a brief introduction on electron donor-acceptor systems and fundamentals of some photophysical processes like nonradiative deactivation, photoinduced electron transfer (PET) and excited state intramolecular proton transfer (ESIPT) reactions. This is followed by description of some of the properties of room temperature ionic liquids (RTILs). Some basic information on protein structure and probing the protein environment by fluorescence techniques is also discussed. Motivation behind the present work has also been briefly discussed. ***Chapter 2*** provides the details of the experimental procedures and methodologies adopted in this investigation. The instrumental details and methods for different calculations have also been discussed in this chapter**.** ***Chapter 3*** describes the transient absorption studies on few structurally related aminophthalimide derivatives in different solvents. ***Chapter 4*** deals with the study of intramolecular PET reaction in some 1,8-naphthalimide systems with *fluorophore-spacer-receptor* architecture in solvents of different polarity. ***Chapter 5*** delineates the ESIPT reaction of 7-hydroxyquinoline in two RTILs. ***Chapter 6*** presents fluorescence and molecular docking results on the interaction of aminocoumarins and aminonitrobenzoxadiazoles with bovine serum albumin and human serum albumin. ***Chapter 7*** summarizes the findings of the present investigations by touching upon the achievements and looking into the future scope of the work.

Chapter 1

Introduction

This chapter introduces some of the characteristics of electron donor-acceptor (EDA) systems, which are frequently used as molecular probes for studying complex environments. A brief outline of some of the photophysical processes, which form the subject matter of the present work, is provided. An introduction to nonradiative processes focusing on the governing principles and the integral role of solvent in the nonradiative transition of some common EDA systems is provided. Fundamental aspects of the excited state intramolecular proton transfer are presented and the different forms involved in this process are illustrated with few common examples. Photoinduced electron transfer (PET) is discussed briefly touching on the principles of intramolecular PET, which is commonly the underlying principle of the fluorescence signaling of various guests. A brief introduction to room temperature ionic liquid highlighting some of its important physical properties is outlined in this chapter. The chapter also includes some structural information of protein molecule followed by a discussion on probing the environment of protein through fluorescence. The chapter concludes on describing the motivation of the thesis and introducing the systems studied in this work.

1.1. Electron donor-acceptor molecules and their characteristics

Considerable attention has been attached to the electron donor-acceptor (EDA) molecules in recent years primarily because of the fact that charge separation is one of the most fundamental processes involved in numerous chemical and biological transformations. A thorough understanding of the photoinduced charge separation process, which plays an important role in the primitive photosynthesis phenomenon in plants,[1] helps in designing and developing of efficient systems for solar energy conversions in modern days.[2-9] Moreover, the EDA systems find usage in sensing environments,[10] as nonlinear optical materials,[11] molecular electronic devices,[12] etc. EDA systems are also considered as a favorite testing ground for the theories of electron transfer and solvation dynamics.[13]

Mulliken was the first to introduce the concept of charge-transfer transition to describe the spectral and bonding interactions of molecular complexes formed between an electron donor and an acceptor.[14,15] The charge transfer can take place either through bond or through space. In systems where the electron donor and acceptor moieties are connected by a flexible spacer, a charge-transfer complex or exciplex is often formed due to the spatial overlap between the donor and acceptor orbitals.[16] But in cases where through-space interaction of the donor and acceptor orbitals is not possible due to limited configurational flexibility, charge separation is made possible by through-bond interaction of the two. In both cases, appropriate model systems[17-19] have been chosen to investigate the dependence of the electron transfer rate on the free energy of reaction, distance and orientation between the donor and acceptor and the medium. When the charge transfer (CT) state is luminescent, the CT emission provides an excellent opportunity to monitor the dynamics because internal structure and environment influence this luminescence in such a way that it could provide a detail information of the thermodynamic and kinetics of photophysical properties. The simple photophysical techniques such as steady state and time-resolved fluorescence as well as transient absorption studies are generally employed for the study of the CT state.

An appreciable increase in the dipole moment is observed for a major chunk of the EDA molecules, when they are subjected to photoexcitation. The emission maxima and quantum yields of these compounds are often very much sensitive to the polarity of the medium. This sensitivity is often exploited to determine the polarity of unknown solvent mixtures or to estimate the polarity of the microenvironments in organized assemblies such as micelles and membranes. Examples of these kinds of probes (Chart 1.1) are 6-propionyl-2-(N,N-dimethylamino)naphthalene (PRODAN),[20,21] 4-aminophthalimide (AP),[22] 1-anilinonaphthalene-8-sulfonate (ANS)[23] and hemicyanine dye.[24]

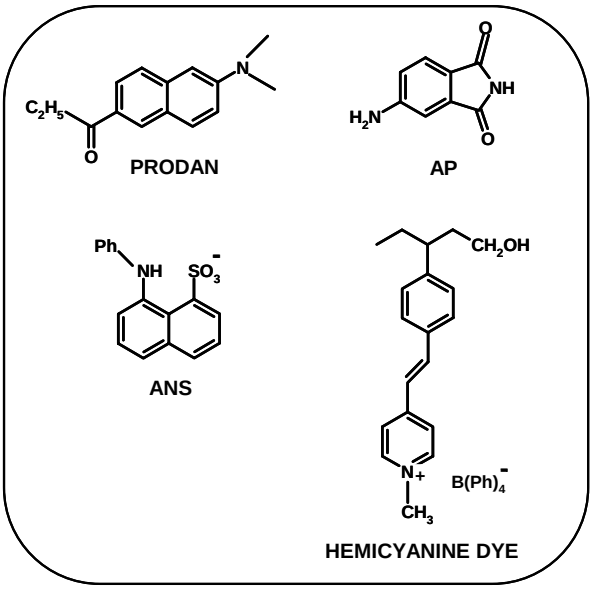

Chart 1.1. Examples of few common EDA probes used for estimation of polarity of environments.

1.2. Nonradiative processes

The nonradiative electronic processes in isolated molecules and condensed phase, take place without breaking of any chemical bond and generally involve the conversion of electronic energy to vibrational energy.[25] The nonradiative decay processes find many useful consequences in dye laser operation,[26] efficiency of fluorescence probes,[27] stereomutation of 'push-pull' stilbenes, polyene and rhodopsin,[28-31] light fastness of dyeing agents,[32] effectiveness of photographic sensitizers[33] and molecular switching devices.[34] Radiationless transition between initial and final electronic states is known to occur at the point of intersection of potential energy surfaces. The nonradiative transition happens irreversibly at this isoenergetic point to the higher vibrational level of the lower energy state and the excess vibrational energy cascades down the vibrational manifold. Thus, the radiationless conversion of energy involves two steps: (i) the transfer of energy

at the isoenergetic point from the higher electronic state to the high vibrational level of the lower electronic state, and (ii) the rapid loss of excess vibrational energy after energy transfer. The first step is the rate determining step and is of prime importance, while the second is merely *vibrational relaxation*. It is to be noted that efficiency of the radiationless transition is directly proportional to the value of the overlap integral (Franck-Condon integral) of the two interacting states. Apart from the Franck-Condon integral, symmetry restrictions and spin multiplicity rule impose their own inefficiency factors in the efficient crossover from one energy state to another. In addition to the above mentioned dependencies, *density of state* is another vital contributing factor for determining the efficiency of the nonradiative process. For example, in solution, the medium may provide a background of its own energy states which are nearly degenerate and in resonance with the initial state, which often facilitates the radiationless transition through the *quasicontinuum* of the final state. Solute-solvent interactions may further perturb the potential energy leading to crossing of surfaces, if such a crossing point was not present initially, then it promotes nonradiative transitions. But in the absence of specific solute-solvent interactions, the medium probably has very little effect on the rates of radiationless transitions. Thus, these three key factors, (1) energy gap between the interacting electronic states, (2) Franck-Condon overlap integral and (3) density of state, are known to govern the efficiency of the nonradiative processes. There are two major types of radiationless transitions: (i) *internal conversion*, and (ii) *intersystem crossing*. When the noradiative loss of energy occurs between electronic energy manifold of the same spin type i.e singlet-singlet or triplet-triplet then such transitions are called internal conversion. The intersystem crossing involves nonradiative energy loss between energy states of two different spin multiplicity. The selection rules for radiationless transitions are opposite to that of radiative transitions. Here, the allowed transitions are: $g \sim\!\!\sim\!\!\rightarrow g$, $u \sim\!\!\sim\!\!\rightarrow u$ and $S_1 \sim\!\!\sim\!\!\rightarrow T_1$ and forbidden transitions are $u \sim\!\!\sim\!\!\rightarrow g$, $S_1 \sim\!\!\sim\!\!\rightarrow S_0$ and

$T_1 \sim\!\!\sim\!\!\rightarrow S_0$. Rigid polyatomic systems like naphthalene, anthracene etc. have a finite rate of nonradiative process due to the inherent factors discussed above. Structurally flexible systems also often exhibits unusually high nonradiative rate due to their internal motion. There are several factors related to the internal motion of the molecule that enhance the nonradiative rate in the systems. These factors are briefly touched upon by illustrating some of the well known fluorescent probes.

1.2.1. Rhodamines

These are a group of popular xanthene dyes (Chart 1.2), known for their interesting photophysical behavior. Rhodamines in frozen solutions or rhodamines with rigid amino group (such as rhodamine 101) show fluorescence quantum yield close to unity.[35,36] It is found that the internal conversion of these dyes is strongly associated with the rigidity of the xanthene-amine C-N bond. Several models have been proposed to explain the unusual dependence of the internal conversion rate on the solvent and molecular structure of the xanthene dyes. Among them the twisted intramolecular charge transfer (TICT) model[37,38] and umbrella like motion (ULM) model[39-41] are noteworthy. Whereas, the TICT model is mainly governed by the viscosity and polarity of the solvent, the ULM model stresses on the importance of specific solute-solvent interactions for unusually high internal conversion rate. Rettig et al. proposed the involvement of nonradiative TICT state for rhodamines and few other xanthene dyes.[37,38] A higher quantum yield and lifetime of the monoalkyl derivative compared to dialkyl substituted rhodamine is attributed to a higher energy of the TICT state of the former system. An alternative mechanism by Arbeloa et al.[39] effectively correlates the internal conversion with a change in the amino group configuration from planar to pyramidal one, known as ULM motion.

1.2.2. Coumarins

In order to account for the dependence of the fluorescence property of coumarins (Chart 1.2) on the structure of the amino moiety and on the polarity of the medium, Jones II and coworkers[42-44] suggested that the planar intramolecular charge transfer state is highly fluorescent, whereas twisted charge transfer state is nonemissive. Later, de Melo et al.[45,46] have shown that the photophysical behavior of some coumarin derivatives is essentially determined by the relative location of two energetically close-lying n-π* and π-π* singlet states. A mixing between the two states depending upon the polarity of the media and the nature of the amino substitution controls the magnitude of the nonradiative rates in methoxycoumarin.

1.2.3. Squaraine

Squaraine is another class of popular dyes (Chart 1.2) emitting in the visible range, which shows interesting nonradiative decay behavior. The nonfluorescent nature of squaraine was interpreted in terms of twisting of the amino moiety around the C-N bond.[47,48] Essentially, the twisting leads to a region close to the funnel of conical intersection, which acts as a nonemissive decay channel.

1.2.4. Cyanine

Among the large organic molecules, cyanine dyes are interesting systems for the study of solvent and temperature dependence on the radiative and nonradiative processes. Fleming et al. have studied DODCI (Chart 1.2), a cyanine dye in a series of polar solvents at different temperatures as well as in rigid matrix and clarified the kinetics for the nonradiative decay.[49] The nonlinear Arrhenius plot was interpreted by invoking the involvement of a second nonradiative decay channel with a low activation energy barrier (~1.55 kcal/mol). This second nonradiative process with low activation barrier is

supposed to be a direct internal conversion which at high temperature cannot compete with the twisting process.

1.2.5. Nitrobenzoxadiazole and naphthalimide derivatives

Recently, two sets of EDA systems, amine-terminated nitrobenzoxadiazole and naphthalimide derivatives (Chart 1.2) have been studied by Samanta and his coworkers with a view to elucidate the nonradiative pathways in these systems.[50,51] It has been found that the nonradiative rate constants of these systems largely depend on the nature of the amino functionality. An increase in the length of the dialkyl groups connected to the amino nitrogen or an increase in the size of the ring containing the amino nitrogen enhances the nonradiative deactivation of the fluorescence state of the systems. It has also been shown that the variation in the nonradiative rate constants in both cases can be best explained in terms of the nitrogen inversion model.

1.2.6. Aminomethoxyflavone derivatives

Very recently Sarkar et al.[52] studied some amine terminated methoxyflavone derivatives to understand the solvent dependency on the nonradiative processes in these systems. The nonradiative rate constants evaluated from the quantum yield and lifetime values show a decreasing trend with increasing polarity of the solvent. The observations have been accounted for taking into consideration the nature of the two excited states involved in the emission process. The results suggest a change in the nature of the state from n-π^* to π-π^* with increase in the polarity of the medium.

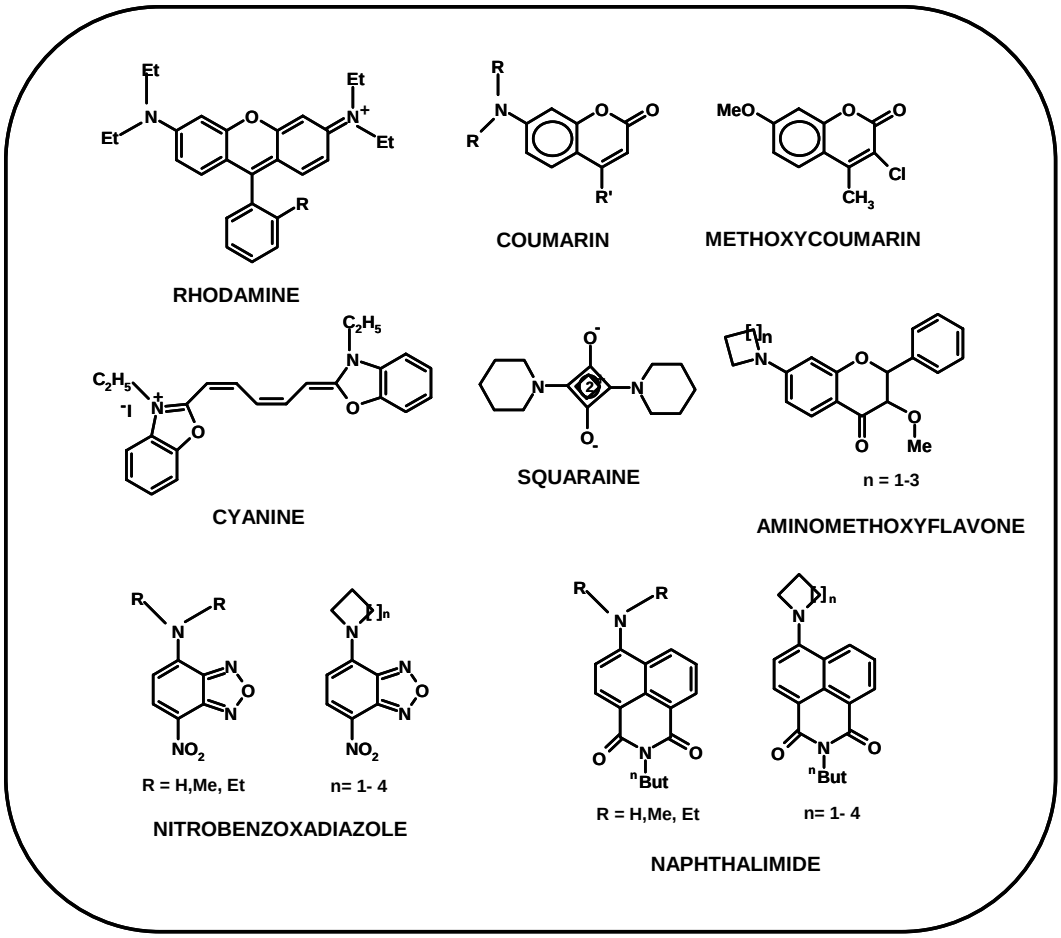

Chart 1.2. Examples of fluorophores known for efficient nonradiative processes.

1.3. Excited state intramolecular proton transfer

Organic bi-functional molecules comprising both hydrogen bond donor and acceptor groups in close proximity form an intramolecular H-bonded structure in the ground state. On photoexcitation, a massive intramolecular redistribution of electronic charge takes place and as a consequence the proton gets translocated from the hydrogen bond donor group to the hydrogen bond acceptor group. This phenomenon is commonly termed as

excited state intramolecular proton transfer (ESIPT). ESIPT reaction has been considered to be one of the simplest photoreactions of great importance in chemical and biological systems and has received a great deal of attention both experimentally and theoretically.[53-64] ESIPT phenomenon is most commonly monitored using fluorescence technique. Excitation of an ESIPT system usually leads to dual fluorescence which is attributed to the normal form and tautomer form of the molecule. The interplay between the molecular structure and potential energy surface has been shown to be quite important for an understanding of the mechanism of ESIPT.[62] The tautomer fluorescence gets highly Stokes' shifted (6000-10000 cm^{-1}) due to enormous change of the electronic distribution in the excited state.[55] Consideration of a double-well potential depicted in the Scheme 1.1 can give a better understanding of this phenomenon.

As can be seen from the Scheme 1.1, due to photoexcitation (from $S_0 \rightarrow S_1$) there occurs huge electronic change and consequently the proton moves on a double-well potential surface as shown in the scheme. In the ground state there exists significant energy barrier for proton transfer, whereas, in the excited state as the barrier becomes small the proton is much easily transferred to generate the excited tautomer species. The $S_1 \rightarrow S_0$ energy gap of the tautomer is much lower than the normal form. Hence the large Stokes' shift observed for the fluorescence originating from the tautomer.

Scheme 1.1

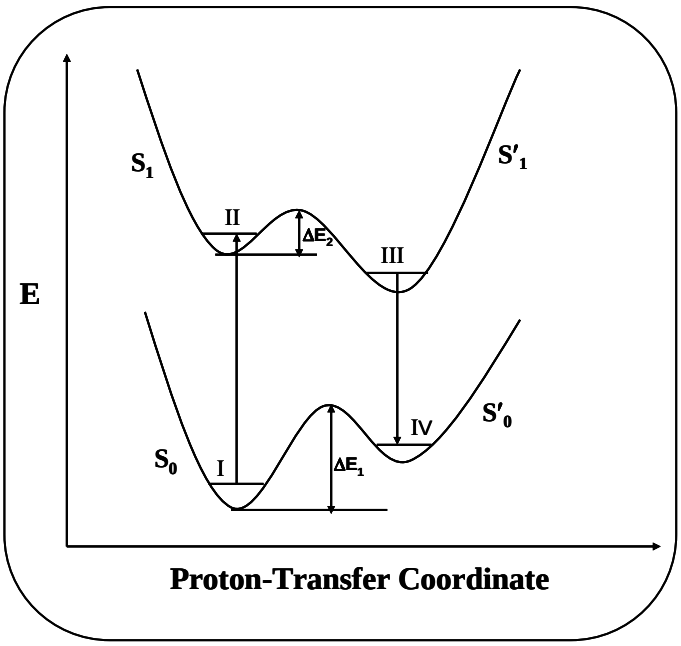

ESIPT requires hydrogen bond formation between the proton donor (generally, a moiety containing –OH or –NH group) and the acceptor (generally, a moiety containing =N– or =O group). The dynamics of this ESIPT phenomenon, on a symmetrical double-well potential, has been well reviewed in literature.[62,65] The presence of an unsymmetrical double-well potential is often visualized as a representation of nearly barrierless proton transfer.[59] Quantum mechanical calculations have shown the impact of tunneling effect and vibration dynamics of bonds involved in hydrogen bonded network on the proton transfer dynamics; thus the potential energy surfaces have shown to be dependent on the nature of the molecules.[60,62,66]

In aprotic solvents, where solvent perturbation is negligible, ESIPT phenomenon normally takes place through the pre-existing strong intramolecular hydrogen bonded structure. However, in protic solvents the solvent perturbation is expected to become

significant, particularly when the intramolecular hydrogen-bonding between the donor and acceptor moieties is weak. In the latter case, the intermolecular hydrogen bonded network inhibits to some extent the ESIPT phenomenon. The most striking feature of the ESIPT dynamics in aprotic solvents is its ultrafast nature, occurring in sub-picosecond to few femtoseconds time scale.

The ESIPT phenomenon has vast utility. Classical examples of these include four-level dye lasers, energy or data storage devices and optical switching,[67-76] Raman filters,[77] scintillation counters,[78] polymer stabilizers.[79,80] Moreover, ESIPT molecules have also been used in metal ion chelates.[81] These ESIPT molecules are known to possess photochemical stability, and are resistant to thermal degradation. Low self-absorption of the tautomer fluorescence has been utilised in electroluminescence.[82]

From the mechanistic point of view, the ESIPT phenomenon can be classified into three groups,[55] (i) intrinsic intramolecular proton transfer, (ii) double proton transfer, and (iii) proton transfer through relay. Each group is discussed separately as follows.

1.3.1. Intrinsic intramolecular proton transfer

This is perhaps the simplest type of proton transfer, occurring in systems in which five/six- membered intramolecularly hydrogen bonded structure is already present. Enormously studied, molecules like methyl salicylate,[83-85] 2-hydroxybenzophenone,[86] salicylidenaniline,[87] 3-hydroxyflavone,[67,88] salicylamide,[89] 2-(2′-hydroxyphenyl)benzimidazole,[90-92] 2-(2′-hydroxyphenyl)benzoxazole[91,93,94] and 2-(2′-hydroxyphenyl)benzothiazole[95,96] (Chart 1.3) serve as good examples for this kind of proton transfer. In each case, specific molecular structure and conformation lead to specific behavior. Environmental and/or solvent-cage perturbations are found to be quite significant in the ESIPT studies of these molecules.

1.3.2. Double proton transfer

This type of proton transfer involves the formation of intermolecular hydrogen bonded network between two same/identical molecules. The first reported example of this kind is 7-azaindole[97-99] (Chart 1.4). At high probe concentration, in addition to the violet emission from the 'normal form' of the molecule, another green fluorescence is observed which is attributed to double proton transfer. Another molecule which shows similar biprotonic transfer is benzanilide[100] (Chart 1.4).

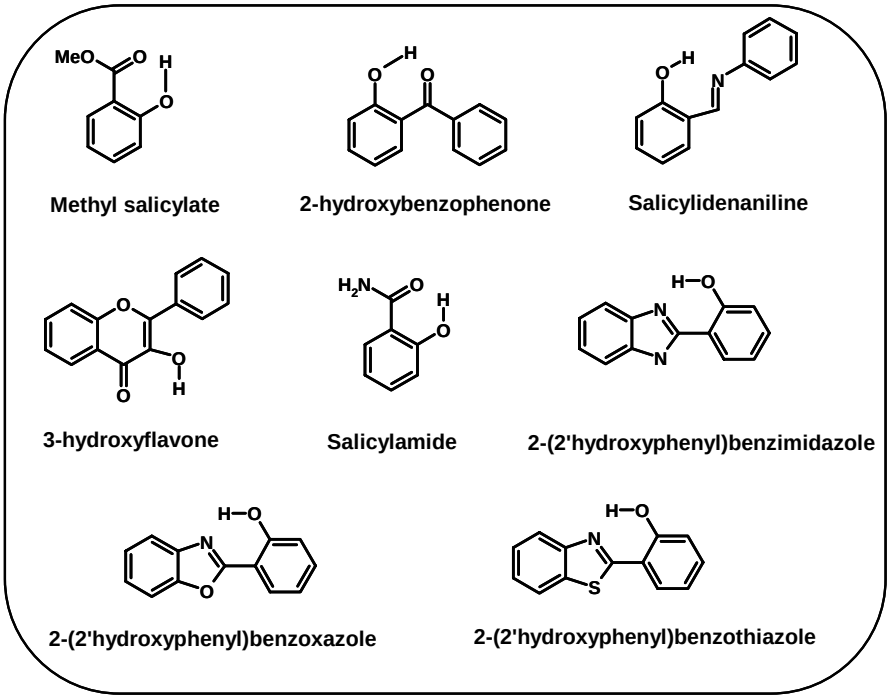

Chart 1.3. Molecules undergoing intrinsic intramolecular proton transfer.

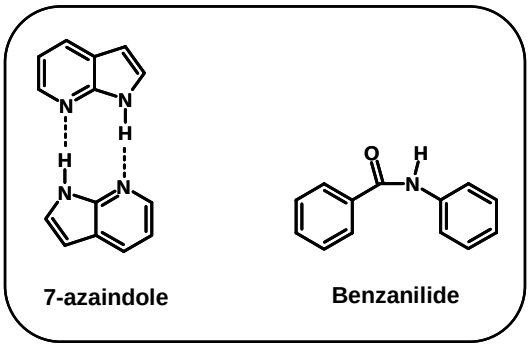

Chart 1.4. Molecules undergoing double proton transfer.

1.3.3. Proton transfer through relay

This is another type of proton transfer, where the proton donor group is at a distance from the proton acceptor. A 'molecular companion', (say acetic acid or alcohol) must be involved in the form of a cyclic H-bonded complex, where protons are transferred in a relay mechanism during the excited state lifetime of the fluorophore. This is observed in case of lumichrome,[101,102] adenine and guanine[55] where acetic acid is involved in the cyclic hydrogen bonded complex (Chart 1.5). While in 7-hydroxyquinoline[66,103] and 3-hydroxyxanthone,[104,105] alcohol molecules form the required H-bonded network (Chart 1.5).

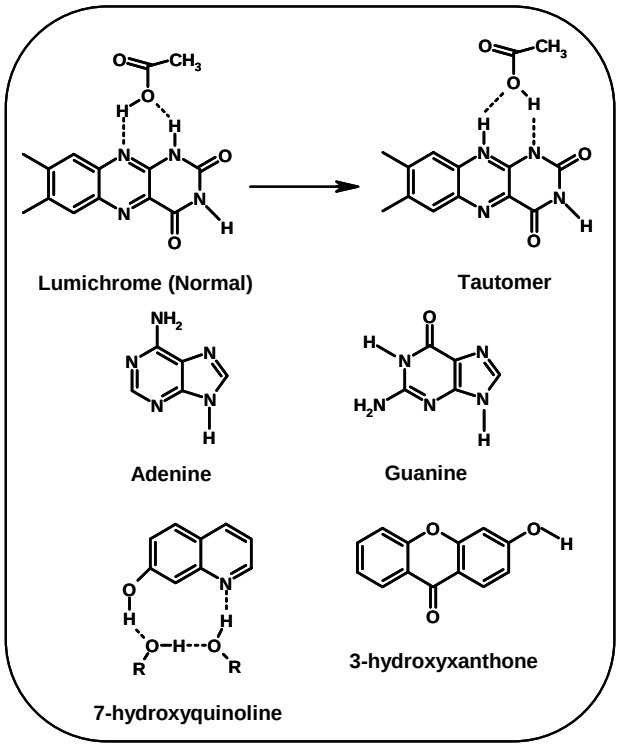

Chart 1.5. Molecules undergoing proton transfer through relay.

1.4. Photoinduced electron transfer

Photoinduced electron transfer (PET) reactions play quite an important role in numerous chemical[106] and biological systems.[107] The application of PET ranges from photosensitized catalysis to solar energy conversion.[108] PET may occur between two separate molecules serving as electron donor and acceptor and also possible in rigid/flexible systems where both the donor and the acceptor are part of the same molecule linked with a spacer.[106]

In case where two separate entities are involved the transfer of an electron occurs between the photoexcited state (singlet or triplet) and ground state molecule to generate a charge transfer species, which may either be an excited state charge transfer complex or a

charge separated radical ion pair.[109] The initial species then may undergo a variety of secondary processes like back electron transfer leading to the ground state of the molecule, ionic dissociation to free, solvent-separated ions, triplet recombination to generate an excited state of one of the reactants, or other charge transfer intermediates and/or stable products[106,109] as shown in Scheme 1.2. In case of such PET reactions, involving singlet excited species, the electron transfer leads to quenching of fluorescence and formation of either an exciplex, often a fluorescent species, formed especially in nonpolar solvents, or a charge separated ion pair, usually called geminate or contact ion pair, which is normally realized in polar solvents.[110,111]

Scheme 1.2

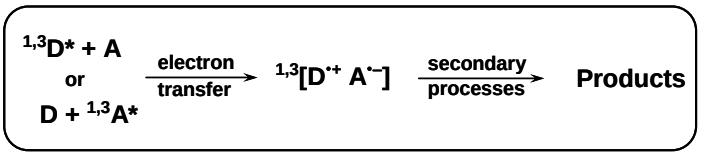

The thermodynamic driving force, ΔG_{ET} of the overall PET process, is given by[111,112]

$$\Delta G = E_D^{ox} - E_A^{red} - E_{0,0} - e^2/\varepsilon r_q \qquad (1.1)$$

where, E_D^{ox} and E_A^{red} are the oxidation and reduction potentials of the donor and the acceptor, respectively. $E_{0,0}$ is the energy corresponding to the 0-0 transition of the photoexcited molecule (donor or acceptor) and $e^2/\varepsilon r_q$ is the coulombic energy of interaction of the ion pair at the effective encounter distance of the donor and acceptor ($r_q = r_d + r_a$). The coulombic energy term depends on solvent polarity and becomes negligible when the solvent is highly polar, cf. acetonitrile.

1.4.1. Intramolecular PET

On photonic excitation, in rigid intramolecular systems the transfer of the electron occurs from the donor end to the acceptor (in the singlet or triplet state of the molecule) to generate the excited charge separated radical ions[106] as depicted in Scheme 1.3.

The efficiency of intramolecular electron transfer is strongly influenced by the separation distance between donor and acceptor and the structure of the molecular link.[106] The characterization of the pathways is possible where donor and acceptor groups form collision complexes or exciplexes, or exchange an electron at a long distance.

Scheme 1.3

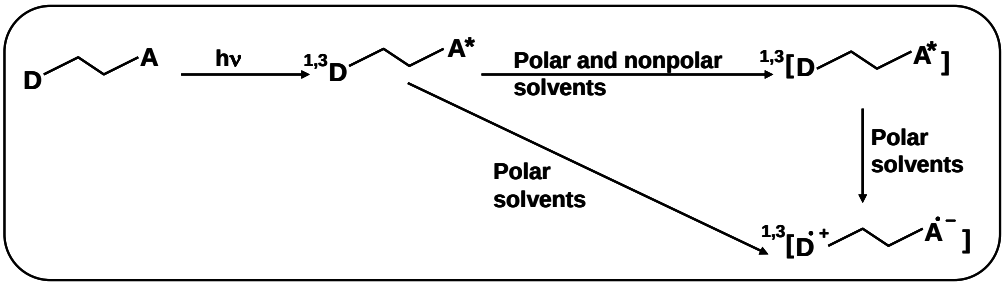

Intramolecular electron transfer can occur where donor and acceptor molecules separated by a (i) short flexible chain, (ii) long flexible chain, and (iii) rigid spacer molecule. In pairs held together by flexible chains, the length and steric nature of the chain, effect of solvent viscosity and temperature on motion of the chain, and the dielectric constant of the solvent generally influence the conformation of the ground state at the moment of electron transfer, i.e, the distance the electron must travel, and the stabilization of exciplex and radical ion intermediates.[113] In case where the chain is long, consideration is given to unrestricted conformational motions in the ground state as well as in intermediate structures. In rigid spacer only the separation distance and orientation of the donor and acceptor are important.[106] Generally in flexible molecules electron

transfer is favorable when the connecting link is short. In these systems, exciplexes are possible intermediates when structure allows for orbital overlap between donor and acceptor.

1.4.2. PET in EDA systems: sensors

Certain multi-component EDA systems constitute a *fluorophore-spacer-receptor* architecture (Scheme 1.4). These molecular systems are weakly fluorescent because of *photoinduced intramolecular electron transfer* from the terminal electron-rich receptor moiety to the electron-deficient fluorophore unit.[114] These systems are most commonly employed for "off-on" fluorescence signaling. In this design, the fluorophore and the receptor sites are connected by an intervening spacer unit. This means that the three separate units: guest-binding unit, terminal fluorophore and spacer serve as quantitative predictors for the sensory properties of the multi-component super-molecule. Thus, a sensor can be designed such that communication between the receptor and the photoexcited fluorophore leads to fluorescence quenching of the system ("off" state) in the absence of a guest. In the presence of a guest, the guest-receptor interaction should lead to a disruption of the communication between the receptor and the fluorophore thereby "switching on" the fluorescence. Sensors based on this mechanism are termed as PET sensors.[114,115]

Scheme 1.4.

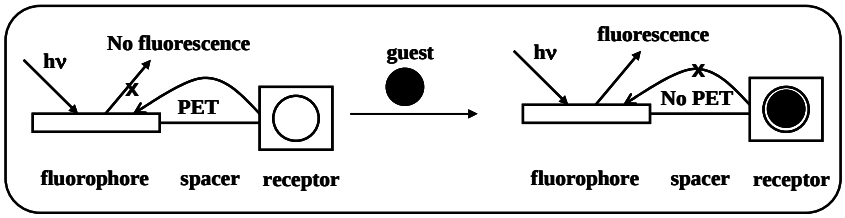

The PET reaction is monitored using a number of experimental techniques. Feasibility of the PET reaction for a particular donor-acceptor pair can be evaluated by calculating ΔG_{ET} using equation (1.1). The best evidence of PET and subsequent reaction comes out of the detection of intermediates, like those described in Scheme 1.2 and in Scheme 1.3. Among the various tools, laser flash photolysis (LFP) detection is most popular as it offers direct determination of the radical ions and other transient species resulted in PET reaction.[109,110,116] The detection of the radical ions intermediates further proves the basic assumption on which the PET sensors are designed. Other techniques like ESR or spin trapping,[117] chemically induced dynamic nuclear polarization (CIDNP),[118] transient photocurrent measurement,[119] scavenging or trapping the intermediates[120] etc have also been employed to elucidate the PET reaction course.

1.5. Room temperature ionic liquids

In the recent years, a significant effort has been directed towards the design and development of environmentally benign media to substitute the traditional solvents, most of which are volatile organic compounds (VOCs), usually employed for laboratory and industrial purposes. These VOCs are major source of environmental pollution, especially when employed in bulk scale for industrial purposes. Therefore, the quest for ***green chemistry***[121] has began and this has led to the realization of the importance of a number of alternatives, such as, solvent-free synthesis,[122] use of water as a solvent,[123] use of supercritical carbon dioxide[124] and ionic liquids as the reaction media.[125-136] The ionic liquids have been invoked as environmentally benign solvents due to a number of suitable properties, but mainly because of their *negligible vapor pressure*, which prevents air and water pollution through emission of VOCs.

The ionic liquids are simply low melting organic salts, composed entirely of ions (i.e., cation and anion). The term '***ionic liquid***' has replaced the older phrase 'molten salt' as the latter suggests a high-temperature, highly corrosive, overtly viscous media, cf.

NaCl at and above its melting point 803°C.[126] In the academic literature, the term '***ionic liquid***' usually refers to liquids composed entirely of ions that are fluid at around or below 100°C.[125] However, ***room temperature ionic liquids*** (RTILs) are the class of ionic liquids which are free-flowing liquid at ambient temperature (*ca*. 20-30°C) and pressure (1 bar), usually having melting point near 0°C or less. The lowest melting point for RTILs reported so far is as low as –96°C.[127]

RTILs are not new; ethyl ammonium nitrate, which is liquid at room temperature, was first described in 1914.[128] The modern chemistry of RTILs was introduced in the early 1980s by the use of the salts based on chloroaluminate anions ($AlCl_4^-$ or $Al_2Cl_7^-$) by Wilkes and his co-workers.[129] However, as these salts were extremely hygroscopic and highly reactive towards water their use was quite limited. Hence, they were soon replaced by air and water stable RTILs based on less reactive anions such as BF_4^-, PF_6^-, $CF_3CO_2^-$, $CH_3CO_2^-$, $CF_3SO_3^-$, $(CF_3SO_2)_2N^-$ etc.[130] The research employing the ionic liquids as reaction media received a boost in 1992 after the invention of air and water stable ionic liquids based on 1-ethyl-3-methylimidazolium cation and tetrafluoroborate anion, abbv. [emim][BF_4].[131] In subsequent years, RTILs based on a number of cationic moieties like (a) imidazolium, (b) pyridinium, (c) pyrrolidinium, (d) ammonium, (e) phosphonium etc (Chart 1.6) have been synthesized.[132,133] Recently, even RTILs based on natural amino acids have been prepared.[134] Since these basic cationic moieties can be functionalized in numerous ways and anions can be introduced through metathetic exchange, a large number of RTILs can be synthesized with the desired physical and chemical properties. Most common RTILs are based on unsymmetrically substituted imidazolium cations (Chart 1.7) and BF_4^-, PF_6^-, $(CF_3SO_2)_2N^-$ (commonly known as Tf_2N^-) anions, though alkylsulfate[135] and dicyanimde[136] anions are also becoming popular.

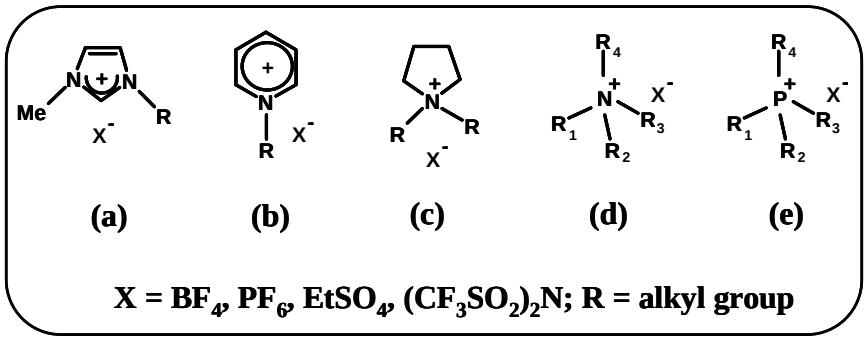

Chart 1.6. Basic structure of some RTILs based on different cationic moieties.

1.5.1. Properties of RTILs

Though nonvolatility (negligible vapor pressure) is the main reason for the choice of RTILs as alternative media, there are a number of useful properties of these substances that make them suitable for diverse application. Among them, wide liquidus, high thermal and chemical stability, moderate to high polarity, high viscosity, non-toxicity and non-flammable nature etc. are noteworthy. Moreover, RTILs can dissolve a large variety of organic/inorganic substances and possess high electrical conductivity and wide electrochemical window.[137] Since the properties of ionic liquids are largely dependent on the constituent ions, it is possible to obtain a RTIL with desired properties by proper choice of the two ionic components, and thus, they are considered as "designer solvent".[138]

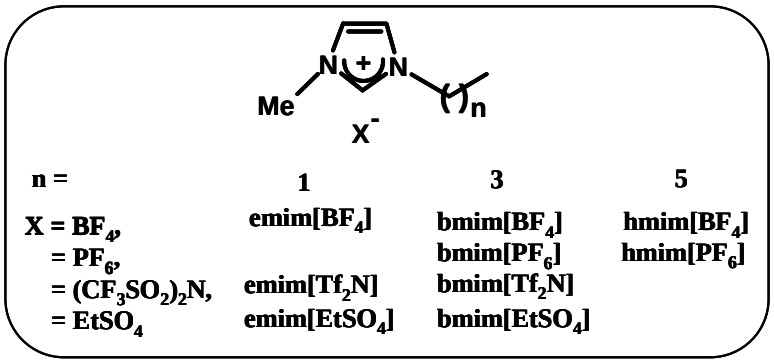

Chart 1.7. Structure and abbreviation of some common imidazolium RTILs.

Melting point: Most RTILs have melting point much below the room temperature (25°C). However, in many RTILs the exact melting point is difficult to determine as they undergo considerable supercooling, which implies that the temperature of phase change may differ considerably depending on whether the sample is heated or cooled.[139] Whence some correlation has been found in terms of the influence of cations, especially for those based on imidazolium salts,[139] the anion effect remains quite uncertain. It has been established that the melting point decreases with increasing size and asymmetry of the cation and increases with increasing branching in the alkyl chain.[140] The effect of hydrogen bonding and delocalization of charge has been invoked to explain the influence of anion, but only a rough correlation can be drawn.[139] For example, low charge density and lack of hydrogen bonding interaction is the main reason for lower melting point of Tf_2N^- salts, whereas more spherical anions like BF_4^-, PF_6^- with potential hydrogen bonding ability result in higher melting point.

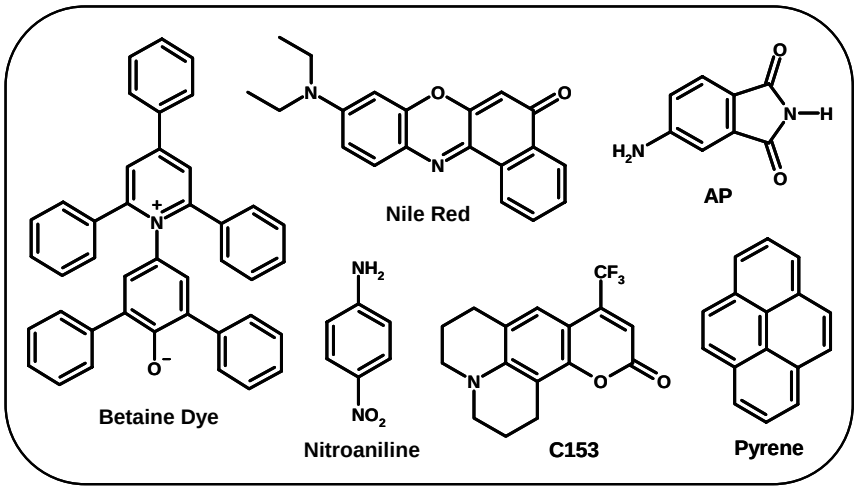

Chart 1.8. Probe molecules used for determination of polarity of RTILs.

Polarity: The microscopic polarity of the RTILs has been determined by using a number of solvatochromic probes (Chart 1.8) in terms of different polarity parameters.[141-147] The $E_T(30)$ or E_T^N values for most of the common RTILs have been determined.[143,144] Other polarity parameters like Kamlet-Taft parameters[145] and multiple polarity parameters[146] have also been employed to review the polarity criteria of RTILs. Most of these studies indicate that polarity of common RTILs (i.e., those having alkyl side-chains) is greater than acetonitrile but less than methanol. $E_T(30)$ values indicate that these RTILs are as polar as short-chain alcohols (cf. butanol). However, recent measurement of static dielectric constant (ε) of a few RTILs indicates that RTILs have very low dielectric constant (in the range of 9-13) which is similar to that of pyridine (ε = 12.3).[147] The reason for such large difference in the polarity estimates of the RTILs is unclear at this moment.

Viscosity and Density: Viscosity of the RTILs is much higher compared to normal solvents like water or alcohols. Even the least viscous RTIL is ~30 times viscous than

water and follow Newtonian-fluid behavior.[139] Generally, RTIL viscosity is sensitive to moisture content and impurities like halide salts.[127,148] Often non-Arrhenius behavior is apparent in the temperature dependence of viscosity,[139,149] especially when measured for a long temperature-range.[149] Examining various anion-cation combinations, the increase in viscosity observed on changing selectively the anion or cation has been primarily attributed to an increase in the van der Waals forces.[150] Hydrogen bonding is always an important parameter and the effect is distinct in the case of alcohol-functionalized RTILs, which are found to be more viscous than their alkyl counterparts.[151] The symmetry of the anion contributes as an additional parameter. Considering the symmetry and hydrogen bonding parameters, the following order of viscosity decrease can be realized: Cl^- > PF_6^- > BF_4^- > Tf_2N^-.[140]

The density of RTILs is also much higher than that of the conventional molecular solvents and the density tends to decrease with increasing anionic volume.[140,150] It is also highly dependent on the molar mass of anions.[152]

Conductivity: The electrical conductivities of RTILs are similar to those of organic solvents with added inorganic electrolytes. The conductivity generally decreases in the following order: 1-alkyl-3-methylimidazolium > N,N- dialkylpyrrolydinium > tetraalkylammonium.[137] This order has been attributed to the decrease in planarity of the cationic component. Among same cationic series with different anions, the conductivity values do not change much.[153] The heat conductivities of the RTILs are also very high. Thus the RTILs permit a very rapid dispersal of the heat of reaction.[139]

Other properties: RTILs usually show high thermal stability, say upto 400°C, though prolonged heating at comparatively lower temperatures, say 200°C, may lead to appreciable thermal degradation. It has been shown that the stability dependence is PF_6^- > Tf_2N^- ~ BF_4^- > halides,[154] and the cation size does not have much effect.[139] Due to extremely low vapor pressure, the RTILs cannot be distilled in normal condition. But,

recently the distillation of some RTILs has been achieved at low pressure.[155] Analysis of the vapor by mass spectroscopic method has shown the existence of neutral ion pairs in vapor state.[155b]

Depending upon the miscibility of RTILs with water they are classified as hydrophobic or hydrophilic. The anion has a dominant role in controlling this property. The PF_6^-, Tf_2N^- etc salts are hydrophobic, while halides, BF_4^-, alkylsulfates are mostly hydrophilic.[139] However, increasing alkyl chain length reduces water solubility, while polar side-chains (those with OH, NH_2) enhance the same. Generally hydrophobic RTILs show more nonpolar behavior in terms of solubility and are readily miscible with the weakly polar organic solvents. However, the solubility of RTILs in aliphatic hydrocarbons is scarce.

1.5.2. Structural features and heterogeneity

Structural features of the ionic liquids have been investigated in the solid state (mainly by crystallography) as well as in the liquid state using various techniques. Even the crystal structures of some RTILs have been determined by in situ crystallization at low temperatures.[156] For imidazolium-based ionic liquids, extensive cation-anion hydrogen bonding network is revealed in the crystal structures, but for the liquid salts presence of such interaction is still not clear.[131,157] Though the hydrogen bonding interaction in some BF_4^- salts[158,159] and its absence in Tf_2N^- salts are revealed in liquid state,[160] the case of the PF_6^- salts is doubtful.[158] Again, some IR studies have revealed that the C–H---X hydrogen bonding remains intact in the liquid state in many cases.[159,161,162]

Many simulation studies have been carried out to obtain an insight into the liquid structure of the RTILs. Molecular dynamics simulations using both atomistic and coarse-grained methods demonstrated the interaction between hydrophobic alkyl tails on the cations, providing local liquid structures reminiscent of membranes and worm-like

micelles.[163,164] The heterogeneity in the liquid structure of RTILs and the presence of '*local structure*' have been indicated in many studies. While some experimental studies have indirectly indicated the heterogeneity or local structures,[165,166] recent X-ray diffraction[167] and Raman scattering[168] studies have shown the evidence of nanoscale ordering and mesoscopic local structure. Using experimental tools like neutron scattering,[169] XAFS,[170] optical Kerr effect[171] etc many aspects of the nanoscale local structure of the RTILs have been revealed. The presence of cation-cation, cation-anion local association has been conclusively shown by NOE and ROESY experiments.[159,162,172] A different variety and level of modeling and simulation studies have also predicted a nanostructured feature of RTILs.[173-175] All simulations confirm a pronounced long-range charge order in RTILs.

1.5.3. Application of RTILs

The early usage of RTILs was mostly confined to their role as alternative solvent system for a large number of organic and inorganic synthesis,[131,149,176-178] catalysis,[126,130] electrochemical[137,179] and separation processes.[180] In recent days, RTILs are emerging as versatile media with potential applicability ranging from synthesis of nanomaterials[181,182] to development of lunar telescope.[183] The RTILs have also been found to be useful in mass spectroscopy,[184] enzyme stabilization,[185] as biocatalysis,[186] gas sensor,[187] and supporting electrolyte for solar[188] and fuel cells.[189] The biphasic acid scavenging utilizing ionic liquids (BASIL) has even met the industrial requirement.[125]

Because functionalization of the RTILs by covalently tethering a functional group to the cation or anion (or both) imparts a particular capability to the ionic liquids, there is considerable current interest in designing and development of various types of functionalized ionic liquids, categorized as "task-specific" ionic liquids (TSILs).[190,191] These TSILs serve specific purposes such as catalysis, organic synthesis, separation of

specific materials, as well as construction of nanostructured materials and ion conductive materials etc.[191]

1.6. Structural aspects of proteins

Proteins are among the most complex and diverse substances known in biological chemistry. Their complexity is related to a great range of biological functions, including enzymatic activity, hormonal and other regulatory activity, immunological activity and a predominant role in structure and morphology of organisms. The diversity of proteins is a reflection of the enormous variety of sequences which result when molecules of high molecular weight are formed by joining 20 different amino acids in a linear series of peptide bonds which is termed as the *primary structure* of protein. The complexity of the protein structure is due to the origin of different structures (Fig. 1.1)[192] from the *primary structure*. *Secondary structure* refers to regular, recurring arrangements in space of adjacent amino acid residues in a polypeptide chain. There are a few common types of secondary structure, the most prominent being the α helix and the β conformation. *Tertiary structure* refers to the spatial relationship among all amino acids in a polypeptide; it is the complete three-dimensional structure of the polypeptide. Proteins with several polypeptide chains have one more level of structure: *quarternary structure*, which refers to the spatial relationship of the polypeptides, or subunits, within the protein. A stable clustering of several elements of secondary structure is sometimes referred to as *supersecondary structure*. A somewhat higher level of structure is the *domain* (Fig. 1.2). This refers to a compact region, including perhaps 40-400 amino acids, that is a distinct structural unit within a larger polypeptide chain. A polypeptide that is folded into a dumbbell-like shape might be considered to have two domains, one at either end. Many domains fold independently into thermodynamically stable structures. A large polypeptide chain can contain several domains that often are readily distinguishable within the overall structure. The stability of the protein conformation is dependent on the

weak interactions like hydrogen bonds, hydrophobic, ionic and van der Waals forces. The role of these interactions is especially important to understand how the polypeptide chains fold into specific secondary, tertiary and quarternary structures. In general, hydrophobic amino acid residues are clustered on the inside of the folded protein, while hydrophilic side chains are present on the surface of the folded protein and favor interaction with the aqueous solvents in which proteins function.

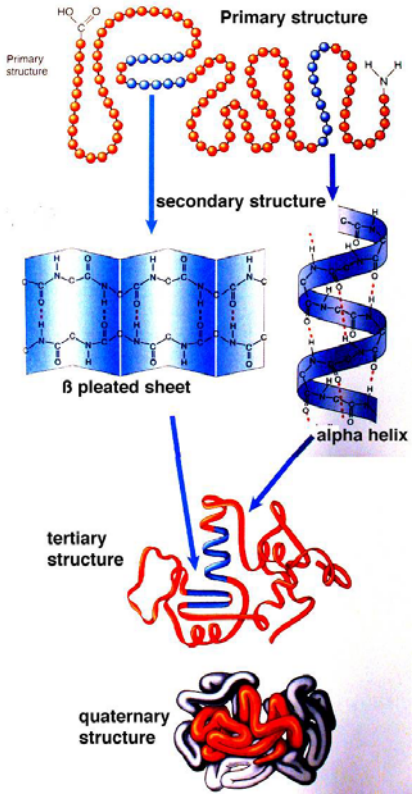

Fig. 1.1. Depiction of three-dimensional structure of protein (due acknowledgement to Brooklyn College, City University of New York- Lecture Outline, Biology 4 section FV).

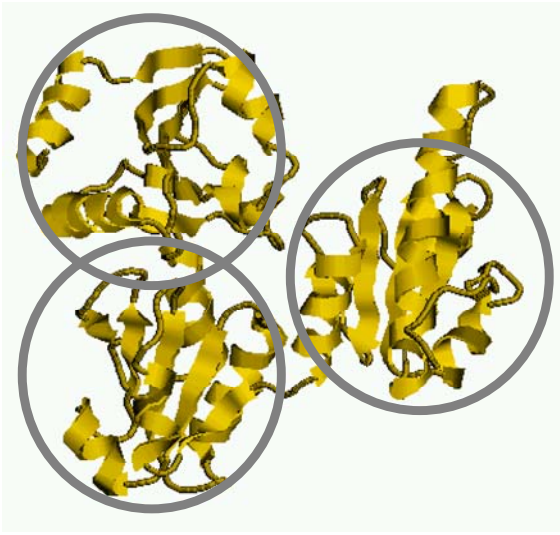

Fig. 1.2. Protein structure with three domains (due acknowledgement to Golan Yona, Colonell University- The Domain Structure of Proteins: Prediction and Organization).

1.7. Probing protein environment through fluorescence

Fluorescence stands out as one of the most popular optical techniques to investigate structure of protein employing molecules whose excited state lifetime is sufficiently long for a variety of chemical and physical interactions to take place prior to emission. These include rotational motion, solvent reorientation, complex formation, proton transfer, and transfer of the excited state energy to another fluorophore. Fluorescence excitation and emission spectra, fluorescence polarization, quantum yields, and decay times provide information about these processes and thereby about the microenvironment of the fluorophores in proteins.[193]

There are fluorescent molecules generally used to investigate such complex environments of the macromolecules (proteins), which are called fluorescence probes. Edelman and McClure[194] have defined *fluorescence probes* as "small molecules which undergo changes in one or more of their fluorescence properties as a result of

noncovalent interaction with a protein or other macromolecule." The typical fluorescence probes for proteins are naphthylamine sufonic acids,[195] of which 1-anilinonaphthalene-8-sulfonic acid (ANS) and 6-(*p*-tulouidinyl)naphthalene-2-sulfonic acid (TNS) are most common (Chart 1.9) wherein noncovalent interactions are responsible for probing the protein environment. Fluorescent probes behave like adsorption indicators, and their interactions with proteins may be described in terms of the stoichiometry and affinity of binding. The structure of a probe may be altered to favor interaction with regions of proteins possessing particular properties. By analyzing the fluorescence of suitably chosen probes, one may study regions of protein molecules of particular interest, such as the active site of enzymes. To interpret the data, it is usually necessary to have information concerning the mechanisms of quenching of fluorescence probe.

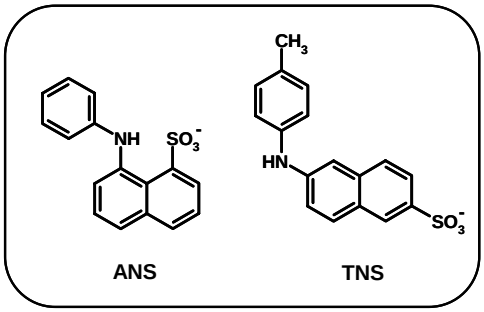

Chart 1.9. Common *fluorescence probes* used for probing the environment of proteins.

1.8. Motivation behind the thesis

The work embodied in this thesis has been undertaken with a view to understand a few photoinduced processes in different environments. While nonradiative processes in certain EDA molecules and PET process in linked systems have been investigated in conventional solvents, proton transfer process is studied in RTILs in order to obtain insight into the mechanistic details of the process in the viscous RTILs. In the later part

of the thesis, the nonradiative process in few EDA molecules has been studied in protein environment.

A substantial amount of work on AP derivatives is aimed at finding out the dependence of their fluorescence efficiency and lifetime on the nature of the amino functionality and polarity of the media.[196] However, these studies did not provide much information on the nature of the nonradiative processes in these systems. This deficiency prompted us to carry out transient absorption studies on three structurally similar AP derivatives comprising cyclic amino functionalities of different ring sizes (Chart 1.10) in less polar (1,4-dioxane), polar aprotic (acetonitrile) and protic (methanol) media by laser flash photolysis technique.

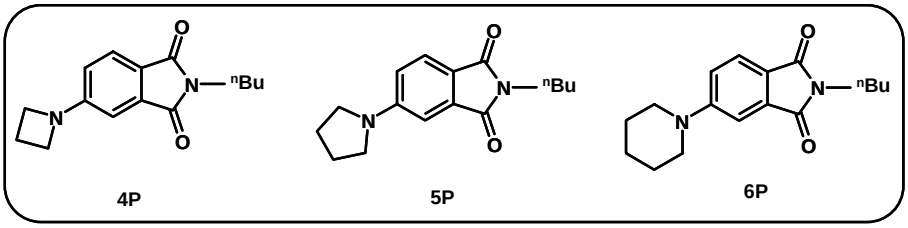

Chart 1.10. Aminophthalimide derivatives comprising cyclic amino functionalities.

Fluorophore-spacer-receptor systems (Chart 1.11) comprising different 1,8-naphthalimide derivatives as fluorophore serve as potential fluorosensors for various guests. The signaling mechanism is believed to be due to photoinduced electron transfer[197] between the fluorophore and receptor moieties, even though direct evidence in favor of this mechanism is so far lacking. We have therefore undertaken the project to obtain compelling evidence for the PET process by probing the transient species in the photoreaction of these systems in different solvents.

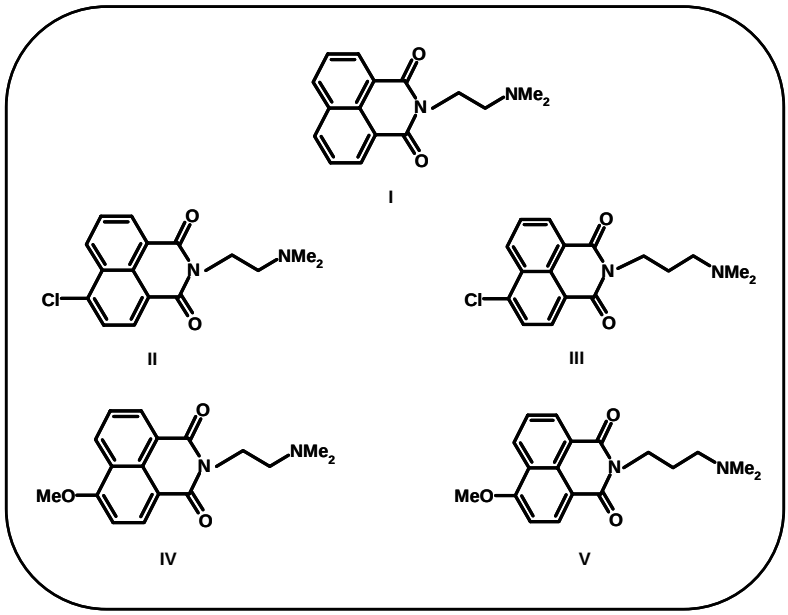

Chart 1.11. 1,8-naphthalimide derivatives bearing the *fluorophore-spacer-receptor* architecture.

Even though excited state proton transfer (ESPT) reaction plays a central role in a wide variety of chemical and biological phenomena,[198] there is hardly any study of this reaction in RTILs. The ESPT reaction in 7-HQ requires participation of protic solvent molecules such as methanol or water to bridge the proton donor and acceptor sites[66,103] and viscosity of the medium plays a crucial role in it.[103e] Thus, this system provides an opportunity to investigate the influence of viscous RTILs on the mechanism and kinetics of the ESPT process. Hence, we studied ESPT reaction of 7HQ mediated by methanol molecules in two RTILs (Chart 1.12) using steady state and time-resolved fluorescence measurements. Apart from the viscosity effects the influence of other factors such as the presence of the ionic constituents and microheterogeneity of the RTILs on the proton transfer process is also investigated.

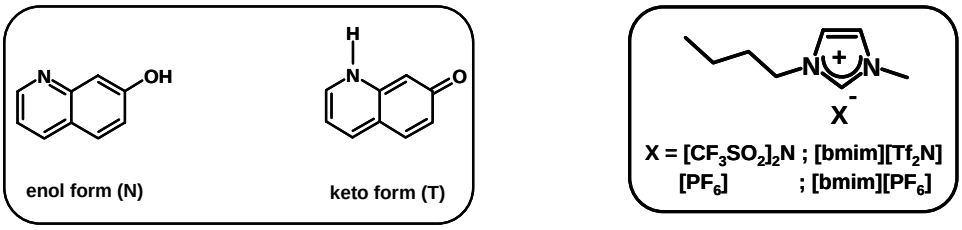

Chart 1.12. Enol and keto forms of 7-hydroxyquinoline and structure and abbreviation of the RTILs used in the present work; [bmim] ≡ 1-butyl-3-methylimidazolium, [Tf_2N] ≡ bis(trifluoromethanesulfonyl)imide.

Twisting of the amino group in aminocoumarins and nitrogen inversion in 4-amino-7-nitrobenz-oxa-1,3-diazoles (NBD) play an important role in dictating their fluorescence efficiencies and lifetimes.[42-44,199,200] An enormous amount of work has been focussed on the interaction of the fluorophores with the protein with a view to obtaining insight into the structure and dynamics of the protein molecule.[192-194,201] However, not much effort has been directed towards finding out whether a protein environment can be profitably exploited for controlling the internal motions in a fluorophore. This work has been undertaken with a view to understand the interaction of the above systems with protein and also to find out whether confinement of these systems in the protein environment can have an influence on their nonradiative processes due to internal motion. Here the steady-state and time-resolved behavior of coumarins and NBD derivatives (Chart 1.13) in presence of BSA and HSA are described. For further support the binding orientation of the molecules to the large protein molecule is investigated through protein docking studies.

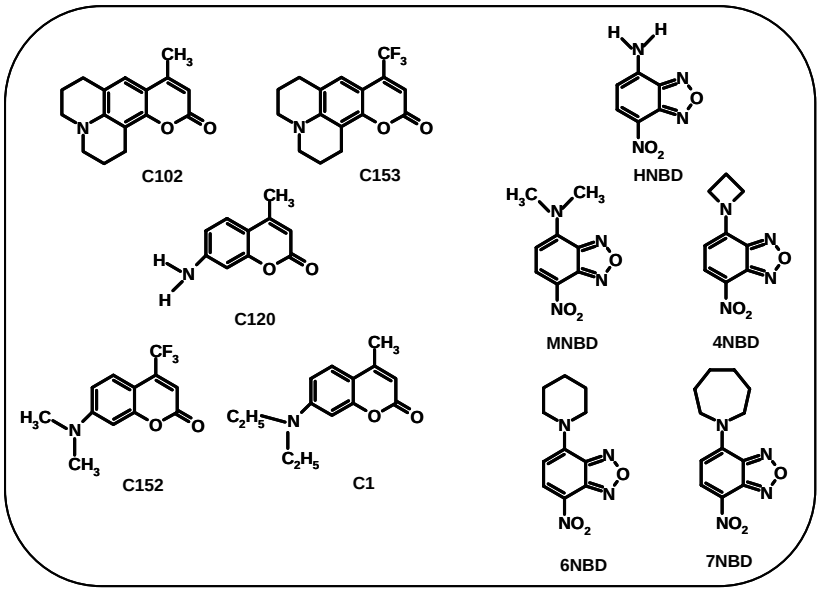

Chart 1.13. Aminocoumarins and 4-amino-7-nitrobenz-oxa-1,3-diazoles (NBD) derivatives used in the study.

References

1. Michel-Beyerle, M. E. In *The Reaction Centre of Photosynthetic Bacteria*; Springer Verlag: Berlin, 1995.
2. Michel-Beyerle, M. E.; Finckh, P.; Heitele, H.; Volk, M. *J. Phys. Chem*. **1988**, *92*, 6584.
3. Wasielewski, M. R. *Chem. Rev*. **1992**, *92*, 435.
4. Gust, D.; Moore, T. A.; Moore, A. L. *Acc. Chem. Res*. **1993**, *26*, 198.
5. Kurreck, H.; Huber, M. *Angew. Chem. Int. Ed. Engl*. **1995**, *34*, 849.
6. Bard, A.; Fox, M. A. *Acc. Chem. Res*. **1995**, *28*, 141.
7. Memming, R. In *Photochemical Conversion and Storage of Solar Energy*; Pelizetti, E., Schiavello, M., Ed.; Kluwer: Holland, 1991.
8. Meyer, T. J. *Acc. Chem. Res*. **1989**, *22*, 163.
9. Diner, B. A.; Babcock, G. T. In *Structure, Dynamics and Energy Conversion Efficiency in Photosystem II*; Diner, B. A., Babcock, G. T., Ed.; Kluwer: Dordrecht, 1996.
10. Fabbrizzi, L.; Poggi, A. *Chem. Soc. Rev*. **1995**, *24*, 197.
11. Shelton, D. B.; Rice, J. E. *Chem. Rev*. **1994**, *94*, 3.
12. Carter, F. L.; Siatoski, R. E.; Woltjen, H. In *Molecular Electronic Devices*; North-Holland: Amsterdam, 1988.
13. Barbara, P. F.; Jarzeba, W. *Acc. Chem. Res*. **1988**, *21*, 195.
14. Mulliken, R. S. *J. Am. Chem. Soc*. **1950**, *72*, 600.
15. Mulliken, R. S. *J. Phys. Chem*. **1952**, *56*, 801.
16. Birks, J. B. In *Photophysics of Aromatic Molecules*; Wiley-Interscience: New York, 1970.
17. Jordan, K. D.; Paddon-Row, M. N. *Chem. Rev*. **1992**, *92*, 395.
18. Verhoeven, J. W.; Scherer, T.; Willemse, R. *J. Pure Appl. Chem*. **1993**, *65*, 1717.
19. Fox, M. A.; Galoppini, E. *J. Am. Chem. Soc*. **1997**, *119*, 5277.
20. Yazdi, P.; McFann, G. J.; Fox, M. A.; Johnston, K. P. *J. Phys. Chem*. **1990**, *94*, 7224.
21. Zhang, J.; Bright, F. V. *J. Phys. Chem*. **1992**, *96*, 5633.
22. (a) Saroja, G.; Soujanya, T.; Ramachandram, B.; Samanta, A. *J. Fluores*. **1998**, *8*, 405. (b) Saroja, G.; Ramachandram, B.; Saha, S.; Samanta, A. *J. Phys. Chem. B* **1999**, *103*, 2906. (c) Soujanya, T.; Krishma, T. S. R.; Samanta, A. *J. Phys. Chem*. **1992**, *96*, 8544.
23. Slavik, J. *Biochem. Biophys. Acta* **1982**, *1*, 694.
24. Narang, V.; Zhav, C. F.; Bhawalkar, J. D.; Bright, F. V.; Prasad, P. N. *J. Phys. Chem*. **1996**, *100*, 4521.
25. Jortner, J.; Levine, R. D. *Adv. Chem. Phys*. **1981**, *47*, 1.
26. Fletcher, A. N. *Appl. Phys*. **1983**, *B31*, 19.
27. Kosower, E. M. *Acc. Chem. Res*. **1982**, *15*, 259.
28. Gorner, H.; Schulte-Frohlinde, D. *J. Mol. Struct*. **1982**, *84*, 227.
29. Baretz, B. H.; Singh, A. K.; Liu, R. S. H. *Nouv. J. Chim*. **1981**, *5*, 297.
30. Keery, K. M.; Fleming, G. R. *Chem. Phys. Lett*. **1982**, *93*, 322.
31. Salem, L. *Science* **1976**, *191*, 822.
32. Allen, N. S.; Bentley, P.; McKellar, J. F. *J. Photochem*. **1976**, *5*, 225.
33. O'Brien, D. F.; Kelly, T. M.; Costa, L. F. *Photogr. Sci. Eng*. **1974**, *18*, 76.
34. Carter, F. L. In *Optical Information Processing Fundamentals*; Lee, S. H., Ed.; Springer-Verlag: New York, 1981.

35. Drexhage, K. H. In *Dye Laser*; Schäfer, F. P., Ed.; Springer: Berlin, 1977.
36. Kubin, R. F.; Fletcher, A. N. *J. Lumin*. **1982**, *27*, 455.
37. Vogel, M.; Rettig, W.; Sens, R.; Drexhage, K. H. *Chem. Phys. Lett*. **1988**, *147*, 461.
38. Vogel, M.; Rettig, W.; Sens, R.; Drexhage, K. H. *Chem. Phys. Lett*. **1988**, *148*, 452.
39. Arbeloa, F. L.; Aguirresacona, U. I.; Arbeloa, I. L. *Chem. Phys*. **1989**, *130*, 371.
40. Arbeloa, F. L.; Arbeloa, T. L.; Arbeloa, I. L.; De Schryver, F. C. *J. Photochem. Photobiol. A: Chem*. **1991**, *56*, 313.
41. Onganer, Y.; Quitevis, E. L. *J. Phys. Chem*. **1992**, *96*, 7996.
42. Jones II, G.; Jackson, W. R.; Kanoktanaporn, S.; Halpern, A. M. *Opt. Commun*. **1980**, *33*, 315.
43. Jones II, G.; Jackson, W. R.; Choi, C.-Y.; Bergmark, W. R. *J. Phys. Chem*. **1985**, *89*, 294.
44. Jones II, G.; Jackson, W. R.; Halpern, A. M. *Chem. Phys. Lett*. **1980**, *72*, 391.
45. de Melo, J. S.; Becker, R. S.; Elisei, F.; Macanita, A. L. *J. Chem. Phys.* **1997**, *107*, 6062.
46. de Melo, J. S.; Becker, R. S.; Macanita, A. L. *J. Phys. Chem*. **1994**, *98*, 6054.
47. Cornelissen-Gude, C.; Rettig, W.; Lapouyade, R. *J. Phys. Chem. A* **1997**, *101*, 9673.
48. Gude, C.; Rettig, W. *J. Phys. Chem. A* **2000**, *104*, 8050.
49. Velsko, S. P.; Fleming, G. R. *Chem. Phys*. **1982**, *65*, 59.
50. Saha, S.; Samanta, A. *J. Phys. Chem. A* **1998**, *102*, 7903.
51. Saha, S.; Samanta, A. *J. Phys. Chem. A* **2002**, *106*, 4763.
52. Sarkar, M.; Kanaparthi, R. K.; Bhattacharya, B.; Samanta, A. *J. Phys. Chem. A* **2008**, *112*, 3302.
53. Klopffer, W. *Adv. Photochem*. **1977**, *10*, 311.
54. Huppert, D.; Gutman, M.; Kaufmann, M. *J. Adv. Chem. Phys*. **1981**, *47*, 643.
55. Kasha, M. *J. Chem. Soc., Faraday Trans. 2* **1986**, *82*, 2379.
56. Barbara, P. F.; Walsh, P. K.; Brus, L. E.; *J. Phys. Chem*. **1989**, *93*, 29.
57. Special Isssue (*Spectroscopy and Dynamics of Elementary Proton Transfer in Polyatomic Systems*, Barbara, P. F., Trommsdorff, H. D., Eds.) *Chem. Phys*. **1989**, *136*, 153.
58. Special Isssue (M. Kasha Festschirift) *J. Phys. Chem*. **1991**, *95*, 10220.
59. Chou, P. T. *J. Chin. Chem. Soc*. **2001**, *48*, 651.
60. Scheiner, S. *J. Phys. Chem. A* **2000**, *104*, 5898.
61. Arnaut, L. G.; Formosinho, S. J. *J. Photochem. Photobiol. A: Chem*. **1993**, *75*, 1.
62. Douhal, A.; Lahmani, F.; Zewail, A. *Chem. Phys*. **1996**, *207*, 477.
63. Aquino, A. J. A.; Lischka, H.; Christof, H. *J. Phys. Chem. A* **2005**, *109*, 3201.
64. Agmon, N. *J. Phys. Chem. A* **2005**, *109*, 13.
65. Shida, N.; Almlof, J. Barbara, P. F. *J. Phys. Chem*. **1991**, *95*, 10457.
66. Kwon, O-H.; Lee, Y-S.; Yoo, B. K.; Jang, D-J. *Angew. Chem. Int. Ed*. **2006**, *45*, 415.
67. Chou, P. T.; McMorrow, D.; Aartsma, T. J.; Kasha, M. *J. Phys. Chem*. **1984**, *88*, 4596.
68. Nishiya, T.; Yamauchi, S.; Hirota, N.; Baba, M.; Hanazaki, I. *J. Phys. Chem*. **1986**, *90*, 5730.
69. Nagaoka, S.; Fujita, M.; Takemura, T.; Baba, M. *Chem. Phys. Lett*. **1986**, *123*, 489.
70. Ernsting, N. P.; Nikolaus, B. *Appl. Phys. B* **1986**, *39*, 155.
71. Kasha, M. In *Molecular Electronic Devices*; Elsevier Science: New York, 1988.

72. Ferrer, M. L.; Acuna, A. U.; Amat-Guerri, F.; Costela, A.; Figuera, J. M.; Florido, F.; Sastre, R. *Appl. Oct*. **1994**, *33*, 2266.
73. Jones, G.; Rahman, M. A. *J. Phys. Chem*. **1994**, *98*, 13028.
74. Liphardt, M.; Gooneskera, A.; Jones, B. E.; Ducharme, S.; Takacs, J. M.; Zhang, L. *Science* **1994**, *263*, 367.
75. Douhal, A.; Sastre, R. *Chem. Phys. Lett*. **1994**, *219*, 91.
76. Kuldova, K.; Corval, A.; Lehn, J. M.; Trommsdorff, H. P. *J. Phys. Chem. A* **1997**, *101*, 6850.
77. Chou, P. T.; Studer, S. L.; Martinez, M. L. *Appl. Spectr*. **1991**, *45*, 513.
78. Renschler, C. L.; Harrah, L. A. In *Nucl. Inst. Methods Phys. Res*. U. S., 1985, Vol. A235.
79. Williams, D. L.; Heller, A. *J. Phys. Chem*. **1970**, *74*, 4473.
80. Heller, H. J.; Blattman, H. R. *Pure Appl. Chem*. **1973**, *36*, 141.
81. Roshal, A. D.; Grigorovich, A. V.; Doroshenko, A. O.; Pivovarenko, V. G.; Demchenko, A. P. *J. Phys. Chem. A* **1998**, *102*, 5907.
82. Tarkka, R. M.; Zhang, X.; Jenekhe, S. A. *J. Am. Chem. Soc*. **1996**, *118*, 9438.
83. Weller, A. Z. *Elektrochem*. **1956**, *60*, 1144.
84. Smith, K. K.; Kauffman, K. J. *J. Phys. Chem*. **1978**, *82*, 2286.
85. Helmbrook, L.; Kenny, J. E.; Kohler, B. E.; Scott, G. W. *J. Phys. Chem*. **1983**, *87*, 280.
86. Lamola, A. A.; Sharp, L. J. *J. Phys. Chem*. **1966**, *70*, 2634.
87. Barbara, P. F.; Rentzepis, P. M.; Brus, L. E. *J. Am. Chem. Soc*. **1980**, *102*, 2786.
88. Sengupta, P. K.; Kasha, M. *Chem. Phys. Lett*. **1979**, *68*, 382.
89. Woolfe, G. J.; Thistlethwaite, P. J. *J. Am. Chem. Soc*. **1980**, *102*, 6917.
90. Sinha, H.; Dogra, S. K. *Chem. Phys.* **1986**, 337.
91. Das, K.; Sarkar, N.; Ghosh, A. K.; Majumdar, D.; Nath, D. N.; Bhattacharyya, K. *J. Phys. Chem*. **1994**, *98*, 9126.
92. Mosquera, M.; Penedo, J. C.; Rodriguez, M. C. R.; Prieto, F. R. *J. Phys. Chem*. **1996**, *100*, 5398.
93. Woolfe, G. J.; Melzig, M.; Schneider, S.; Dorr, F. *Chem. Phys. Lett*. **1983**, *77*, 213.
94. Itoh, H.; Fujiwara, Y. *J. Am. Chem. Soc*. **1985**, *107*, 1561.
95. Barbara, P. F.; Brus, L. E.; Rentzepis, P. M. *J. Am. Chem. Soc*. **1980**, *102*, 5631.
96. Potter, C. A. S.; Brown, R. G.; *Chem. Phys. Lett*. **1988**, *153*, 7.
97. Taylor, C. A.; El-Bayoumi, M. A.; Kasha, M. *Proc. Natl. Acad. Sci. USA* **1969**, *63*, 253.
98. Ingham, K. C.; Abu-Elgheit, M.; El-Bayoumi, M. A. *J. Am. Chem. Soc*. **1971**, *93*, 5023.
99. Hetherington, W. H.; Micheels, R. H.; Eisenthal, K. B. *Chem. Phys. Lett*. **1979**, *66*, 230.
100. Tang, G. Q.; Macinnis, J.; Kasha, M. *J. Am. Chem. Soc*. **1987**, *109*, 2531.
101. Song, P. S.; Sun, M.; Koziolawa, A.; Koziol, J. *J. Am. Chem. Soc*. **1974**, *96*, 4319.
102. Choi, J. D.; Fugate, R. D.; Song, P. S. *J. Am. Chem. Soc*. **1980**, *102*, 5293.
103. (a) Mason, S. F.; Philip, J.; Smith, B. E. *J. Chem. Soc*. **1968**, 3051. (b) Thistlethwaite, P. J.; Corkill, P. J. *Chem. Phys. Lett*. **1982**, *85*, 317. (c) Itoh, M.; Adachi, T.; Tokumara, K. *J. Am. Chem. Soc*. **1983**, *105*, 4828. (d) Nakagawa, T.; Kohtani, S.; Itoh, M. *J. Am. Chem. Soc*. **1995**, *117*, 7952. (e) Ochoa-G.; Bisht, P. B.; Sanchez, F.; Martinez-Ataz, E.; Santos, L.; Tripathi, H. B.; Douhal, A. *J. Phys. Chem. A* **1998**, *102*, 8871.
104. Schipfer, R.; Wolfbeis, O. S.; Knierzinger, A. *J. Chem. Soc., Perkins Trans. 2* **1981**, 1443.

105. Itoh, M.; Yoshida, N.; Takashima, M. *J. Am. Chem. Soc*. **1985**, *107*, 4819.
106. Kavarnos, G. J.; Turro N. J. *Chem. Rev.* **1986**, *86*, 401.
107. Marcus, R. A.; Sutin, N. *Biochim. Biophys. Acta* **1985**, *811*, 265.
108. (a) Julliard, M.; Chanon, M. *Chem. Rev.* **1983**, *83*, 425. (b) Whitten, D. G. *Acc. Chem. Res.* **1980**, *84*, 981. (c) Balzani, V.; Scandola, F. In *Photochemical Conversion and Storage of Solar Energy*; Connolly, J. S., Ed.; Academic: New York, 1981; Chapter 4.
109. *The Exciplex*; Gordon, M., Ware, W. R., Eds.; Academic Press: New York, 1974.
110. (a) Mataga, N. *Pure & Appl. Chem.* **1984**, *56*, 1255. (b) Weller, A. *Pure & Appl. Chem.* **1984**, *56*, 1255.
111. (a) Rehm, D.; Weller, A. *Ber. Bunsen-Ges. Phys. Chem.* **1969**, *73*, 834. (b) Knibbe, H.; Rehm, D.; Weller, A. *Ber. Bunsen-Ges. Phys. Chem.* **1968**, *72*, 257.
112. Rehm, D.; Weller, A. *Isr. J. Chem.* **1970**, *8*, 259.
113. (a) Beecroft, R. A.; Davidson, R. S.; Goodwin, D.; Pratt, J. E. *Pure. Appl. Chem*. **1982**, *54*, 1605. (b) Beecroft, R. A.; Davidson, R. S.; Whelan, T. D. *Chem. Commun*. **1978**, 911.
114. de Silva, A. P.; Gunaratne, H. Q. N.; Gunnlaugsson, T.; Huxley, A. J. M.; McCoy, C. P.; Rademacher, J. T.; Rice, T. E. *Chem. Rev.* **1997**, *97*, 1515.
115. Bissel, R. A.; de Silva, A. P.; Gunaratne, H. Q. N.; Lynch, P. L. M.; Maguire, G. E. M.; McCoy, C. P.; Sandanayake, K. R. A. S. *Top. Curr. Chem.* **1993**, *168*, 223.
116. (a) Hinto, T.; Akazawa, H.; Mashuhara, H.; Mataga N. *J. Phys. Chem.* **1976**, *80*, 33. (b) Hirata, Y.; Kanda Y.; Mataga, N. *J. Phys. Chem.* **1983**, *87*, 1659. (c) Mataga, N; Okada, T.; Kanda, Y.; Shioyama, H. *Tetrahedron* **1986**, *42*, 6143.
117. (a) Schaap, A. P.; Zaklika, K. A.; Kaskar, B.; Fung, L. V.-M. *J. Am. Chem. Soc.* **1980**, *102*, 389. (b) Sostero, S.; Traverso, O.; Bernardo, F. D.; Kemp, T. J. *J. Chem. Soc., Dalton Trans.* **1979**, 659. (c) Janzen, E. G. In *Creation and Detection of the Excited State*; Ware, W. R., Ed; Marcel Dekker, Inc.: New York, 1976; Chapter 3.
118. (a) Glarum, S. H. In *Chemically Induced Magnetic Polarization*; Lepley, A. R., Closs, G. L., Eds.; Wiley-Interscience: New York, 1973; Chapter 1. (b) Roth, H. D.; Schilling, M. L. M. *J. Am. Chem. Soc.* **1980**, *102*, 4303. (c) Closs, G. L.; Czeropski, M. S. *J. Am. Chem. Soc.* **1977**, *99*, 6126.
119. (a) Jarnigan, R. C. *Acc. Chem. Res.* **1971**, *4*, 420. (b) Taniguchi, Y.; Nishina, Y.; Mataga, N. *Bull. Chem. Soc. Jpn.* **1972**, *45*, 764.
120. (a) Gassman, P. G.; Olson, K. D. *J. Am. Chem. Soc.* **1982**, *104*, 3740. (b) Maioulis, A. J.; Shigemitsu, Y.; Arnold, D. R. *J. Am. Chem. Soc.* **1978**, *100*, 535.
121. Nelson, W. M. In *Green Chemistry*; Anastas, P. T., Williamson, T. C., Eds.; Oxford University Press: Oxford, 1998.
122. Tanaka, K.; Toda, F. *Chem. Rev*. **2000**, *100*, 1025.
123. Hang, C. T.; Lianhai, L.; Yang, Y.; Wenshuo, L. Developing green chemistry: Organometallic reactions in aqueous media. In *Clean Solvents: Alternative Media for Chemical Reactions and Processing*; Abraham, M., Moens, L., Eds.; ACS Symposium Series 819; American Chemical Society: Washington, DC, 2002; p 166.
124. Kajimoto, O. *Chem. Rev.* **1999**, *99*, 355.
125. (a) Seddon, K. R. *Nature (Materials)* **2003**, *2*, 363. (b) Rogers, R. D.; Seddon, K. R. *Science* **2003**, *302*, 792.

126. Wasserscheid, P.; Keim, W. *Angew. Chem., Int. Ed.* **2000**, *39*, 3772.
127. Seddon, K. R.; Stark, A.; Torres, M. J. *Pure Appl. Chem.* **2000**, *72*, 2275.
128. Walden, P. *Bull. Acad. Imper. Sci. (St. Petersberg)* **1914**, 1800.
129. (a) Wilkes, J. S.; Levinsky, J. A.; Wilson, R. A.; Hussey, C. L. *Inorg. Chem*. **1982**, *21*, 1263. (b) Boon, J. A.; Levinsky, J. A.; Pflug, J. L.; Wilkes, J. S. *J. Org. Chem*. **1986**, *51*, 480.
130. Sheldon, R. *Chem. Commun.* **2001**, 2399.
131. Wilkes, J. S.; Zaworotko, M. J. *Chem. Commun*. **1992**, 965.
132. Welton, T. *Chem. Rev.* **1999**, *99*, 2071.
133. (a) MacFarlane, D. R.; Meakin, P.; Sun, J.; Amini, N.; Forsyth, M. *J. Phys. Chem. B* **1999**, *103*, 4164. (b) Henderson, W. A.; Passerini, S. *Chem. Mater.* **2004**, *16*, 2881.
134. (a) Tao, G.; He, L.; Sun, N.; Kou, Y. *Chem. Commun.* **2005**, 3562. (b) Fukumoto, K.; Yoshizawa, M.; Ohno, H. *J. Am. Chem. Soc.* **2005**, *127*, 2398. (c) Ohno, H.; Fukumoto, K. *Acc. Chem. Res.* **2007,** *40,* 1122.
135. Holbrey, J. D.; Reichert, W. M.; Swatloski, R. P.; Broker, G. A.; Pitner, W. R.; Seddon, K. R.; Rogers, R. D. *Green Chem.* **2002**, *4*, 407.
136. (a) McFarlane, D. R.; Golding, J.; Forsyth, S.; Forsyth, M.; Deacon, G. B. *Chem. Commun.* **2001**, 1430. (b) McFarlane, D. R.; Forsyth, S. A.; Golding, J.; Deacon, G. B. *Green Chem.* **2002**, *4*, 444.
137. Buzzeo, M. C.; Evans, R. G.; Compton, R. G. *Chem. Phys. Chem.* **2004**, *5*, 1106.
138. Freemantle, M. *Chem. Eng. News* **1998**, *76*, 32.
139. Chiappe, C; Pieraccini, D. *J. Phys. Org. Chem.* **2005**, *18*, 275.
140. (a) Huddleston, J. G.; Visser, A. E.; Reichert, W. M.; Willauer, H. D.; Broker G. A.; Rogers, R. D. *Green Chem.* **2001**, *3*, 156. (b) Dzyuba, S.; Bartsch, R. A. *Chem. Phys. Chem.* **2002**, *3*, 161. (c) Carda-Broch, S.; Berthold, A.; Armstrong, D. W. *Anal. Bioanal. Chem.* **2003**, *375*, 191.
141. Carmichael, A. J.; Seddon, K. R. *J. Phys. Org. Chem.* **2000**, *13*, 591.
142. Aki, S. N. V. K.; Brennecke, J. F.; Samanta, A. *Chem. Commun.* **2001**, 413.
143. Muldoon, M. J.; Gordon, C. M.; Dunkin, I. R. *J. Chem. Soc., Perkin Trans. 2* **2001**, 433.
144. Reichardt, C. *Green Chemistry* **2005**, *7*, 339.
145. Crowhurst, L.; Mawdsley, P. R.; Perez-Arlandis, J. M.; Salter, P. A.; Welton, T. *Phys. Chem. Chem. Phys.* **2003**, *5*, 2790.
146. Anderson, J. L.; Ding, J.; Welton, T.; Armstrong, D. W. *J. Am. Chem. Soc.* **2002**, *124*, 14247.
147. (a) Wakai, C.; Oleinikova, A.; Ott, M.; Weingartner, H. *J. Phys. Chem. B* **2005**, *109*, 17028. (b) Daguenet, C.; Dyson, P. J.; Krossing, I.; Oleinikova, A.; Slattery, J.; Wakai, C.; Weingartner, H. *J. Phys. Chem. B* **2006**, *110*, 12682.
148. Widegren, J. A.; Laesecke, A.; Magee, J. W. *Chem. Commun.* **2005**, 1610.
149. Seddon, K. R.; Stark, A.; Torres, M. J. In *Clean Solvents: Alternative Media for Chemical Reactions and Processing*; Abraham, M., Moens, L., Eds.; ACS Symposium Series 819; American Chemical Society: Washington, DC, 2002; p 34.
150. Xu, W.; Wang, L.-M.; Nieman, R. A.; Angell C. A. *J. Phys. Chem. B* **2003**, *107*, 11749.

151. (a) Holbrey, J. D.; Turner, M. B.; Reichert, W. M.; Rogers, R. D. *Green Chem.* **2003**, *5*, 731. (b) Branco, L. C.; Rosa, J. N.; Ramos, J. J. M.; Afonso, C. A. M. *Chem. Eur. J.* **2002**, *8*, 3671.
152. Pringle, J. M.; Golding, J.; Baranyai, K.; Forsyth, C. M.; Deacon, G. B.; Scott, J. L.; MacFarlane, D. R. *New J. Chem.* **2003**, *27*, 1504.
153. Every, H. A.; Bisop, A. G.; MacFarlane, D. R.; Oradd, G.; Forsyth, M. *Phys. Chem. Chem. Phys.* **2004**, *6*, 1758.
154. Ngo, H. L.; LeCompte, K.; Hargens, L.; McEwen, A. B. *Thermochim. Acta* **2000**, *357*, 97.
155. (a) Earle, M. J.; Esperanca, J. M. S. S.; Gilea, M. A.; Lopes, J. N. C.; Rebelo, L. P. N.; Magee, J. W.; Seddon, K. R.; Widegren, J. A. *Nature* **2006**, *439*, 831. (b) Armstrong, J. P.; Hurst, C.; Jones, R. G.; Licence, P.; Lovelock, K. R. J.; Satterley, J.; Villar-Garcia, I. J. *Chem. Phys. Chem.* **2007**, *9*, 982.
156. Choudhury, A. R.; Winterton, N.; Steiner, A.; Cooper, A. I.; Johnson, K. A. *J. Am. Chem. Soc.* **2005**, *127*, 16792.
157. (a) Kölle, P.; Dronskowski, R. *Inorg. Chem.* **2004**, *43*, 2803. (b) van de Broeke, J.; Stam, M.; Lutz, M.; Kooijman, H.; Spek, A. L.; Deelman, B.-J.; van Koten, G. *Eur. J. Inorg. Chem.* **2003**, *26*, 2798. (c) Gordon, G. M.; Holbrey, D. M.; Kennedy, A. R.; Seddon, K. R. *J. Mater. Chem.* **1998**, *8*, 2627.
158. Suarez, P. A. Z.; Dullius, J. E. L.; de Souza, R. F.; Dupont, J. *J. Chim. Phys. Phys.-Chim. Biol.* **1998**, *95*, 1626.
159. Mele, A.; Tran, C. D.; De Paoli Lacerda, S. H. *Angew. Chem. Int. Ed.* **2003**, *42*, 4364.
160. Bonhote, P.; Dias, A. P.; Papageorgiou, N.; Kalyanasundaram, K.; Gratzel, M. *Inorg. Chem.* **1996**, *35*, 1168.
161. Avent, A. G.; Charloner, P. A.; Day, M. P.; Seddon K. R.; Welton, T. *J. Chem. Soc., Dalton Trans.* **1994**, *23*, 3405.
162. Mele, A.; Romano, G.; Giannone, M.; Ragg, E.; Fronza, G.; Raos, G.; Marcon, V. *Angew. Chem. Int. Ed.* **2006**, *45*, 1123.
163. (a) Wang, Y.; Voth, G. A. *J. Am. Chem. Soc.* **2005**, *127*, 12192. (b) Lopes, J. N. C.; Padua, A. A. H. *J. Phys. Chem. B* **2006**, *110*, 3330. (c) Jiang, W.; Wang, Y.; Voth, G. A. *J. Phys. Chem. B* **2007**, *111*, 4812.
164. Wang, Y.; Jiang, W.; Yan, T.; Voth, G. A. *Acc. Chem. Res.* **2007**, *40*, 1193.
165. Mandal, P. K.; Sarkar, M.; Samanta, A. *J. Phys. Chem. A* **2004**, *108*, 9048.
166. Funston, A. M.; Fadeeva, T. A.; Wishart, J. F.; Castner, E. W., Jr. *J. Phys. Chem. B* **2007**, *111*, 4963.
167. (a) Triolo, A.; Russina, O.; Bleif, H.-J.; Di Cola, E. *J. Phys. Chem. B* **2007**, *111*, 4641. (b) Moutiers, B. G.; Labet, A.; Azzi A. E.; Gaillard, C.; Mariet, C.; Lutzenkirchen, K. *Inorg. Chem.* **2003**, *42*, 1726. (c) Carmichael, A. J.; Hardacre, C.; Holbrey, J. D. *Mol. Phys.* **2001**, *99*, 795.
168. (a) Hayashi, S.; Ozawa, R.; Hamaguchi, H. *Chem. Lett.* **2003**, *32*, 498. (b) Ozawa, R.; Hayashi, S.; Saha, S.; Kobyashi, A.; Hamaguchi, H. *Chem. Lett.* **2003**, *32*, 948. (c) Iwata, K.; Okazima, H.; Saha, S.; Hamaguchi, H. *Acc. Chem. Res.* **2007,** *40,* 1174.
169. Hardacre, C.; Holbrey, J. D.; McMath, S. E. J.; Bowron, D. T.; Soper, A. K. *J. Chem. Phys.* **2003**, *118*, 273.

170. Carmichael, A. J.; Hardacre, C.; Holbrey, J. D.; Nieuwenhuyzen, M.; Seddon, K. R. *Anal. Chem.* **1999**, *71*, 4572.
171. (a) Xiao, D.; Rajian, J. R.; Li, S.; Bartsch, R. A.; Quitevis, E. L. *J. Phys. Chem. B* **2006**, *110*, 16174. (b) Xiao, D.; Rajian, J. R.; Cady, A.; Li, S.; Bartsch, R. A.; Quitevis, E. L. *J. Phys. Chem. B* **2007**, *111*, 4669.
172. Dupont, J.; Suarez, P. A. Z.; de Suza, R. F.; Burrow, R. A.; Kintzinger, J. *Chem. Eur. J.* **2000**, *6*, 2377.
173. (a) Hu, Z.; Margulis, C. J. *Proc. Natl. Acad. Sci.* **2006**, *103*, 831. (b) Hu, Z.; Margulis, C. J. *J. Phys. Chem. B* **2006**, *110*, 11025. (c) Hu, Z.; Margulis, C. J. *Acc. Chem. Res.* **2007**, *40*, 1097.
174. (a) Popolo, M.; Kohanoff, J.; Lynden-Bell, R. M.; Pinilla, C. *Acc. Chem. Res.* **2007**, 40, 1156. (b) Padua, A. A. H.; Costa Gomes, M. F.; Lopes, J. N. C. *Acc. Chem. Res.* **2007**, *40*, 1087.
175. (a) Hardacre, C.; Holbrey, J. D.; Nieuwenhuyzen, M.; Youngs, T. G. A. *Acc. Chem. Res.* **2007**, *40*, 1144. (b) Castner, E. W., Jr.; Wishert, J. F.; Shirota, H. *Acc. Chem. Res.* **2007**, *40*, 1144.
176. Dupont, J.; de Souza, R. F.; Suarez, P. A. Z. *Chem. Re*v. **2002**, *102*, 3667.
177. *Ionic Liquids in Synthesis*; Welton, T., Wasserscheid, P., Eds.; VCH-Wiley: Weinheim, Germany, 2002.
178. *Ionic Liquids, Industrial Applications for Green Chemistry*; Rodgers, R., Seddon, K. R., Eds.; ACS Symposium Series 818; American Chemical Society: Washington, DC, 2002.
179. (a) Abedin, S. Z. E.; Endres, F. *Acc. Chem. Res.* **2007**, *40*, 1106. (b) MacFarlane, D. R.; Forsyth, M.; Howlett, P. C.; Pringle, J. M.; Sun, J.; Annat, G.; Neil, W.; Izgorodina, E. I. *Acc. Chem. Res.* **2007**, *40*, 1165.
180. (a) Huddleston, J. G.; Willauer, H. D.; Swatlowski, R. P.; Visser, A. E.; Rodgers, R. D. *Chem. Commun.* **1998**, 1765. (b) Dai, S.; Ju, Y. H.; Barnes, C. E. *J. Chem. Soc., Dalton Trans.* **1999**, 63.
181. (a) Itoh, H.; Naka, K.; Chujo, Y. *J. Am. Chem. Soc.* **2004**, *126*, 3026. (b) Wei, G.-T.; Yang, Z.; Lee, C.-Y.; Yang, H.-Y.; Wang, C. R. C. *J. Am. Chem. Soc.* **2004**, *126*, 5036. (c) Tatumi, R.; Fujihara, H. *Chem. Commun.* **2005**, 83.
182. (a) Yu, B.; Zhou, F.; Liu, G.; Liang, Y.; Huck, W. T. S.; Liu, W. *Chem. Commun.* **2006**, 2356. (b) Wang, Y.; Yang, H. *Chem. Commun.* **2006**, 2545. (c) Zhao, D.; Fei, Z.; Ang, W. H.; Dyson, P. J. *Small* **2006**, *7*, 879. (d) Green, M.; Rahmana, P.; Smyth-Boyle, D. *Chem. Commun.* **2007**, 574.
183. Borra, E. F.; Seddiki, O.; Angel, R.; Eisenstein, D.; Hickson, P.; Seddon, K. R.; Worden, S. P. *Nature* **2007**, *447*, 979.
184. Armstrong, D. W.; Zhang, L. K.; He, L.; Gross, M. L. *Anal. Chem.* **2001**, *73*, 3679.
185. Park, S.; Kazlauskas, R. J. *Curr. Opin. Biotech.* **2003**, *14*, 432.
186. van Rantwijk, F.; Lau, R.; Sheldon, R. A. *Trends Biotechnol.* **2003**, *21*, 131.
187. (a) Bates, E. D.; Mayton, R. D.; Ntai, I.; Davis, J. H., Jr. *J. Am. Chem. Soc.* **2002**, *124*, 926. (b) Buzzeo, M. C.; Hardacre, C.; Compton, R. G. *Anal. Chem.* **2004**, *76*, 4583.
188. Wang, P.; Zakeeruddin, S. M.; Comte, P.; Exnar, I.; Gratzel, M. *J. Am. Chem. Soc.* **2003**, *125*, 1166.

189. Kimizuka, N.; Nakashima, T. *Langmuir* **2001**, *17*, 6759.
190. For review on this subject, see (a) Davis, J. H. *Chem. Lett.* **2004**, *33*, 1072. (b) Lee, S. *Chem. Commun.* **2006**, 1049.
191. Ref. 190 and references therein.
192. Lehninger, A. L.; Nelson, D. L.; Cox, M. M. In *Principles of Biochemistry*, 2nd Ed.; Worth Publishers, Inc., USA, 1982.
193. Brand, L.; Gohlke, J. R. *Annu. Rev. Biochem*. **1972**, *41*, 843.
194. Edelman, G. M.; McClure, W. O. *Acc. Chem. Res*. **1968**, *3*, 65.
195. Lakowicz, J. R. In *Principles of Fluorescence Spectroscopy*; 2nd Ed.; Kluwer Academic/Plenum Press: New York, 1999.
196. (a) Soujanya, T.; Fessenden, R. W.; Samanta, A. *J. Phys. Chem*. **1996**, *100*, 3507. (b) S. Saha, Ph. D. Thesis. University of Hyderabad, 2002.
197. (a) Ramachandram, B.; Samanta, A. *Chem. Commun*. **1997**, 1037. (b) Ramachandram, B.; Saroja, G.; Sankaran, N. B.; Samanta, A. *J. Phys. Chem. B*. **2000**, *104*, 11824. (c) Ramachandram, B.; Sankaran, N. B.; Karmakar, R.; Saha, S.; Samanta, A. *Tetrahedron*. **2000**, *56*, 7041.
198. (a) Tanner, C.; Manca, C.; Leutwyler, S. *Science* **2003**, *302*, 1736. (b) Rini, M.; Magnes, B.-Z.; Pines, E.; Nibbering, E. T. J. *Science* **2003**, *301*, 349. (c) Gutman, M.; Nachliel, E. *Annu. Rev. Phys. Chem*. **1997**, *48*, 329. (d) Douhal, A.; Kim, S. K.; Zewail, A. H. *Nature* **1995**, *378*, 260. (e) Lill, M. A.; Helms, V. *Proc. Natl. Acad. Sci. USA* **2002**, *99*, 2778.
199. Bhattacharyya, K.; Chowdhury, M. *Chem. Rev*. **1993**, *93*, 507.
200. Saha, S.; Samanta, A. *J. Phys. Chem. A* **1998**, *102*, 7903.
201. Stryer, L. *J. Mol. Biol*. **1965**, *13*, 482.

Chapter 2

Materials, Methods and Instrumentation

This chapter lists the materials used in this study followed by the methods of purification of reagents and solvents. Synthesis of the electron donor-acceptor (EDA) molecules used in the studies is briefly described. Synthesis and purification of the RTILs employed in one of the present studies have also been described. The instrumental details, especially the time-correlated single-photon counting technique (TCSPC) based picosecond setup and nanosecond laser flash photolysis setup has been outlined. Various methodologies, like sample preparation for different experiments, measurements of fluorescence quantum yield, triplet-triplet extinction coefficient, triplet quantum yield and analysis of TCSPC data have been discussed. In addition, some introductory information on the protein docking is also provided.

2.1. Materials

4-Aminophthalimide (AP) was obtained from TCI (Japan) and recrystallized twice from ethanol/water mixture prior to photophysical experiments. 1,8-naphthalimide (Aldrich), monosodium salt of 4-chlorophthalic acid (CPA, Acros), hexamethylenimine (Fluka), azetidine (Fluka), 1,8-naphthalic anhydride, N,N-dimethylethylenediamine and N,N dimethylpropylenediamine (Aldrich), 4-chloro-1,8-naphthalic anhydride (Acros), 4-chloro-7-nitrobenzoxadiazole (NBD-chloride, Acros) and sodium azide (Loba Chemicals, India) were used as received for synthesis. 7-HQ was procured from Acros and recrystallized from ethanol prior to use. The coumarin derivatives (laser grade, Exciton), BSA (Sigma) and cetyltrimethylammonium bromide (CTAB, Aldrich) were used as received. Phosphate buffer tablets (pH = 7.0) were obtained from Qualigens. Pyrrolidine and Piperidine (Aldrich), dimethylamine and n-butylamine (Acros) were distilled before use. The purities of all compounds were checked by single spot in thin layer chromatography (TLC), nuclear magnetic resonance spectroscopy (NMR) as well as by matching the absorption and emission spectra with literature.

The various drying agents and chemicals such as phosphorous pentoxide (P_2O_5), sodium metal, magnesium turnings and iodine used at different stages of the purification procedure, were purchased from local companies. Calcium hydride (CaH_2) was obtained from Spectrochem (India). GR grade solvents were obtained from Merck (India) for spectroscopic and synthetic purposes and their purification procedures are outlined in the following section. Deuteriated solvents, chloroform-d, methanol-d_4 and acetone-d_6 used for NMR spectral measurements were obtained either from Aldrich or from Merck (India).

The reagents required for synthesis of the two RTILs were obtained from various sources and carefully purified following standard procedure. The materials like 1-methylimidazole, 1-chlorobutane, were obtained from Acrös. Hexafluorophosphoric acid (65% solution in water) was procured from Lancaster, whereas lithium bis(trifluoromethanesulfonyl)imide ($LiTf_2N$) was obtained from Aldrich and potassium hydroxide (KOH) from local company.

2.2. Purification of conventional solvents and reagents

The solvents used at various stages of the study were purified using the procedures available in the literature.[1] We adopted the following procedures for the purification of various solvents.

1,4-dioxane: The solvent was refluxed over metallic sodium for 3-4 hr and then benzophenone was added after cooling. The dark blue solution was refluxed for another one hour and distilled under dry condition. The purified solvent was optically transparent in the spectral region of interest.

Acetonitrile (ACN): The solvent was stirred with CaH_2 overnight or refluxed with P_2O_5 for 3-4 hr and then distilled. The distilled solvent was collected and stored in desiccator.

Methanol (MeOH): The solvent was refluxed with magnesium turnings and little quantity of iodine for 3-4 hr and distilled over molecular sieves and stored under dry condition.

Ethyl acetate: After stirring with P_2O_5 for some hours, the solvent was distilled out.

Water: MilliQ water (Millipore) was used for the study.

2.3. Synthesis of EDA systems

A brief description of synthesis of 4-aminophthalimide (AP) derivatives used for the work in Chapter 3, 1,8-naphthalimide derivatives studied in Chapter 4 and 4-amino-7-nitrobenz-oxa-1,3-diazole (NBD) derivatives for Chapter 6 is provided in this section.

AP derivatives: AP derivatives bearing 4-, 5- and 6- membered cyclic amino moiety (4P, 5P and 6P, Chapter 1) were prepared following the procedure in literature.[2] The monosodium salt of 4-chlorophthalic acid was treated with HCl and then dry acetic anhydride to obtain the anhydride. The anhydride was treated with n-butylamine to form 4-chloro-N-(n-butyl)phthalimide, which was subsequently treated with the appropriate amine (like azetidine, pyrroline and piperidine) to yield the desired product.

1,8-naphthalimide derivatives: This set of naphthalimide derivatives with and without *fluorophore-spacer-receptor* architecture (I, II, III, IV, V, NP, CNP and MNP, Chapter 1 and Chapter 4) were prepared following the literature procedure.[3] N-Ethyl-1,8-naphthalimide (NP) was obtained from 1,8-naphthalimide on treatment with previously washed sodium hydride followed by ethylbromide in dry DMF at room temperature for 24 hr with constant stirring. N-Butyl-4-chloro-1,8-naphthalimide (CNP) was obtained by refluxing 4-chloro-1,8-naphthalic anhydride with butylbromide for 6 hr. 4-Methoxy-N-butyl-1,8-naphthalimide (MNP) was obtained on treating CNP with sodium methoxide at room temperature for 6 hr. 2-(N,N-Dimethylamino)-1-(1,8-naphthalimido)ethane (I) was obtained on treating 1,8-naphthalic anhydride with N,N-dimethylethylenediamine in presence of ethanol and refluxed for 5 hr. 2-(N,N-Dimethylamino)-1-(4-chloro-1,8-

naphthalimido)ethane (II) was obtained on refluxing 4-chloro-1,8-naphthalic anhydride with N,N-dimethylethylenediamine in ethanol for 6 hr. 3-(N,N-Dimethylamino)-1-(4-chloro-1,8-naphthalimido)propane (III) was obtained on refluxing 4-chloro-1,8-naphthalic anhydride with N,N dimethylpropylenediamine in ethanol for 6 hr. 2-(N,N-Dimethylamino)-1-(4-methoxy-1,8-naphthalimido)ethane (IV) was obtained on refluxing II with sodium methoxide at room temperature for 6 hr. 3-(N,N-Dimethylamino)-1-(4-methoxy-1,8-naphthalimido)ethane (V) was obtained on refluxing III with sodium methoxide at room temperature for 6 hr.

NBD derivatives: This set of aminonitrobenzoxadiazoles (HNBD, MNBD, 4NBD, 6NBD and 7NBD, Chapter 1) were prepared according to the literature procedure.[2,4] 4-amino-7-nitrobenzoxadiazole (HNBD) was obtained on treating NBD-Cl with sodium azide in DMSO for 5-10 min. The precipitate recrystallised was then refluxed in toluene for 30 min. The other derivatives, MNBD, 4NBD, 6NBD and 7NBD were prepared following a general procedure.[2,4] The suitable amine (like dimethylamine, azetidine, piperidine and hexamethylenimine) was added dropwise to NBD-Cl in ethyl acetate in ice-cold condition. After 30 min stirring in ice-bath, the reaction mixture was further stirred for 2 hr at room temperature and red precipitate of the product was obtained.

2.4. Synthesis and purification of RTILs

Methods for the preparation of two imidazolium RTILs used in one of the work have been depicted in Scheme 2.1. A brief description of synthesis of individual RTIL is outlined in the following discussion.

2.4.1. [bmim][PF_6]

[bmim][PF_6] was prepared from its chloride salt, [bmim]Cl, following a standard procedure.[5] The latter was first prepared by treating a mixture of 1-methylimidazole (distilled from KOH under reduced pressure) and 1-chlorobutane (distilled from P_2O_5),

taken in 1:2 mole ratio, at 65 °C for 48-60 hrs under nitrogen.[6] It should be noted that the addition of 1-chlorobutane has to be slow and under cooling condition. The reaction mixture was then cooled down to room temperature and kept overnight in an ice-acetone bath in tightly sealed condition. The white solid salt so obtained was washed several times with dry warm ethyl acetate until the washings were free from unreacted 1-methylimidazole. The halide salt was then rigorously dried under high vacuum before proceeding to the next reaction step.

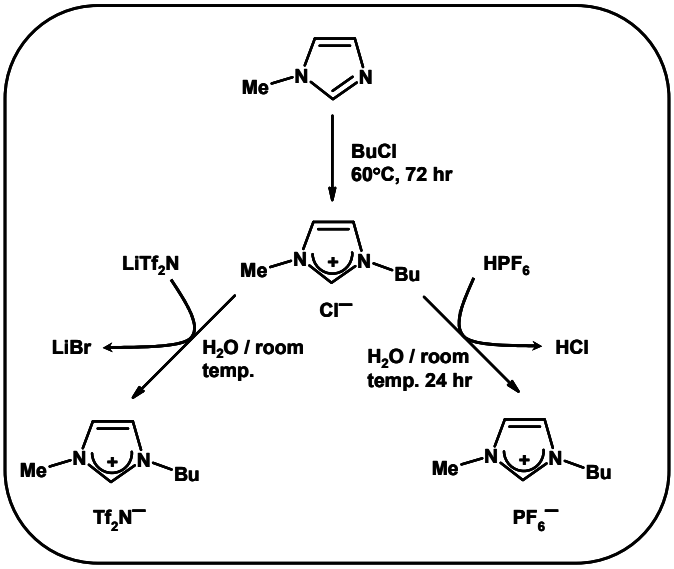

Scheme 2.1. Synthetic steps of the two RTILs employed the present study.

A dilute aqueous solution of [bmim]Cl was prepared in a plastic box and cooled to 0-4°C in an ice bath. To this ice-cold solution was added ice-cooled HPF_6 (65% solution in water), maintaining 1:1.5 molar proportion, dropwise over an hour or so with constant vigorous stirring. This slow addition prevented significant rise of the temperature and avoided rapid exothermic reaction. The reaction mixture was then stirred for 24 hr at room temperature. After decanting the upper acidic layer, the lower viscous ionic liquid

portion was washed with excess water until it was free from acid (checked by a pH paper).

2.4.2. [bmim][Tf_2N]

[bmim][Tf_2N] was prepared from [bmim]Cl in the following way.[7] The chloride salt and $LiTf_2N$ were dissolved in equimolar amount of milliQ water and the mixture was stirred for at least 18 hrs, first in room temperature and then at 50-60°C, but always under nitrogen atmosphere. After cooling the mixture, the viscous lower part (hydrophobic) was separated and washed with water for 4-5 times, until and unless no trace of halide was detected in the wash-liquid by $AgNO_3$ test.

2.4.3. Purification of the RTILs

The purification of RTILs is the most crucial step as these liquids are used as solvents for spectroscopic purposes. Care was taken to ensure that these liquids are free from impurities, particularly those which might contribute to the absorption/fluorescence in the wavelength region of interest. The freshly prepared [bmim][PF_6] and [bmim][Tf_2N] liquids were washed many times with water to remove the unreacted precursors and halides as these RTILs are hydrophobic. The removal of the halide impurities was ensured by the fact that the ionic liquids or the washings did not form any precipitate of silver halide when treated with aqueous $AgNO_3$ solution.

The RTILs were then dried under high vacuum (pressure 10^{-2}-10^{-3} mbar), for at least 10-12 hrs to minimize the water content and for the removal of the traces of organic impurities, if any, present in these liquids.[8] In this way effectively dry ionic liquids were obtained. The RTILs thus prepared were characterized by NMR and IR spectroscopic techniques (compared with the literature data)[5-7] and then stored in vacuum desiccator under nitrogen atmosphere wrapped by aluminum foil.

2.5. Instrumentation

The IR and NMR spectra were measured using Jasco FTIR 5300 spectrometer and Bruker AVAnce 400 MHz NMR spectrometer, respectively. Steady-state absorption and fluorescence spectra were recorded on a UV-vis spectrophotometer (Cary100, Varian) and a spectrofluorimeter (FluoroLog-3, Jobin Yvon), respectively. The fluorescence spectra were corrected for the instrumental response. The viscosity of the RTILs and other viscous solvents was measured by a LVDV-III Ultra Brookfield Cone and Plate viscometer (1% accuracy and 0.2% repeatability).

2.5.1. Picosecond time-correlated single-photon counting setup

Time-resolved fluorescence measurements were carried out using a time-correlated single-photon counting (TCSPC) spectrometer (5000, IBH)[9] (Scheme 2.2). Diode lasers were used as excitation sources and a micro-channel plate (MCP) photomultiplier tube was used as the detector. Depending on the system involved, three different excitation sources, nanoLED (331 nm, FWHM = 1 ns), diode laser (374 nm, FWHM = 65 ps) and diode laser (439 nm, FWHM = 90 ps) were employed. The maximum repetition rate of the diode lasers was 1 MHz. A Hamamatsu R3809U-50 MCP-PMT (160-850 nm range) was used as a detector.

The lamp profile was recorded by placing a scatterer (dilute solution of Ludox in water) in place of the sample. Decay curves were analyzed by nonlinear least-squares iteration procedure using IBH DAS6 (Version 2.2) decay analysis software.

The time-resolved anisotropy measurements were performed with the same setup, using two polarizers (300-800 nm) by placing one of them in the excitation beam path and the other in front of the detector. The same software was used to analyze the anisotropy data.

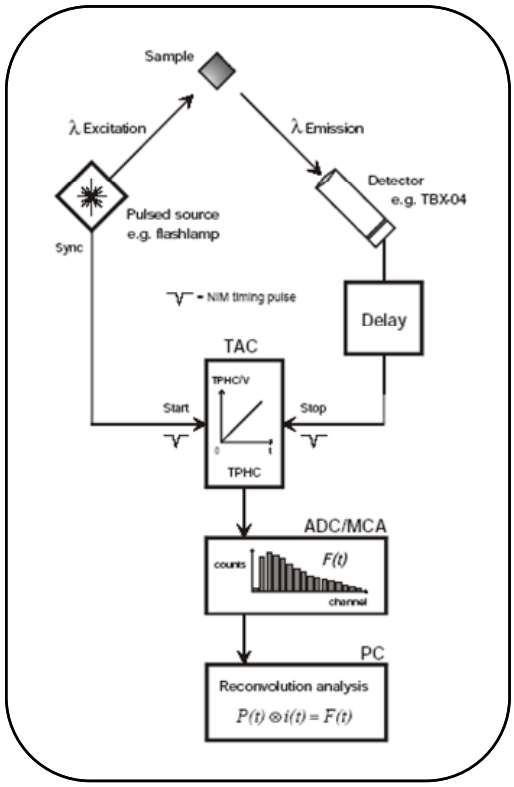

Scheme 2.2. Schematic block diagram for a TCSPC setup (from DataStation Hub User manual, IBH).

2.5.2. Nanosecond laser flash photolysis setup

The transient absorption measurements were performed by a laser flash photolysis (LFP) setup (Scheme 2.3) which was equipped with a laser system (Q-switched Nd:YAG, pulse width ~8 ns) from Spectra Physics (Quanta-Ray INDI series) and a spectrometer from Applied Photophysics (model LKS.60). The spectrometer consisted of a 150 W pulsed xenon lamp, a programmable f/3.4 grating monochromator, a digitized oscilloscope (Agilent, 600 MHz), and an R-928 photomultiplier tube. The solutions were excited by the third harmonic (355 nm) of the laser. A perpendicular configuration was

chosen for the excitation of the sample. Applied Photophysics LKS.60 Kinetic Spectrometer workstation software was used for the collection and analysis of the data.

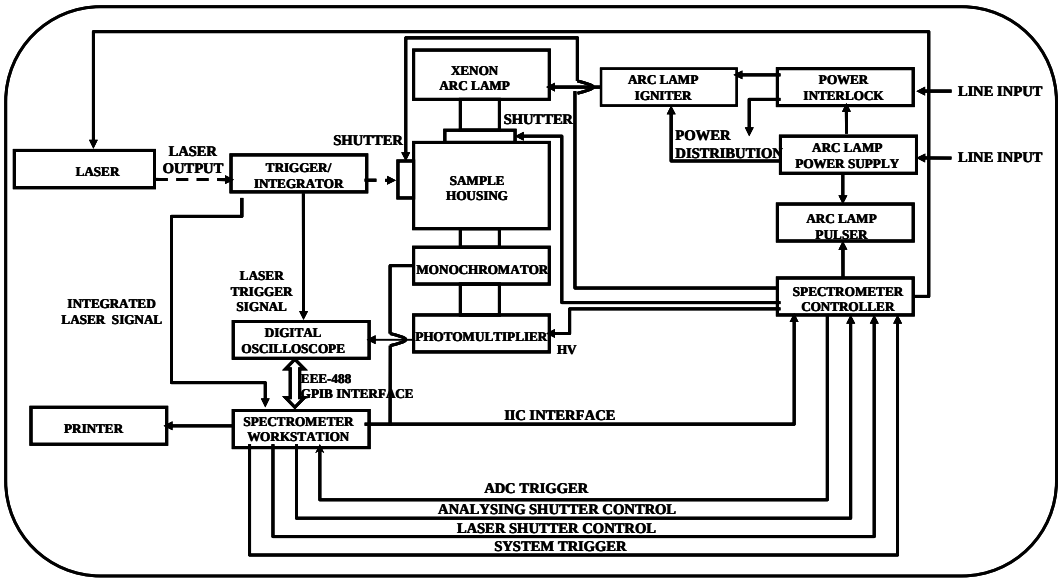

Scheme 2.3. Schematic diagram of the LFP setup (from LKS.60 hardware section of the user handbook of Applied Photophysics).

2.6. Sample preparation for spectral measurements

For measurements in conventional solvents, the solutions were prepared such that the absorbance of the solution (1 cm pathlength) at the excitation wavelength was around 0.1-0.2. The concentration of the probe molecules corresponding to an absorbance value of 0.2 was found to be in the range of 10^{-6}-10^{-4} M.

For laser flash photolysis experiments, quartz cuvettes with pathlength of 0.3 cm were used and the probe concentrations were such that the absorbance was around 0.2-0.5 at the excitation wavelength (355 nm). The solutions were deaerated by purging argon gas into the cuvettes for about 30 minutes prior to the experiments.

In case of experiments in RTILs, the sample preparation was not so straightforward. Prior to the sample preparation, these liquids were dried under high vacuum at 50-60°C for 10-12 hr in order to ensure the removal of the trapped moisture, if any, in RTILs. Generally 2.5 ml of RTIL was used to prepare sample solution in 1 cm quartz cuvette. After addition of sample solute, the cuvettes were tightly sealed with septum and parafilm. Since the dissolution of the solid probes in RTILs is slow, the absorption spectra were measured from time to time to ensure the complete dissolution. The concentration of the solute was optimized to have 0.2-0.3 absorbance at the excitation wavelength.

In dealing with experiments of Chapter 6, solutions of probes and protein were made in phosphate buffer. 1 tablet (pH=7.0) was dissolved in 100 ml milliQ water to obtain buffer solution at pH = 7.0.

2.7. Measurement of photophysical parameters

2.7.1. Fluorescence quantum yield

For fluorescence quantum yield measurements, optically matched solutions (or solutions with very similar absorbances) of the sample and the standard at a given absorbing wavelength (the excitation wavelength) were prepared. The quantum yield was calculated by measuring the integrated area under the emission curves and by using the following equation,[10]

$$\Phi_{sample} = \frac{A_{sample} \times OD_{std} \times n^2_{sample}}{A_{std} \times OD_{sample} \times n^2_{std}} \times \Phi_{std} \qquad (2.1)$$

where, Φ is the quantum yield, A is the integrated area of emission, OD is the optical density at the excitation wavelength, and n is the refractive index. The subscripts ‘sample’ and ‘std’ refer to the fluorophore of unknown quantum yield and the reference fluorophore of known quantum yield, respectively.

2.7.2. Molar extinction coefficient of triplet-triplet absorption

This quantity was determined by energy transfer technique using the triplet of reference molecule as the energy donor. The quenching of the reference molecule was assumed to be entirely dominated by exothermic triplet energy transfer process. Experiments were carried out (355 nm excitation) in acetonitrile (experimental standard solvent) containing both reference and the sample. The end of the pulse absorbance change $(\Delta OD)_0^R$ caused by reference triplet at its triplet-triplet absorption maxima (λ_{max}^T) was compared with the absorbance change $(\Delta OD)_\infty$ of the sample at its corresponding λ_{max}^T. The ε_T value was calculated from the following equation.[11]

$$\varepsilon_T = \frac{\varepsilon_T^R (\Delta OD)_\infty k_{obs}}{(\Delta OD)_0^R (k_{obs} - k_0)} \qquad (2.2)$$

where, ε_T^R is the extinction coefficient of the reference triplet-triplet absorption and k_{obs} and k_0 are the rate constant for the decay of reference triplet in the presence and absence of the sample, respectively.

2.7.3. Triplet quantum yield

The triplet quantum yield (Φ_T) was determined by comparative actinometry method in our studies. The triplet-triplet extinction coefficient values (ε_T) was assumed to be independent on the solvent polarity.[11] The end of pulse absorbance change $(\Delta OD)_0$ due to the triplet of the sample at λ_{max}^T was compared with the absorbance change $(\Delta OD)_0^R$ due to the reference triplet at its λ_{max}^T, the latter being observed in a solution optically matched at the exciting wavelength with that of sample.

$$\Phi_T = \frac{\Phi_T^R (\Delta OD)_0 \varepsilon_T^R}{(\Delta OD)_0^R \varepsilon_T} \qquad (2.3)$$

2.8. Data analysis

A brief outline of analysis of the fluorescence lifetimes and anisotropy profiles are discussed.

2.8.1. Fluorescence lifetime

The lifetimes of the samples were estimated from the measurements of fluorescence decay curves and the instrumental profiles using a nonlinear least-squares iterative fitting procedure (using decay analysis software IBH DAS6, Version 2.2). This program uses a reconvolution method for the analysis of the experimental data.[12] When the decay time is long compared to the pulse width of the excitation pulse, the excitation may be described as a δ-function. However, when the lifetime is short, distortion of the experimental data occurs by the finite decay time of the lamp pulse and response time of the photomultiplier and associated electronics. Since the measured decay function is convolution of the true fluorescence decay and the instrumental pulse, it is necessary to analyze the data by deconvolution in order to get the actual fluorescence lifetime. The mathematical statement of the problem is given by the following equation:

$$D(t) = \int_0^t P(t')G(t-t')dt' \tag{2.4}$$

where, D(t) is the fluorescence intensity at any given time t, P(t') is the intensity of the exciting light at time t' and G(t–t') is the response function of the experimental system. The experimental data D(t) and P(t') from the MCA were fed into a personal computer (PC) to determine the lifetime. We used the IBH program to analyze the multi-exponential decays. An excitation pulse profile was recorded and then deconvolution started with mixing of the excitation pulse and a projected decay to form a new reconvoluted set. The data was compared with the experimental set and the difference between the data points was summed, generating χ^2 function for fitting. The

deconvolution proceeded through a series of such iterations until an insignificant change of χ^2 occurred between iterations. The inspection of reduced χ^2, a plot of weighted residuals and autocorrelation function of the residuals allowed assessment of the quality of the fit.

2.8.2. Fluorescence anisotropy

The anisotropy decay function, r(t) is defined by:[13]

$$r(t) = \frac{I_p(t) - I_x(t)}{I_p(t) + 2I_x(t)} = \frac{I_d(t)}{I_s(t)} \tag{2.5}$$

I represents idealized (undistorted) fluorescence intensity, the subscripts p and x refer to parallel and crossed polarisers while d and s denote difference and sum respectively. I_x and I_p need to be measured under identical conditions for satisfying equation 2.5. Experimentally fluorescence decay data Y(i) is observed not I(t). The static sensitivities of the instrument in the two polarizer orientations may not be the same, and so instrument G-factor was calculated using the DEPOL program.

A key aspect of anisotropy analysis is error analysis, as anisotropy information is extracted as relatively small differences between large numbers. The total fluorescence data $Y_s(i)$ for instance, could be obtained by combining parallel and crossed data as follows:

$$Y_s(i) = GY_p(i) + 2Y_x(i) \tag{2.6}$$

Using the decay curves $Y_x(i)$ and $Y_p(i)$, together with the G-factor, anisotropy decay curve was directly calculated point by point:

$$Y_r(i) = \frac{GY_p(i) - Y_x(i)}{GY_p(i) + 2Y_x(i)} = \frac{Y_d(i)}{Y_s(i)} \tag{2.7}$$

This $Y_r(i)$ curve obtained was then analysed using any of the exponential fit programs, (IBH DAS6, Version 2.2) in terms of a number of exponential decay components,

superimposed on a static anisotropy r_∞ (=A in the notation of the fit programs). The main disadvantage of the method was that the instrumental distortions remained unaccounted and it was therefore difficult to extract very short anisotropy decay times.

2.9. Protein docking

Protein docking is basically an optimization process which gives a best fit orientation of a small molecule that binds to a particular protein of interest. Docking comprises two components: (1) Configurational and conformational degrees of freedom and (2) Scoring function. The search algorithm searches the potential energy landscape adequately to find out the global energy minimum. In rigid docking, the search algorithm explores different positions for the small molecule in the receptor active site using the translational and rotational degrees of freedom. Flexible ligand docking adds exploration of torsional degrees of freedom of the small molecule. These algorithms are complimented by scoring functions that are designed to predict the biological activity through the evaluation of interactions between compounds and potential targets. The scoring function has to be realistic enough to assign the most favorable scores to the experimentally determined complex. Usually, the scoring function assesses both the steric as well as the chemical complimentaries between the ligand and the receptor.

The process of evaluating the particular conformation of molecule when bound to protein uses a number of descriptive features such as, number of intermolecular interactions including hydrogen bonds, hydrophobic contacts and van der Waals energy. Scoring function used in docking is a mathematical function whose values are proportional to the binding affinities of the lead molecules. A good scoring function should be able to give reliable estimates of binding affinities of structurally diverse lead molecules for different protein targets while considering the thermodynamic aspects of binding.[14] The success of docking program depends on both the search algorithm and the scoring function.

Computational tool such as MODELLER, a module in homology of INSIGHT II (version 2000, Accelrys, Sandiego, CA) was used for comparative protein structure modeling.[15] For structure validation of the protein PROCHECK and Profiles-3D were used. PROCHECK is a program measuring the stereochemical quality of the protein structure.[16] Profiles-3D is known to measure the compatibility between the protein sequence and known protein structures.[17]

2.10. Standard error limits

Standard error limits involved in the measurements are:

λ_{max} (abs./fluo.)	± 1 nm
Φ_f	± 10%
τ_f (> 1 ns)	± 5%
τ_f (< 1 ns)	± 5-8% (depending on the excitation source used)
Relaxation time	± 5%
Viscosity	± 2%

References

1. Perrin, D. D.; Armerego, W. L. F.; Perrin, D. R. In *Purification of Laboratory Chemicals*; Pergamon Press: New York, 1980.
2. Saha, S. Ph. D Thesis. University of Hyderabad. 2002.
3. (a) Ramachandram, B.; Saroja, G.; Sankaran, N. B.; Samanta, A. *J. Phys. Chem. B* **2000**, *104*, 11824. (b) Ramachandram, B.; Sankaran, N. B.; Karmakar, R.; Saha, S.; Samanta, A. *Tetrahedron* **2000**, *56*, 7041.
4. Saha, S.; Samanta, A. *J. Phys. Chem. A* **1998**, *102*, 7903.
5. Huddleston, J. G.; Willauer, H. D.; Swatlosky, R. P.; Visser, A. E.; Rogers, R. D. *Chem. Commun.* **1998**, 1765.
6. Hasan, M; Kozhevnikov, I. V.; Siddiqui, M. R. H.; Steiner, A.; Winterton, N. *Inorg. Chem.* **1999**, *38*, 5637.
7. Bonhote, P.; Dias, A. P.; Papageorgiou, N.; Kalyanasundaram, K.; Gratzel, M. *Inorg. Chem.* **1996**, *35*, 1168.
8. Seddon, K. R.; Stark, A.; Torres, M. J. In *Clean Solvents: Alternative Media for Chemical Reactions and Processing*; Abraham, M., Moens, L., Eds.; ACS Symposium Series 819; American Chemical Society: Washington, DC, 2002.
9. O'Connor, D. V.; Philips, D. In *Time-Correlated Single Photon Counting*; Academic Press: New York, 1984.
10. Austin, E.; Gouterman, M. *Bioinorg. Chem.* **1978**, *9*, 281.
11. Carmichael, I.; Hug, G. L. *J. Phys. Chem. Ref. Data* **1986**, *15*, 1.
12. Bevington, P. R. In *Data Reduction and Analysis for the Physical Sciences*; McGraw-Hill: New York, 1969.
13. User Manual; Decay analysis software IBH DAS6, Version 2.2.
14. Ajay; Murcko, M. A. *J. Med. Chem*. **1995**, *38*, 4953.
15. Sali, A.; Blundell, TL. *J. Mol. Biol*. **1993**, *234*, 779.
16. Laskowski, R. A.; MacArthur, M. W.; Moss, D. S.; Thornton, J. M. *J. Appl. Cryst*. **1993**, *26*, 283.
17. Lüthy, R.; Bowie, J. U.; Eisenberg, D. *Nature* **1992**, *356*, 83.

Chapter 3

Nonradiative Deactivation Pathway in Aminophthalimide Derivatives

In this chapter, transient absorption studies have been carried out on structurally similar 4-aminophthalimide derivatives, wherein the amino nitrogen forms part of a cyclic system of different ring sizes. The triplet states of these systems have been probed in less polar (1,4-dioxane), polar aprotic (acetonitrile) and protic (methanol) media by laser flash photolysis technique. The results suggest that an enhanced internal conversion process is responsible for the reduction of fluorescence efficiency of the aminophthalimides in highly polar and protic media.

3.1. Introduction

4-Aminophthalimide (AP) and its derivatives are highly fluorescent substances, which have received considerable attention in recent years.[1-27] Electronic excitation of the AP derivatives leads to enhanced separation of charge between the amino nitrogen and the carbonyl moieties. The state from which these systems fluoresce is intramolecular charge transfer (ICT) in nature and is highly sensitive to the polarity of the medium and hydrogen bond donating ability of the solvent.[4-6] Because of the sensitivity of the fluorescence properties on the nature of the solvent, one of the most common utilities of AP has been in the estimation of microscopic polarity of the organized assemblies such as the micelles, cyclodextrins, etc. as a reporter molecule.[5-8] AP is also an extensively used probe molecule for the study of solvation dynamics in conventional solvents and in complex systems.[3,9-15] The long fluorescence lifetime of AP allows study of slow solvation process in relatively viscous media such as in room temperature ionic liquids.[13-15] Highly fluorescent nature of the AP derivatives has also been exploited in the design and development of fluorescence sensors for the transition metal ions and protons.[16-18]

The dependence of the fluorescence efficiency and lifetime of the AP derivatives on the nature of the amino functionality and polarity of the media has been studied previously.[4,20] A lower fluorescence quantum yield of 4-dimethylaminophthalimide compared to AP in polar media was interpreted by postulating a nonfluorescent twisted intramolecular charge transfer state below the fluorescent state of the former system.[4] However, a later study on large number of dialkylamino derivatives of AP has indicated the important role of inversion of the amino nitrogen in making these systems less fluorescent in polar media.[20] The protic solvents exert a profound influence on the fluorescence properties of the AP derivatives.[1-3,5,6] Specific hydrogen-bonding interaction of the AP moiety with the protic solvents leads to a drastic reduction of the fluorescence efficiency and lifetime and a significant stabilization of the emitting state of the molecules. In a recent paper,[27] Maciejewski and coworkers have proposed various possible mechanisms of deactivation of AP in different kind of solvents. According to these schemes, the emitting state of AP is deactivated by both internal conversion and intersystem crossing processes.[27] On the other hand, Valeur attributed the drop of fluorescence efficiency of AP in protic solvents to an increase in the rate constant of the intersystem crossing process.[28] It is surprising to note that while the singlet state of AP and its derivatives has been probed extensively by monitoring the fluorescence, no attempt has so far been made to find out whether low fluorescence efficiency of these systems in polar and protic media is due to an enhancement of internal conversion or intersystem crossing process or both. Since it is possible to obtain an answer to this fundamental question by directly monitoring the triplet state of the systems, we have carried out transient absorption studies on three structurally similar AP derivatives to address this issue. In this context, we note that except for the work of Basu and coworkers,[19] in which the charge transfer character of the triplet state of AP was established, there is hardly any literature dealing with the triplet state properties of AP or

its derivatives. This could perhaps be due to the fact that since the aminophthalimide derivatives are highly fluorescent, the triplet yield is inherently low making detection of the triplet state rather difficult by the transient absorption technique. Low triplet extinction coefficient can also contribute to the lack of studies involving the triplet state of AP and its derivatives. In the present work, we first highlight the fluorescence behaviour of three different aminophthalimide derivatives comprising cyclic amino functionalities of different ring sizes (Chart 3.1) in less polar (1,4-dioxane), polar aprotic (acetonitrile) and protic (methanol) media and then report on the results of the triplet state of the systems probed by laser flash photolysis technique. The results suggest that these systems are characterised by moderate values of the molar extinction coefficient of the triplet-triplet absorption and low triplet yield. The results also unambiguously suggest that an enhanced internal conversion ($S_1 \sim\!\!\sim\!\!\rightarrow S_0$) is responsible for low fluorescence quantum yield of these systems in polar aprotic and protic media.

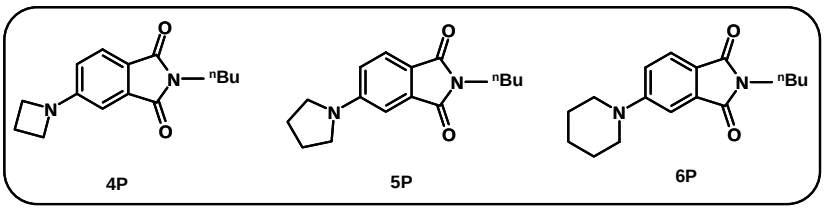

Chart 3.1. Aminophthalimide derivatives comprising cyclic amino functionalities.

3.2. Steady-state absorption and fluorescence behavior

3.2.1. Absorption

The absorption spectra of the AP derivatives are characterised by broad bands. The longest wavelength absorption maximum for the present systems appears between 380 and 400 nm depending on the system and the medium. This band has been attributed to intramolecular charge transfer transition from the amino moiety to the phthalimide unit.[20] In consistent with this nature of the transition, a Stokes shift of the absorption maximum

is observed on increase in the polarity of the media (Table 3.1). Representative spectra illustrating these features are shown in Fig. 3.1.

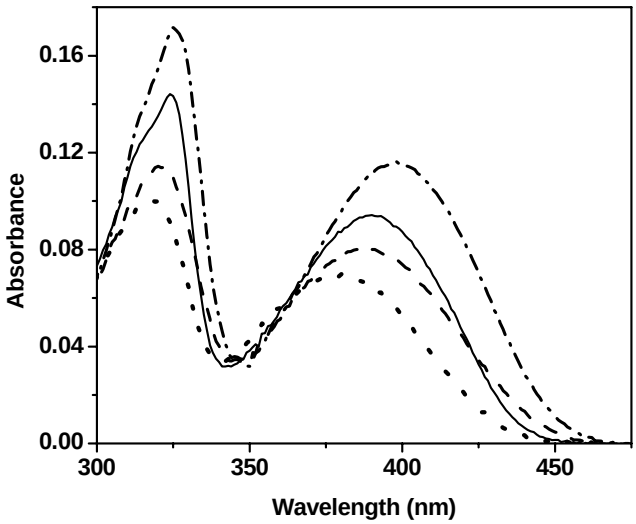

Fig. 3.1. Typical absorption spectra of the AP derivatives: 4P (····) in dioxane, (- - -) in acetonitrile and 5P (—) in dioxane, (– · –) in acetonitrile.

3.2.2. Fluorescence

The systems exhibit broad structureless fluorescence. Unlike the absorption, the fluorescence spectra of AP and its derivatives show more pronounced solvent effect. Typical influence of the solvent on the fluorescence spectra of the systems is illustrated in Fig. 3.2. Table 3.1 summarises the spectral characteristics of the systems in different solvents. The observed solvent effect is partly due to more polar nature of the fluorescent state of the systems and partly to enhanced hydrogen bonding interaction of the fluorescent state with the protic solvents.[5,6] It is evident from the data shown in the table, the shift of the fluorescence maximum of any given system on changing the solvent from 1,4-dioxane to acetonitrile is due to general solvent effect and that on changing the

solvent from acetonitrile to methanol is due to specific hydrogen bonding interaction. These features are found common to the AP derivatives studied till date.[3,5,6]

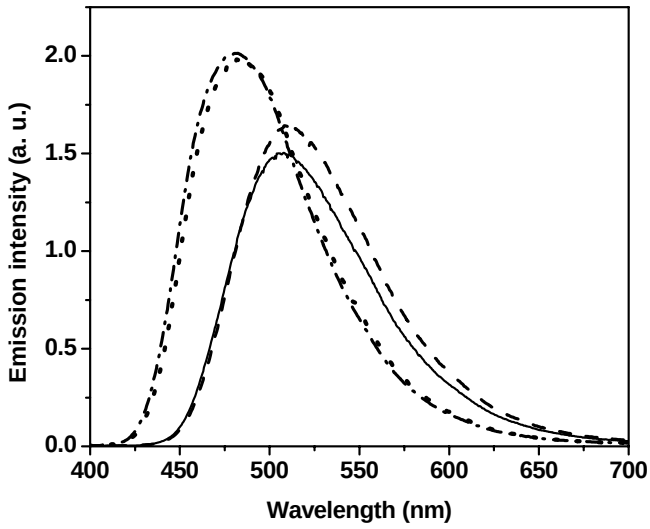

Fig. 3.2. Fluorescence spectra of 4P (····) in dioxane, (- - -) in acetonitrile and 5P (– · –) in dioxane, (—) in acetonitrile.

Table 3.1. Steady state absorption and emission data of the systems in different solvents at room temperature.

System	λ_{max}^{abs} (nm)[a]			λ_{max}^{ems} (nm)[a]			Φ_f[b]		
	diox.	acn	MeOH	diox.	acn	MeOH	diox.	acn	MeOH
4P	381	390	394	471	508	567	0.67	0.59	0.098
5P	390	399	404	468	505	567	0.68	0.54	0.05
6P	381	390	396	473	516	570	0.65	0.28	0.009

[a]± 1 nm, [b]±10%, measured in aerated solution using 4-aminophthalimide as the reference compound (Φ_f = 0.63 in acetonitrile).[4] Even though these values are lower than those reported in for the nitrogen-bubbled solutions,[20] the trend of variation of the Φ_f values with the amino functionality or polarity of the medium is very similar.

Interesting to note in this context is the variation of the fluorescence quantum yield of the various AP derivatives in different media (Table 3.1). Leaving aside the origin of the variation of the fluorescence efficiency of the systems with the amino functionality (the ring size), which has already been studied,[20] we concentrate on the solvent dependence of the fluorescence efficiency of the systems. For all three systems, the fluorescence yield drops as the solvent is changed from 1,4-dioxane to acetonitrile. This drop is most significant for 6P. What is most significant in this context is the drastic reduction of the fluorescence efficiency of the systems in protic solvent, methanol. While it is known for some time that hydrogen bonding interaction with the protic solvents leads to a reduction of the fluorescence efficiency of the AP derivatives,[5,6] it is still a matter of speculation which one of the two competing nonradiative process, internal conversion or intersystem crossing, is actually responsible for this.[19,27,28] Both higher triplet yield[19] and rate constant of intersystem crossing process[28] have been used to explain the low fluorescence yield of AP.

3.3. Time-resolved absorption studies

Laser flash photolysis (λ_{exc} = 355 nm) of the AP derivatives gives rise to a weak and broad transient absorption band in the 450-550 nm region. While the maximum absorption is observed around 470 nm in dioxane, a red shift of the peak is noticeable on increase in polarity of the medium (Fig. 3.3). That this absorption is due to triplet-triplet transition is evident from the facts that (i) bubbling of O_2 or air leads to the disappearance or diminishing intensity of the band (ii) long lifetime (~ 1.9 μs) of the transient and (iii) the literature data on the triplet-triplet absorption of 4-amino-N-methylphthalimide.[19] Additional support in favour of this assignment is obtained from a triplet sensitization study using thioxanthone. As can be seen, the transient absorption spectrum obtained on direct excitation is very similar to the sensitized spectrum (Fig. 3.4). The red shift of the spectral maximum in acetonitrile, as has been observed here, could be due to the charge

transfer character of the triplet-triplet absorption.[19] In any given solvent, the spectral variation for different derivatives is found to be minimal.

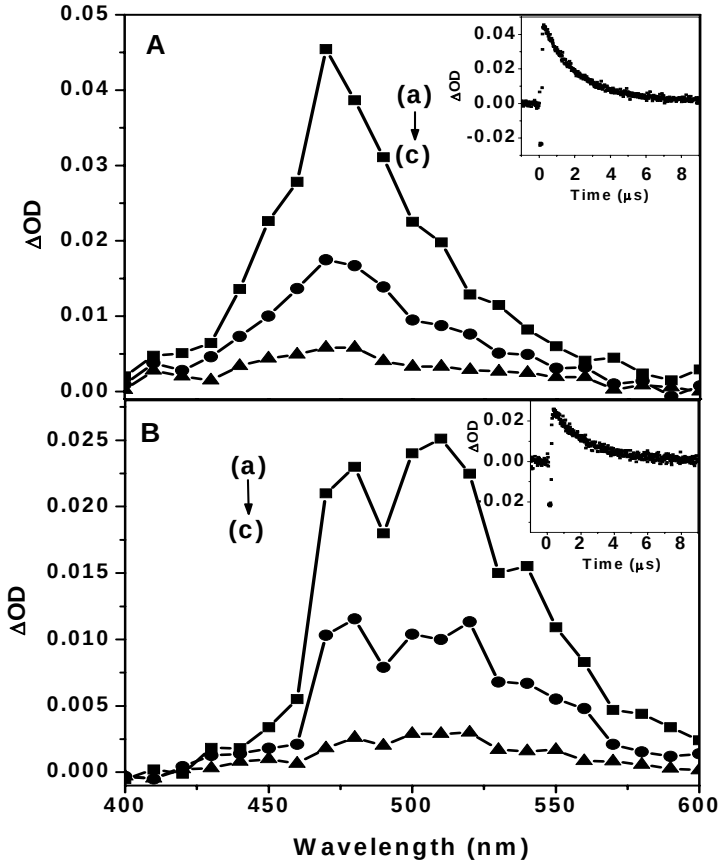

Fig. 3.3. Transient absorption spectra of 4P in 1,4 dioxane (A) 270 ns, 2 μs and 5 μs (a→c) after excitation and in acetonitrile (B) 400 ns, 2 μs, and 5 μs (a→c) after excitation. The inset shows the transient absorption decay curves at 470 nm and 510 nm in dioxane and acetonitrile, respectively.

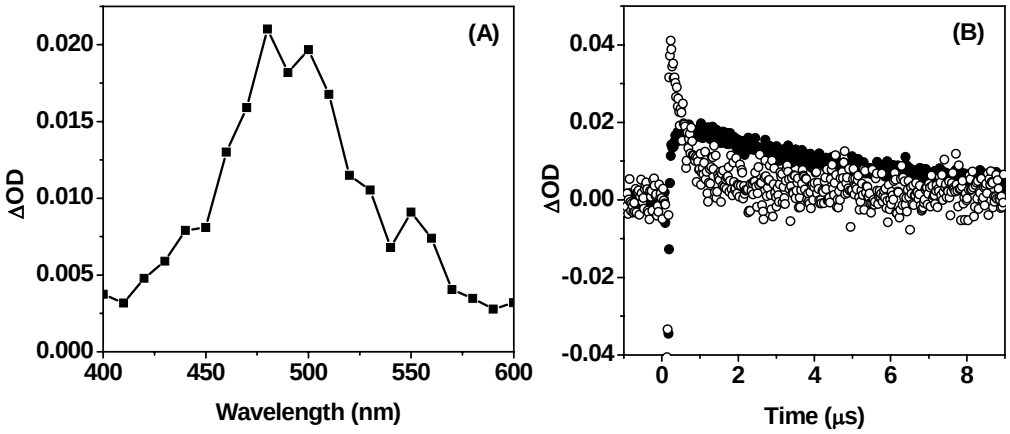

Fig. 3.4. Thioxanthone sensitized triplet-triplet absorption spectra of 4P in acetonitrile (A) recorded 1 μs after excitation. The sensitized decay curves (B) at 470 nm (●) and 600 nm (○) respectively.

As the estimation of the triplet yield from the triplet-triplet absorption data requires knowledge of the extinction coefficient (ε_T) of the triplet-triplet absorption, we have determined this quantity for the present AP derivatives by energy transfer technique using the triplet of thioxanthone as the energy donor. The quenching of the latter (E_T = 65.5 kcal/mol)[29] was assumed to be entirely dominated by exothermic triplet energy transfer process. Experiments were carried out (355 nm excitation) in acetonitrile containing both thioxanthone and the sample. The end of the pulse absorbance change $(\Delta OD)_0^R$ caused by thioxanthone triplet at 630 nm was compared with the absorbance change $(\Delta OD)_\infty$ of the sample at 500 nm. The ε_T values were calculated from the following equation.[30]

$$\varepsilon_T = \frac{\varepsilon_T^R (\Delta OD)_\infty k_{obs}}{(\Delta OD)_0^R (k_{obs} - k_0)}$$

where, ε_T^R is the extinction coefficient of the thioxanthone triplet-triplet absorption (ε_T^R = 3×10^{-4} M^{-1} cm^{-1} at 630 nm),[30] and k_{obs} and k_0 are the rate constant for the decay of thioxanthone triplet in the presence and absence of the AP derivatives, respectively. As can be seen, the measured ε_T values, which are collected in Table 3.2, are moderate. However, it is to noted that these ε_T values are significantly lower than those reported for 4-amino-N-methylphthalimide.[19] We found that this discrepancy is due to the fact that previous estimation of the ε_T values were based on the incorrect assumption that the triplet yield of the AP derivatives is simply given by $(1-\phi_f)$.[19]

The triplet quantum yield (Φ_T) was determined by comparative actinometry method using 4,4′ - dimethoxybenzophenone (ε_T^R = 5200 $M^{-1}cm^{-1}$ at 545 nm, Φ_T^R = 1.0)[30] as the standard and assuming that the triplet-triplet extinction coefficient values (ε_T) do not vary significantly with the solvent polarity. While it is a standard practice to estimate the triplet yield of a system assuming the solvent independence of the molar extinction coefficient value,[30] our assumption is justified by the results of independent test measurements on one of the present systems. The results show that the triplet-triplet extinction coefficients of 6P in acetonitrile and 1,4-dioxane do not differ by more than 15%.

The end of pulse absorbance change $(\Delta OD)_0$ due to the triplet of the sample at λ_{max}^T was compared with the absorbance change $(\Delta OD)_0^R$ due to the 4,4′-dimethoxybenzophenone triplet at 545 nm, the latter being observed in a solution optically matched at the exciting wavelength with that of sample.

$$\Phi_T = \frac{\Phi_T^R (\Delta OD)_0 \varepsilon_T^R}{(\Delta OD)_0^R \varepsilon_T}$$

The estimated Φ_T values for the systems are collected in Table 3.2.

Table 3.2. Triplet state parameters of the systems in different solvents at room temperature.

System	$\log\varepsilon_T$[a]	Φ_T[b]		
		diox.	ACN	MeOH
4P	3.76	0.18	0.19	0.029
5P	3.67	0.23	0.23	0.035
6P	3.56	0.28	0.16	0.033

[a]± 10%, measured in acetonitrile, [b]± 15%

The trends that emerge from the data are the following. First, the triplet yield of the systems in least polar solvent (1,4-dioxane) is the maximum (0.18 – 0.28). In this solvent, the singlet and triplet yields account for nearly 85 – 93% of the absorbed light implying that the efficiency of the internal conversion process is between 7 and 15%. In highly polar aprotic solvent, acetonitrile, there is hardly any variation in the triplet yield of 4P and 5P, though some reduction of the triplet yield for 6P could be observed. Since the fluorescence and triplet yields account for 44 - 78% of the absorbed light, the efficiency of the internal conversion process in this medium is found to be between 22 and 56%. In protic solvent, methanol, where the systems are very weakly fluorescent, the triplet yield is also very low. This implies that contrary to what is commonly believed, the internal conversion process becomes highly efficient in protic solvent. According to the present data, the internal conversion accounts for nearly 87-96% of the absorbed photons in methanol. It is therefore concluded based on the collected data that because of an increased efficiency of the internal conversion process the AP derivatives are weakly fluorescent in polar and protic media.

3.4. Conclusion

We conclude that the aminophthalimides are characterized by low triplet yields and moderate values of the molar extinction coefficients of the triplet-triplet absorption. Even in protic media, where the systems are very weakly fluorescent, the triplet yield is also found to be quite low. The results presented in this work suggest that an enhanced internal conversion process is responsible for the low fluorescence efficiency of the systems in polar protic and aprotic media.

References

1. Ware, W. R.; Lee, S. K.; Brant, G. J.; Chow, P. P. *J. Chem. Phys*. **1971,** *11*, 4729.
2. Noukakis, D.; Suppan, P. *J. Lumin*. **1991,** *47*, 285.
3. Nagarajan, V.; Brearley, A. M.; Kang, T.-J.; Barbara, P. F. *J. Chem. Phys*. **1987**, *86*, 3183.
4. Soujanya, T.; Fessenden, R. W.; Samanta, A. *J. Phys. Chem*. **1996**, *100*, 3507.
5. Soujanya, T.; Krishna, T. S. R.; Samanta, A. *J. Photochem. Photobiol. A: Chem*. **1992**, *66*, 185.
6. Soujanya, T.; Krishna, T. S. R.; Samanta, A. *J. Phys. Chem*. **1992**, *96*, 8544.
7. Saroja, G.; Samanta, A. *Chem. Phys. Lett*. **1995**, *246*, 506.
8. Saroja, G.; Ramachandram, B.; Saha, S.; Samanta, A. *J. Phys. Chem. B* **1999**, *103*, 2906.
9. Chapman, C. F.; Fee, R. S.; Maroncelli, M. *J. Phys. Chem*. **1995**, *99*, 4811.
10. Laitinen, E.; Salonen, K.; Harju, T. *J. Chem. Phys*. **1996**, *104*, 6138.
11. Das, S.; Datta, A.; Bhattacharyya, K. *J. Phys. Chem. A* **1997**, *101*, 3299.
12. Sen, S.; Sukul, D.; Dutta, P.; Bhattacharyya, K. *J. Phys. Chem. A* **2001**, *105*, 10635.
13. Karmakar, R.; Samanta, A. *J. Phys. Chem. A* **2003**, *107*, 7340.
14. Ingram, J. A.; Moog, R. S.; Ito, N.; Biswas, R.; Maroncelli, M. *J. Phys. Chem. B* **2003**, *107*, 5926.
15. Mandal, P. K.; Samanta, A. *J. Phys. Chem. B* **2005**, *109*, 15172.
16. Ramachandram, B.; Samanta, A. *Chem. Commun*. **1997**, 1037.
17. Banthia, S.; Samanta, A. *J. Phys. Chem. B* **2002**, *106*, 5572.
18. Sarkar, M.; Banthia, S.; Samanta, A. *Tet Lett*. **2006**, *47*, 7575.
19. Aich, S.; Raha, C.; Basu, S. *J. Chem. Soc., Faraday Trans*. **1997**, *93*, 2991.
20. Saha, S. Ph. D. Thesis. University of Hyderabad, 2002.
21. Wetzler, D. E.; Chesta, C.; Fernandez-Prini, R.; Aramendia, P. F. *J. Phys. Chem. A* **2002**, *106*, 2390.
22. Yuan, D.; Brown, R. G. *J. Phys. Chem. A* **1997**, *101*, 3461.
23. Morimoito, A.; Yatsuhashi, T.; Shimada, T.; Biczok, L.; Tryk, D. A.; Inoue, H. *J. Phys. Chem*. **2001**, *105*, 10488.
24. Chen, Y.; Topp, M. R. *Chem. Phys*. **2002**, *283*, 249.
25. Maciejewski, A.; Kubicki, J.; Dobek, K. *J. Phys. Chem. B* **2003**, *107*, 13986.
26. Maciejewski, A.; Kubicki, J.; Dobek, K. *J. Phys. Chem. B* **2005**, *109*, 9422.
27. Krystkowiak, E.; Dobek, K.; Maciejewski, A. *J. Photochem. Photobiol. A: Chem*. **2006**, *184*, 250.
28. Valeur, B. In *Molecular Fluorescence*; VCH-Wiley: Weinheim, Germany, 2002.
29. Murov, S. L. In *Handbook of Photochemistry*; Dekker: New York, 1973.
30. Carmichael, I.; Hug, G. L. *J. Phys. Chem. Ref. Data* **1986**, *15*, 1.

Chapter 4

Photoinduced Electron Transfer in 1,8-naphthalimide Derivatives

This chapter describes transient absorption measurements on fluorophore-spacer-receptor molecules bearing 1,8-naphthalimide moiety as fluorophores in 1,4-dioxane and acetonitrile. Laser flash photolysis studies allow detection of the imide radical anions providing direct evidence of intramolecular photoinduced electron transfer (PET) process in these systems. The studies indicate participation of the triplet state in the PET process and role of the solvent polarity in dictating the involvement of the excited state in the above process. Triplet quantum yield, imide radical ion yield and triplet state lifetime of the 1,8-naphthalimide systems are estimated in these media.

4.1. Introduction

Naphthalimide and its derivatives have been the subject of several investigations dealing with their photophysical[1-8] and photobiological behavior.[9-13] Substituted 1,8-naphthalimides and bisnaphthalimides are promising anticancer agents[9] and the sulfonated derivatives are good antiviral agents with selective *in vitro* activity against the human immunodeficiency virus, HIV-1.[10] Brominated mono and bisnaphthalimide derivatives are photochemotherapeutic inhibitors for enveloped viruses in blood and blood products.[11] The photoactivity and DNA-intercalation properties of 1,8-naphthalimide derivatives have also prompted studies on sequence-specific DNA-photonucleases.[12] Saito et al.[13] demonstrated photoinduced DNA cleavage via electron transfer between a guanine base and 1,8-naphthalimide. The photophysical and excited-state reactivity of 1,8-naphthalimide derivatives have been extensively studied by Kossyani and co-workers,[1] Pardo et al.,[2] and Samanta and co-workers.[3-8]

In recent past, multi-component systems (I-V, Chart 4.1) bearing the *fluorophore-spacer-receptor* architecture and comprising 1,8-naphthalimide or substituted

naphthalimide derivatives as fluorophores have been designed and developed for signaling purpose.[5-8] The basic underlying principle involved in the design of these systems is *photoinduced intramolecular electron transfer* (PET) from the electron-rich receptor moiety to the electron-deficient fluorophore unit. These systems are characterized with low fluorescence quantum yields in the absence of guests such as metal ions or protons.[5,8] Addition of the metal ions leads to fluorescence enhancement as the PET communication between the receptor and fluorophore is disrupted. Although the fluorescence behavior of these systems is interpreted in terms of the PET process, no evidence in favor of the PET mechanism is available so far. The fluorescence measurements merely indicate the involvement of a competing process from the excited singlet state that leads to fluorescence quenching of the systems. Since identification of the products of the PET reaction can only provide the clinching evidence in favor of the process, we have taken up this investigation. A second objective of the present study based on laser flash photolysis technique has been to determine whether PET reaction occurs from the triplet state of the molecules as well. As in the recent past,[14-19] extensive PET studies have been carried out on 1,8-naphthalimide derivatives, these results are expected to serve as a guide to the identification of the various transient species involved in the PET reaction.

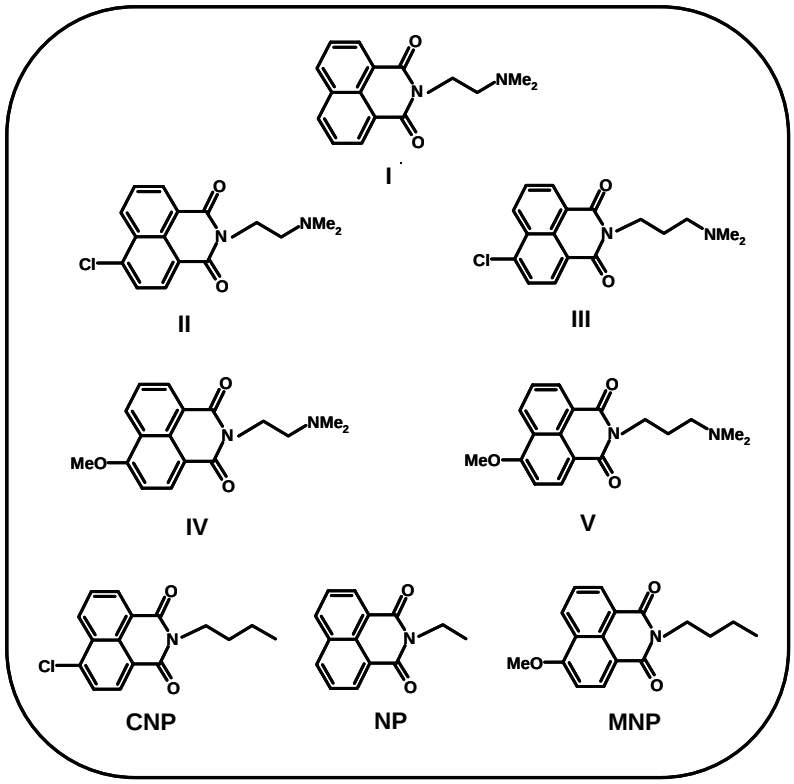

Chart 4.1. 1,8-naphthalimide derivatives bearing the *fluorophore-spacer-receptor* architecture along with the parent fluorophores.

In the present study, the transient absorption measurements have been confined to the multi-component systems (I-V, Chart 4.1). Characteristic absorption due to the corresponding imide radical anion has been detected for all the systems bearing the *fluorophore-spacer-receptor* architecture. The triplet quantum yields of the systems have been determined. The estimation of radical ion yield allowed determination of the extent of intramolecular electron transfer in all the multi-component systems. The solvent effect on the yield and lifetime of the triplet and pathway of the PET process has been

investigated by carrying out the measurements in two solvents, 1,4 dioxane and acetonitrile.

4.2. Steady-state absorption and fluorescence

The absorption spectra of the multi-component systems, I-III, exhibit vibronic structures, which are very similar to those exhibited by their parent fluorophores, NP and CNP. The other two multi-component systems, IV and V, display broad absorption bands similar to the parent fluorophore, MNP and this broad nature can be attributed to intramolecular charge transfer transition from the methoxy group to the carbonyl oxygen in these systems.[20] Representative absorption spectra are shown in Fig. 4.1. The systems I-III show weak structured fluorescence, while IV and V exhibit fluorescence bands that are broad and structureless. The nature of the fluorescence spectra of the multi-component systems is similar to their respective parent fluorophores. Polarity of the solvent does not have much influence on the fluorescence spectra of I-III, but considerable red-shift is observed for the fluorescence spectra of IV and V with increasing polarity of the media, which is in agreement with the charge transfer character in the latter systems (Fig. 4.2). Although the absorption and fluorescence spectral behavior of the two sets of molecules, I-III and IV-V, are not very similar, the fluorescence quantum yields (as indicated in Table 4.1) of all the multi-component systems (I-V) are significantly lower than those of their respective parent fluorophore in any given solvent. It is generally believed that PET process, which is thermodynamically feasible,[5,8] is responsible for the low fluorescence yield of the systems. It is evident from the fluorescence quantum yield data of IV and V (Table 4.1) in different solvents that PET process is more feasible in polar solvents. However, the involvement of the PET cannot be judged only by the thermodynamic feasibility of the process as fluorophore-receptor distance and relative orientation of the two components in the multi-component systems are also crucial factors on which the efficiency of PET process depends.[21] The

fluorescence quenching in the absence of a guest and subsequent enhancement (FE) of these multicomponent systems in presence of guest[5,8] suggest only about a quenching mechanism, but nothing about its nature.

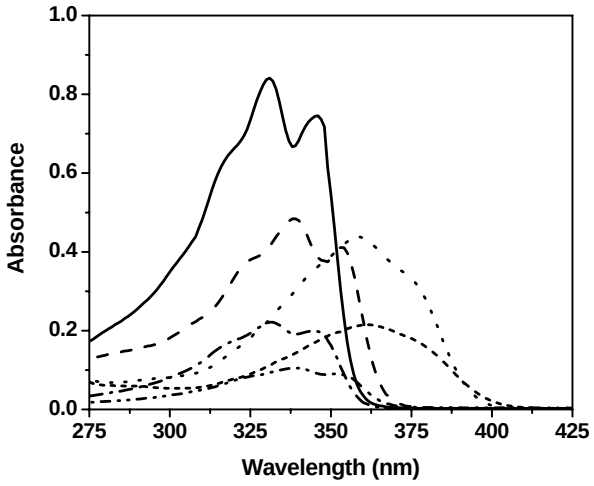

Fig. 4.1. Representative absorption spectra of the multi-component systems: I (—), III (– – –), V (····) in 1,4 dioxane and I (– · –), III (- ·· - ·· - ··), V (- - -) in acetonitrile.

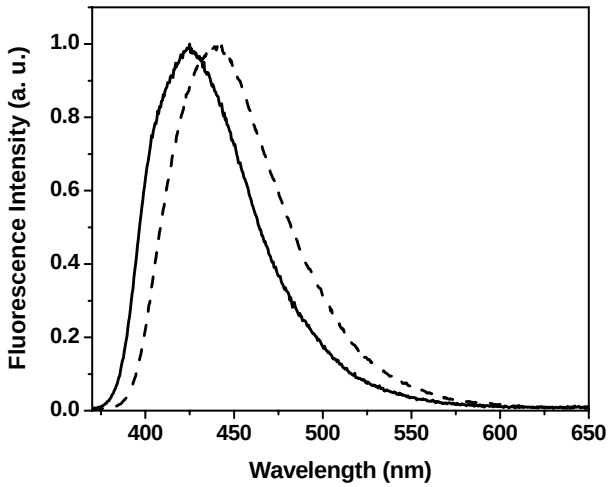

Fig. 4.2. Representative fluorescence spectra of V (—) in 1,4 dioxane, and (– – –) in acetonitrile.

Table 4.1. Fluorescence quantum yield† of the multi-component systems and parent fluorophores.

Systems	Φ_f	
	dioxane	acetonitrile
NP	0.01	0.03
CNP	0.02	0.06
MNP	0.76	0.78
I	0.0003	0.007
II	0.0002	0.0005
III	0.001	0.002
IV	0.065	0.03
V	0.15	0.05

†From reference 20.

4.3. Time-resolved absorption

4.3.1. Results

The transient absorption spectrum of NP in acetonitrile (Fig. 4.3) is characterized by absorption in the 350-550 nm wavelength range with maxima at 360 and 470 nm. The other parent compound MNP shows slightly broader transient absorption at 400-500 nm wavelength region (Fig. 4.4) in acetonitrile. In addition to the transient absorption band around 470 nm, the multi-component systems I-V also exhibit a long-lived absorption band (λ_{max} = 400 - 420 nm) in acetonitrile unlike their parent systems NP and MNP (see Fig. 4.5 - Fig. 4.7). A significant blue-shift of the peak maxima of the transient absorption band is observed for MNP, IV and V in 1,4 dioxane (Fig. 4.8, Fig. 4.9). The long-lived band of I at λ = 410 nm is characterized with a risetime of 450 ns (Fig. 4.5). It is to be

noted that the long-lived absorption at 410-420 nm which is observable in acetonitrile is not observed in dioxane for the multi-component systems, I-V.

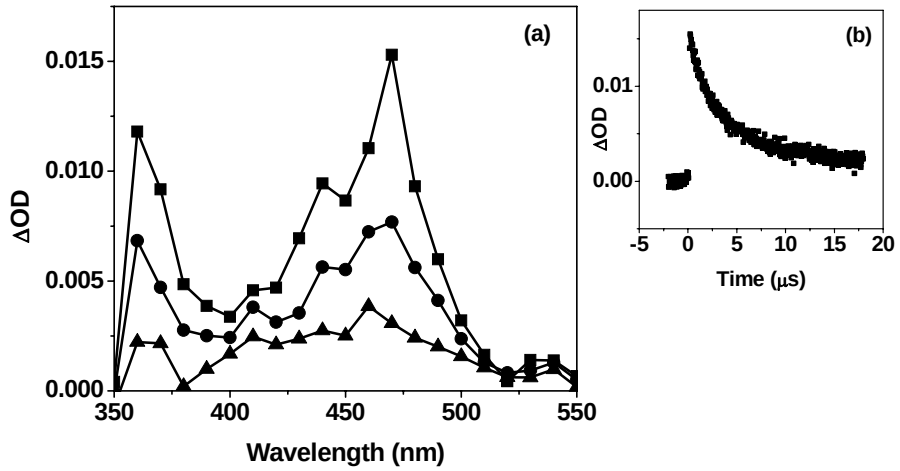

Fig. 4.3. Transient absorption spectra of NP in acetonitrile (a) at different delay times, 240 ns (■), 2.7 μs (●) and 9.6 μs (▲). Decay curve of T-T absorption (b) at 470 nm.

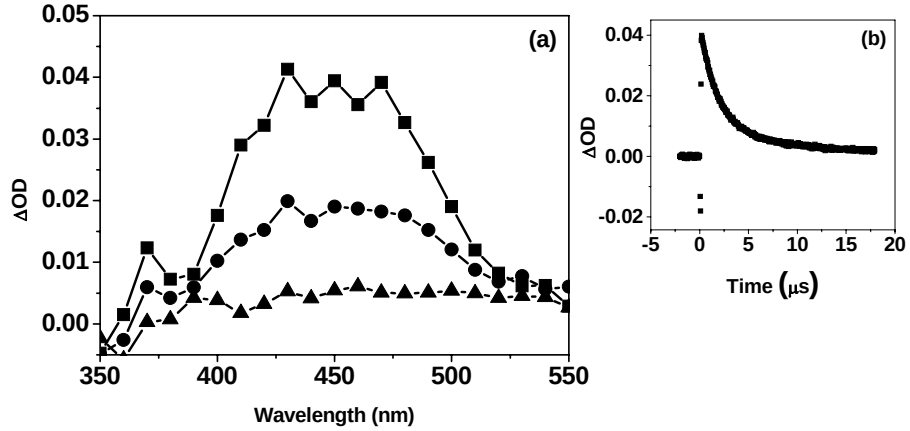

Fig. 4.4. Transient absorption spectra of MNP in acetonitrile (a) at different delay times, 240 ns (■), 2.0 μs (●) and 7.9 μs (▲). Decay curve of T-T absorption (b) at 470 nm.

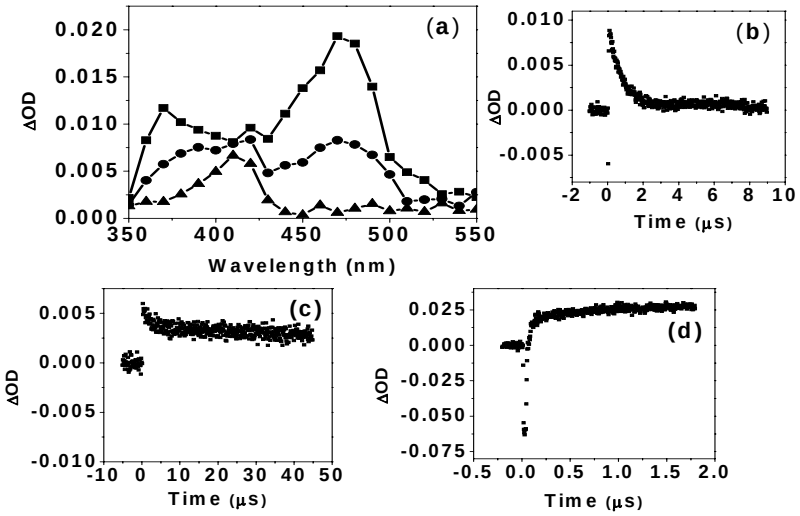

Fig. 4.5. Transient absorption spectra of I in acetonitrile (a) at different delay times, 160 ns (■), 960 ns (●) and 4.9 μs (▲). Decay curve of T-T absorption at 470 nm (b), decay trace of the imide radical anion at 410 nm (c), growth profile of imide radical anion at 414 nm (d).

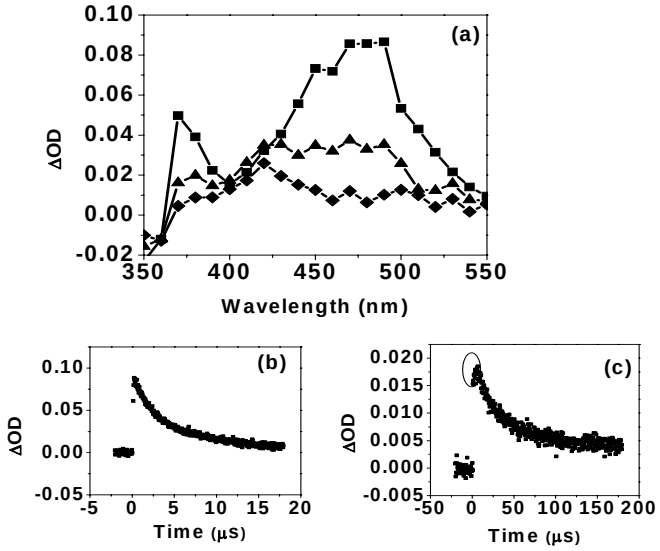

Fig. 4.6. Transient absorption spectra of III in acetonitrile (a) at 280 ns (■), 3.8 μs (▲) and 11.9 μs (♦). Decay curves of T-T absorption at 470 nm (b) and radical anion at 410 nm highlighting the rise (c).

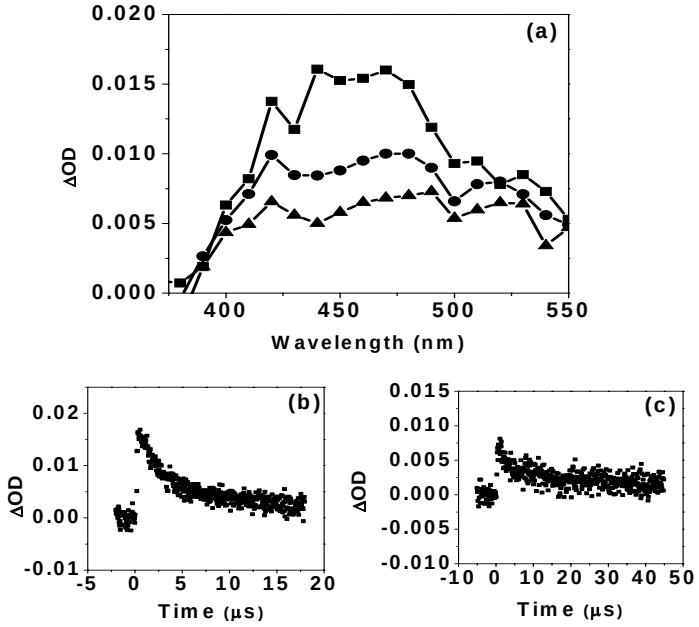

Fig 4.7. Transient absorption spectra of IV (a) in acetonitrile, at 270 ns (■), 1.9 μs (▲) and 3.6 μs (♦). Decay curves of T-T absorption at 470 nm (b) and decay profile at 400 nm (c).

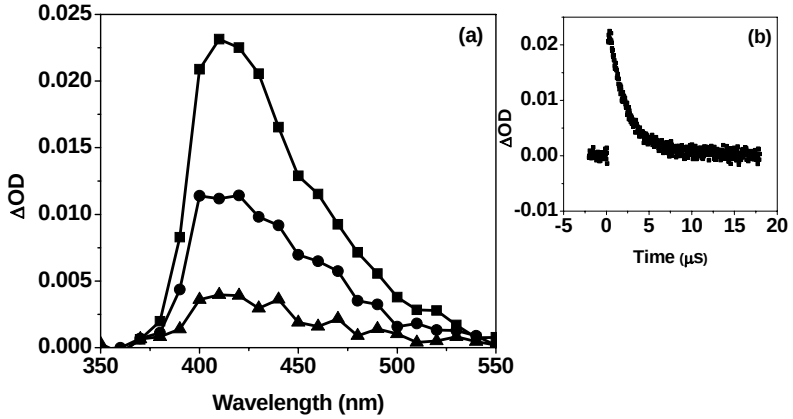

Fig. 4.8. Transient absorption spectra of MNP (a) in dioxane at different delay times, 360 ns (■), 1.8 μs (●) and 4.2 μs (▲). Decay curve of T-T absorption (b) at 420 nm.

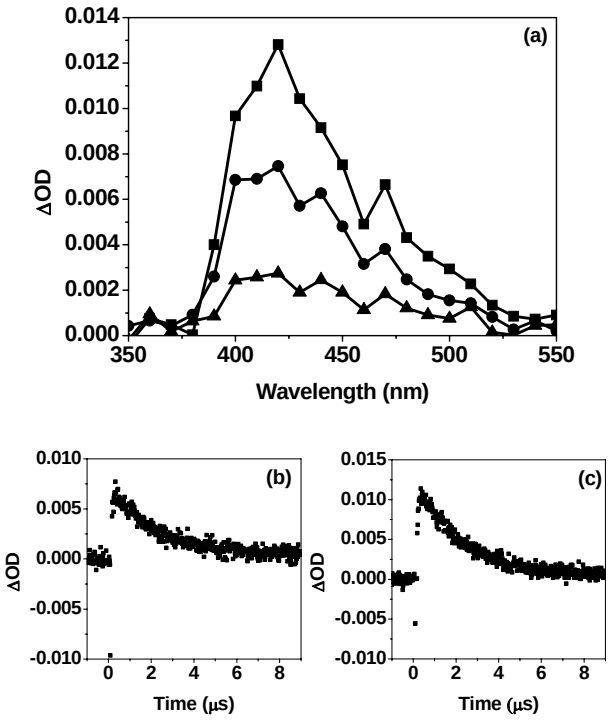

Fig 4.9. Transient absorption spectra of IV (a) in dioxane, at 340 ns (■), 1.4 μs (▲) and 3.8 μs (♦). Decay profile of T-T absorption at 470 nm (b) and decay trace at 410 nm (c).

Determination of triplet-state parameters: Since estimation of the triplet yield of a system from the triplet-triplet absorption data requires the knowledge of the extinction coefficient (ε_T) of the triplet-triplet absorption, this quantity is first determined for the parent fluorophores NP and MNP by energy transfer technique using the triplet of thioxanthone as the energy donor. The quenching of the latter (E_T = 65.5 kcal/mol)[22] was assumed to be entirely dominated by exothermic triplet energy transfer process. Experiments were carried out in acetonitrile containing both thioxanthone and the sample with 355 nm excitation. The end of the pulse absorbance change $(\Delta OD)_0^R$ caused by

thioxanthone triplet at 630 nm was compared with the absorbance change $(\Delta OD)_{\infty}^{S}$ of the sample at 470 nm. ε_T^S value was calculated from the following equation.[23]

$$\varepsilon_T^S = \frac{\varepsilon_T^R (\Delta OD)_{\infty}^S k_{obs}}{(\Delta OD)_0^R (k_{obs} - k_0)} \quad (1)$$

where, ε_T^R is the extinction coefficient of the thioxanthone triplet-triplet absorption (ε_T^R = 3×10^{-4} M^{-1} cm^{-1} at 630 nm)[23] and k_{obs} and k_0 are the rate constants for the decay of thioxanthone triplet in the presence and in the absence respectively of the NP/MNP derivative. The ε_T^S values for NP and MNP are estimated to be 6.875×10^3 M^{-1} cm^{-1} and 6.028×10^3 M^{-1} cm^{-1} respectively at 470 nm. The ε_T^S values for the compounds I-V are assumed to be same to that of their parent fluorophore.

Once the triplet-triplet extinction coefficient ε_T^S was known, the triplet quantum yield (Φ_T^S) was determined by comparative actinometry method using 1,8 naphthalimide (ε_T^R = 10,300 M^{-1} cm^{-1} at 470 nm, Φ_T^R = 0.92)[4] as the standard assuming that the extinction coefficient of the systems does not change with solvent polarity.[23,24] The end of pulse absorbance change $(\Delta OD)_0^S$ due to the triplet of the sample was compared with the absorbance change $(\Delta OD)_0^R$ due to the 1,8 naphthalimide triplet at 470 nm, the latter being observed in a solution optically matched at the exciting wavelength with that of the sample.

$$\Phi_T^S = \frac{\Phi_T^R (\Delta OD)_0^S \varepsilon_T^R}{(\Delta OD)_0^R \varepsilon_T^S} \quad (2)$$

Using the extinction coefficient ($\Delta\varepsilon$) of 1,8-naphthalimide radical anion, ($\Delta\varepsilon$ = 35,000 M^{-1} cm^{-1} at 410 nm)[16,19] the yields (Φ) of the radical anion ($A^{\cdot-}$) for the systems, I-

V are determined using the equation (3) below.[16,17] Here the process of self-quenching is neglected as the experiments were carried out in dilute solutions of the sample and also PET has been considered as the major pathway for deactivation of the triplet states of the systems.

$$\Delta A = \Delta\varepsilon\left[{}^3A^*\right]_0 \Phi \qquad (3)$$

where ΔA is the transient absorbance due to the imide radical anion (extrapolating to time zero), $[{}^3A^*]_0$ is the triplet state concentration of the imide produced by the laser pulse.

The triplet quantum yields estimated for the systems (Table 4.2) are considerably high in acetonitrile than in dioxane. The yield of the radical ion is found to vary with the nature of the substituent. Table 4.2 indicates that radical ion yield is slightly higher for the chloro derivatives (II and III) than that for the methoxy ones (IV and V).

Table 4.2. Triplet state parameters of the compounds in non-polar and polar media.

Systems	Φ_T		Φ_{A^-}	τ_T (μs)		τ_{A^-} /μs
	acn	dioxane	(acn)	acn	dioxane	(acn)
I	0.12	0.063	0.024	0.7	1.9	2.8
II	0.11	0.037	0.025	2.0	1.0	30.0
III	0.13	0.094	0.028	1.8	3.3	60.0
IV	0.18	0.034	0.018	3.2	2.7	7.1
V	0.17	0.037	0.022	2.0	2.5	10.9

4.3.2. Discussion

The transient absorption bands observed for NP, MNP and the multi-component systems (I-V) in and around 470 nm are due to triplet-triplet transition.[4,14,19] The broadness of the triplet-triplet absorption band of MNP, IV and V and the shift of its peak maxima to the long wavelength region with increasing polarity of the solvent is due to the charge transfer nature of the transition. Thus, the charge transfer character of the methoxy derivatives is also reflected in the triplet-triplet absorption spectra. The long-lived absorption at 410-420 nm region observed for systems I-V in acetonitrile is attributed to the absorption of the imide radical anion ($A^{\cdot-}$). This assignment is in agreement with literature.[14-19] The generation of imide radical anion is only possible if there is electron transfer from the dimethyamino moiety to the naphthalimide fluorophores in the concerned *fluorophore-spacer-receptor* systems, I-V. Thus the detection of radical anion provides conclusive evidence of PET in the multi-component systems. In this context, it is to be kept in mind that although the long-lived band corresponds to the absorption due to the radical anion of the acceptor moiety (i.e the imide radical ion), for the intramolecular systems where the donor and acceptor moieties are linked with a spacer, it is more practical to represent the species as ($D^{\cdot+}$-$A^{\cdot-}$).

The long risetime (450 ns) of the absorption due to radical anion of I suggests that the PET occurs from the triplet state of these systems in acetonitrile, as the singlet state lifetime is only 185 ps.[20] The occurrence of the PET process from the triplet state is further evident from the similarity of the triplet lifetime (τ_T = 700 ns for I) and the risetime of the radical ion absorption. The higher triplet yields of I-V in acetonitrile than in dioxane (Table 4.2) suggest that the probability of occurrence of PET from the triplet state is more in acetonitrile compared to dioxane. This observation is in agreement with literature,[19] which states that in non polar solvent, like toluene, the ISC efficiency is approximately 50% of that in acetonitrile for some 1,8-naphthalimide systems. Thus, PET

from dimethylamino unit to the naphthalimide moiety for the systems I-V occurs in the singlet excited state (S_1) as well as in the triplet excited state (T_1) in acetonitrile, or in other words, D-^{1}A undergoes intersystem crossing to give D-^{3}A with competition of the charge transfer process (D-^{1}A $\rightarrow$ ^{1}($D^{\bullet+}$-$A^{\bullet-}$)) in polar solvents. In dioxane, the absence of the long-lived band due to the radical anion ^{3}($D^{\bullet+}$-$A^{\bullet-}$), probably suggests rapid recombination of the products of the electron transfer reaction in non polar solvents. As ISC is less efficient in dioxane, PET occurs mainly through D-^{1}A compared to D-^{3}A in non-polar solvents. That the polarity of the solvent dictates the involvement of the singlet or the triplet states in the PET process of systems I-V is in agreement with the literature.[14]

4.4. Conclusion

While the fluorescence quantum yield data of the systems, I-V, indicated the presence of a quenching mechanism, the present measurements, wherein we have detected the product of the electron transfer reaction, offer direct evidence of the PET reaction occurring in these systems. The transient absorption studies have also shown the involvement of the triplet state in the PET process of the molecules. The triplet quantum yield and radical ion yield of the 1,8-naphthalimide derivatives have been determined which depict that the polarity of the solvent dictates the participation of the excited state (singlet/triplet) in the electron transfer process for these systems.

References

1. (a) Nemes, P.; Demeter, A.; Biczok, L.; Berces, T.; Wintgens, V.; Valat, P.; Kossanyi, J. *J. Photochem. Photobiol. A: Chem*. **1998**, *113*, 225. (b) Wintgens, V.; Valat, P.; Kossanyi, J.; Demeter, A.; Biczok, L.; Berces, T. *J. Photochem. Photobiol. A: Chem*. **1996**, *93*, 109. (c) Wintgens, V.; Valat, P.; Kossanyi, J.; Demeter, A.; Biczok, L.; Berces, T. *New. J. Chem*. **1996**, *20*, 1149. (d) Demeter, A.; Biczok, L.; Berces, T.; Wintgens, V.; Valat, P.; Kossanyi, J. *J. Phys. Chem*. **1993**, *97*, 3217. (e) Demeter, A.; Biczok, L.; Berces, T.; Wintgens, V.; Valat, P.; Kossanyi, J. *J. Phys. Chem*. **1996**, *100*, 2001. (f) Valat, P.; Wintgens, V.; Kossanyi, J.; Biczok, L.; Demeter, A.; Berces, T. *J. Am. Chem. Soc*. **1992**, *114*, 946.
2. (a) Pardo, A.; Poyato, M.; Martin, E. *J. Photochem*. **1986**, *36*, 323. (b) Pardo, A.; Martin, E. Poyato, J. M. L.; Camacho, J. J.; Brana, M. F.; Castellano, J. M. *J. Photochem. Photobiol. A: Chem*. **1987**, *41*, 69. (c) Pardo, A.; Poyato, J. M. L.; Martin, E. Camacho, J. J.; Reyman, D. *J. Lumin*. **1990**, *46*, 381. (d) Pardo, A.; Martin, E.; Poyato, J. M. L.; Camacho, J. J.; Guerra, J. M.; Weigand, R.; Brana, M. F.; Castellano, J. M. *J. Photochem. Photobiol. A: Chem*. **1989**, *48*, 259.
3. Samanta, A.; Saroja, G. *J. Photochem. Photobiol. A: Chem*. **1994**, *84*, 19.
4. Samanta, A.; Ramachandram, B.; Saroja, G. *J. Photochem. Photobiol. A: Chem*. **1996**, *101*, 29.
5. Ramachandram, B.; Saroja, G.; Sankaran, N. B.; Samanta, A. *J. Phys. Chem. B* **2000**, *104*, 11824.
6. Ramachandram, B.; Samanta, A. *Chem. Commun*. **1997**, 1037.
7. Ramachandram, B.; Sankaran, N. B.; Samanta, A. *Res. Chem. Interm*. **1999**, *25*, 843.
8. Ramachandram, B.; Sankaran, N. B.; Karmakar, R.; Saha, S.; Samanta, A. *Tetrahedron* **2000**, *56*, 7041.
9. (a) Brana, M. F.; Castellano, J. M.; Roldan, C. M.; Sntos, A.; Vazquez, D.; Jimenez, A. *Cancer Chemother. Pharmacol*. **1980**, *4*, 61. (a) Brana, M. F.; Castellano, J. M.; Sanz, A. M.; Roldan, C. M.; Roldan, C. Eur. *J. Med. Chem*. **1981**, *16*, 207.
10. Rideout, D.; Schinazi, R.; Pauza, C. D.; Lovelace, K.; Chiang, L.-C.; Calogeropoulou, T.; Mccarthy, M.; Elder, J. H. *J. Cell. Biochem*. **1993**, *51*, 446.
11. (a) Chanh, T. C.; Lewis, D. E.; Allan, J. S.; Sogandares-Bernal, F.; Judy, M. M.; Utecht, R. E.; Matthews, J. L. *AIDS Res. Hum. Retroviruses* **1993**, *9*, 891. (b) Chanh, T. C.; Archer, B. J.; Utecht, R. E.; Lewis, D. E.; Judy, M. M.; Matthews, J. L. *Biomed. Chem. Lett*. **1993**, *3*, 555. (c) Chanh, T. C.; Lewis, D. E.; Judy, M. M.; Sogandares-Bernal, F.; Michalek, G. R.; Utecht, R. E.; Skiles, H.; Chang, S. C.; Matthews, J. L. *Antiviral Res*. **1994**, *25*, 133.
12. Bailly, C.; Brana, M.; Waring, M. J. *Eur. J. Biochem*. **1996**, *240*, 195.
13. Saito, I.; Takayama, M.; Sugiyama, H.; Nakatani, K.; Tsuchida, A.; Yamamoto, M. *J. Am. Chem. Soc*. **1995**, *117*, 6406.
14. van Dijk, S. I.; Groen, C. P.; Hartl, F.; Brouwer, A. M.; Verhoeven, J. W. *J. Am. Chem. Soc*. **1996**, *118*, 8425.
15. Aveline, B. M.; Matsugo, S.; Redmond, R. W. *J. Am. Chem. Soc*. **1997**, *119*, 11785.
16. Rogers, J. E.; Kelly, L. A. *J. Am. Chem. Soc*. **1999**, *121*, 3854.
17. Rogers, J. E.; Weiss, S. J.; Kelly, L. A. *J. Am. Chem. Soc*. **2000**, *122*, 427.
18. Abraham, B.; Kelly, L. A. *J. Phys. Chem. B* **2003**, *107*, 12534.

19. Cho, D. W.; Fujitsuka, M.; Sugimoto, A.; Yoon, U. C.; Mariano, P. S.; Majima, T. *J. Phys. Chem. B* **2006**, *110*, 11062.
20. Ramachandram, B. Ph. D. Thesis. University of Hyderabad, 1999.
21. (a) Weller, A.; Staerk, H.; Trichel, R. *Faraday Discuss. Chem. Soc*. **1984**, *79*, 271. (b) Gust, D.; Moore, T. A. In *Photoinduced Electron Transfer*; Mattey, J. Ed.; *Topics in Current Chemistry* 159; Springer-Verlag: New York, 1991; Vol III, pp 105. (c) Verhoeven, J. W. *Pure Appl. Chem*. **1990**, *62*, 1585. (d) Jordan, K. D.; Paddon-Row, M. N. *Chem. Rev*. **1992**, *92*, 395. (e) Wasielewski, M. R. *Chem. Rev*. **1992**, *92*, 435.
22. Murov. S. L. In *Handbook of Photochemistry*; Dekker: New York, 1973.
23. Carmichael, I.; Hug, G. L. *J. Phys. Chem. Ref. Data* **1986**, *15*, 1.
24. Bhattacharya, B. Samanta, A. *Chem. Phys. Lett*. **2007**, *442*, 316.

Chapter 5

Excited-State Proton-Transfer Dynamics of 7-Hydroxyquinoline in Room Temperature Ionic Liquids

This chapter deals with excited-state proton transfer (ESPT) reaction of 7-hydroxyquinoline (7-HQ) mediated by methanol molecules in two Room Temperature Ionic Liquids (RTILs). While no ESPT is observable in neat RTILs, characteristic tautomer fluorescence of 7-HQ could be observed in the presence of small quantity of methanol (0.5 – 4.1 M). The observation of a rise time (350 ps – 1.4 ns) associated with the tautomer fluorescence suggests that proton transfer in 7-HQ is indeed an excited state phenomenon that requires considerable solvent reorganization prior to the relay of proton from the hydroxyl group to the distant ring nitrogen atom through suitably organized dimeric chain of methanol molecules. The rise time of the tautomer fluorescence, which has been found to decrease with increasing methanol concentration, is attributed to the change of viscosity of the medium upon methanol addition. While the influence of viscosity on the ESPT kinetics is evident from the data, lack of any definite correlation between the bulk viscosity and rise time has been interpreted in terms of the microheterogeneous nature of the media that does not allow assessment of the microviscosity around 7-HQ from the bulk viscosity.

5.1. Introduction

Though RTILs are emerging as media of diverse application, the number of photophysical studies carried out in this novel solvent system is still comparatively less. Since proton transfer reactions play a central role in a wide variety of chemical and biological phenomena[1] and that there is hardly any study of the proton transfer reaction involving photoexcited molecules in RTILs, we have undertaken this work on 7-hydroxyquinoline (7-HQ, Chart 5.1), an amphoteric molecule that contains both acidic (–OH group) and basic (–N= group) moieties. Unlike commonly encountered excited state intramolecular proton transfer (ESIPT) reaction such as in 3-hydroxyflavone (3-HF),[2] where the proton moves from the hydroxy group to an adjacent carbonyl group on

photoexcitation without the involvement of the solvent molecules, excited state proton transfer (ESPT) reaction in 7-HQ requires participation of protic solvent molecules as the functional groups involved are far apart.[3-9] Since this process closely resembles proton relay over large distance observed in several systems, 7-HQ serves as a simple model system for understanding the mechanism of long distance proton translocation mediated by a hydrogen bonded network.

Extensive fluorescence studies have indicated that ESPT reaction in 7-HQ proceeds through the formation of 1:2 complexes (7HQ/$(ROH)_2$) (Chart 5.2) in monohydroxy alcohols such as in methanol or in hexane-alcohol.[3-10] However, in polyhydroxy alcohols such as glycerol (GL) or ethylene glycol (EG), a single alcohol molecule can give rise to ESPT in the system through 1:1 complexation.[11] The rate constant of ESPT in the complex is found to be dependent on the H-bond donating ability of the alcohols, as measured by the Kamlet-Taft acidity (α) of the alcohols.[9,12] In a recent work Jang and coworkers[9] have demonstartated that ESPT in 7HQ-$(ROH)_2$ complexes in n-alkanes is characterized by an unsually large temperature independent, and viscosity dependent kinetic isotope effect. It is shown that ESPT in this system is initiated by proton transfer from alcohol molecule to the imino nitrogen atom of 7-HQ and completed by rapid proton transfer from the enol group of the molecule to the transient alkoxide moiety. Interestingly, in viscous media such as in GL and EG[11] as well as in argon[13] and polymer matrices,[14] the keto-tautomer of 7-HQ has been observed in the ground state, but not in conventional less viscous media like hexane-alcohol, alcohols, etc.

While ESIPT reaction such as in 3-HF is hardly dependent on the viscosity of the media because of its intrinsic nature, Douhal and co-workers[11] have shown that solvent viscosity plays an important role in determining the dynamics of solvent mediated proton transfer reaction in 7-HQ. This has later been confirmed by Jang and coworkers.[9] Since two monohydroxy alcohol molecules are required to bridge the proton donor and acceptor

sites of 7-HQ for ESPT in the system and viscosity of the medium plays a crucial role in it, we realized that this system provides an opportunity to investigate the influence of viscous RTILs on the mechanism and kinetics of the ESPT process. A number of specific issues that we have addressed apart from the influence of viscosity are the following. Firstly, since the C-2 hydrogen of the imidazolium cation is acidic and known to be hydrogen bonded to the H-bond acceptors such as the anionic component of the RTILs, it is of interest to find out whether the hydrogen bonded network available in the RTILs can reorganize to give rise to ESPT in 7-HQ. Secondly, it is also of interest to find out whether small amount of methanol can break the hydrogen bonded network of the viscous RTILs and form a bridge consisting of two methanol molecules that is essential for ESPT in 7-HQ. Thirdly, unlike the conventional solvents, where the constituents are neutral molecules, RTIL provides an opportunity to study how/whether its ionic constituents can influence the long distance movements of proton in 7-HQ. In this work, methanol mediated ESPT reaction of 7-HQ has been studied in two RTILs, [bmim][Tf_2N] and [bmim][PF_6] (Chart 5.3), which differ in their viscosities significantly.

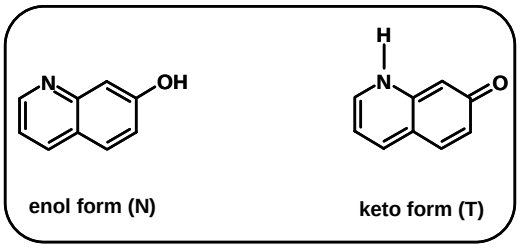

Chart 5.1. Enol and keto forms of 7-hydroxyquinoline.

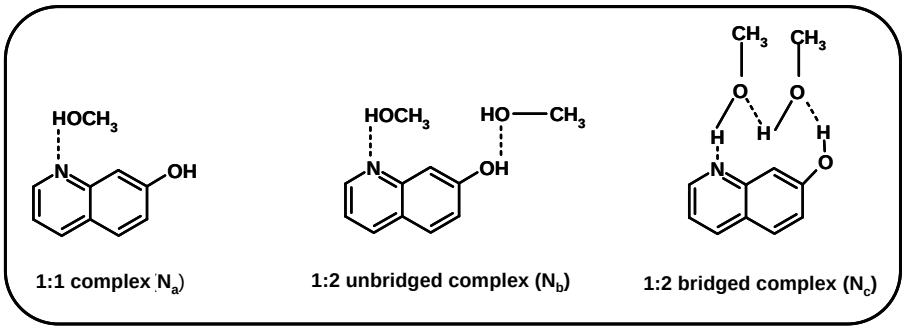

Chart 5.2. Various hydrogen-bonded enol forms of 7-hydroxyquinoline with methanol.

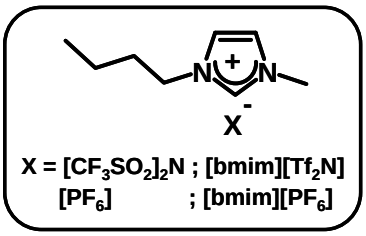

Chart 5.3. Structure and abbreviation of the RTILs used in the present work; [bmim] ≡ 1-butyl-3-methylimidazolium, [Tf_2N] ≡ bis(trifluoromethanesulfonyl)imide.

5.2. Results

5.2.1. Steady-state behavior

The absorption spectra of 7-HQ in RTILs are found similar to that observed in acetonitrile.[11] With gradual addition of methanol, the vibrational structure of the main absorption band is lost and enhanced absorption in the long wavelength region can be observed (Fig. 5.1). These changes are similar to those observed in acetonitrile-glycerol or acetonitrile-ethylene glycol systems.[11] A similar enhancement of absorption is also observed in hexane-methanol.[8,10]

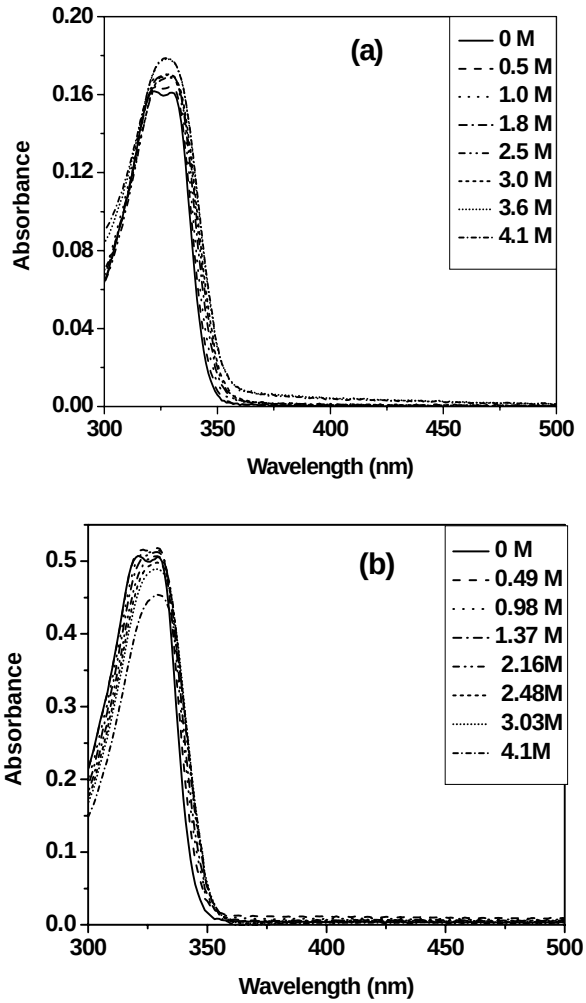

Fig. 5.1. Absorption spectra of 7-HQ in [bmim][Tf_2N] (a) and in [bmim][PF_6] (b) for different concentrations of methanol (0 – 4.1) M. Any absorption due to the RTILs in this region has been eliminated by baseline correction with neat ILs.

7-HQ in neat RTILs, when excited at around 320-330 nm, shows a single emission band with maximum at 360 nm (Fig. 5.2), a behavior very similar to that observed in acetonitrile.[11] On addition of methanol, dual emission with maxima at 360-380 nm and 540 nm (Fig. 5.2) is observed. The changes observed around the 360 nm band (small shift

and changes in intensity) in the presence of methanol are similar to those observed for the system in hexane-methanol or in acetonitrile-glycerol/ethylene glycol. With increase in concentration of methanol, a small decrease in intensity of the short wavelength emission band is accompanied with noticeable increase in the intensity of the green emission at 540 nm. The variation of the ratio of the fluorescence intensities at 540 nm and 360-380 nm is shown in Fig. 5.2.

A study of the excitation wavelength dependence of the fluorescence behavior reveals the following: With increase in the excitation wavelength, the overall fluorescence intensity of the system is decreased progressively. However, no significant change in the relative intensities of the two emission bands is observed. This is evident from the insert to Fig. 5.3. The dual emission of 7-HQ could be observed upto an excitation wavelength of 350 nm. For excitation wavelengths higher than 350 nm, where the absorption due to 7-HQ is very low, the emission due to the imidazolium ionic liquids starts interfering with the measurements.[15] However, it is found that the 540 nm emission band due to 7-HQ could not be observed for excitation wavelength higher than 375 nm. The steady state fluorescence behavior of 7-HQ in two RTILs in the presence of methanol is found qualitatively rather similar.

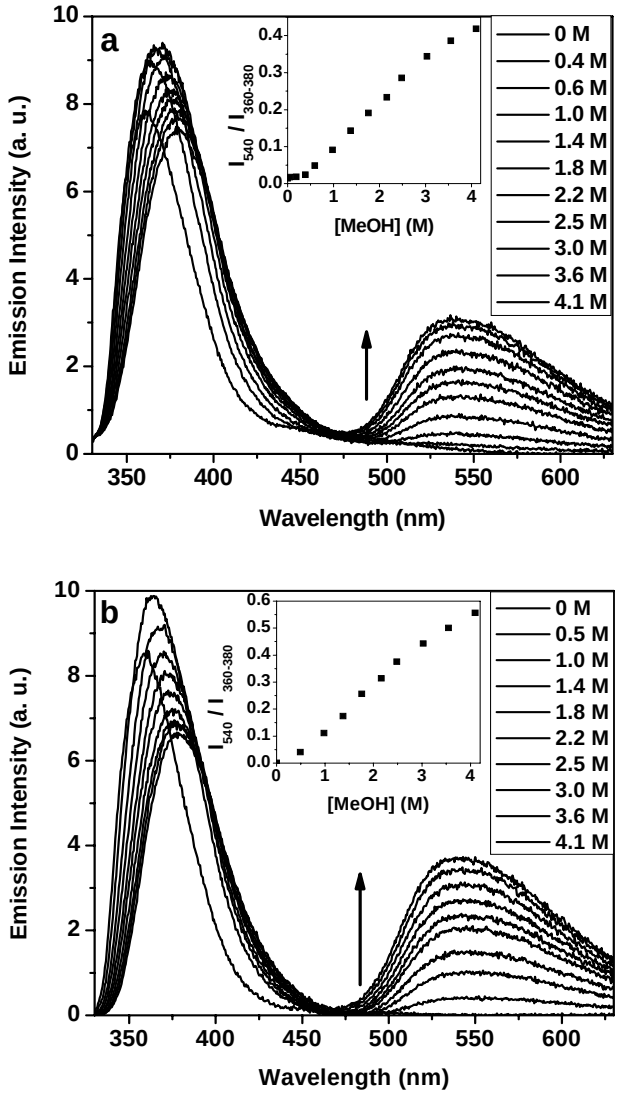

Fig. 5.2. Fluorescence spectra of 7-HQ in [bmim][Tf_2N] (a) and [bmim][PF_6] (b) for different concentrations of methanol, (0 - 4.1) M. λ_{exc} = 320 nm. Weak emission due to neat RTILs was subtracted from each of the spectra. Insert shows variation of I_{540} / $I_{360-380}$ with concentration of methanol. $I_{360-380}$ was measured at the wavelength where the fluorescence intensity is maximum.

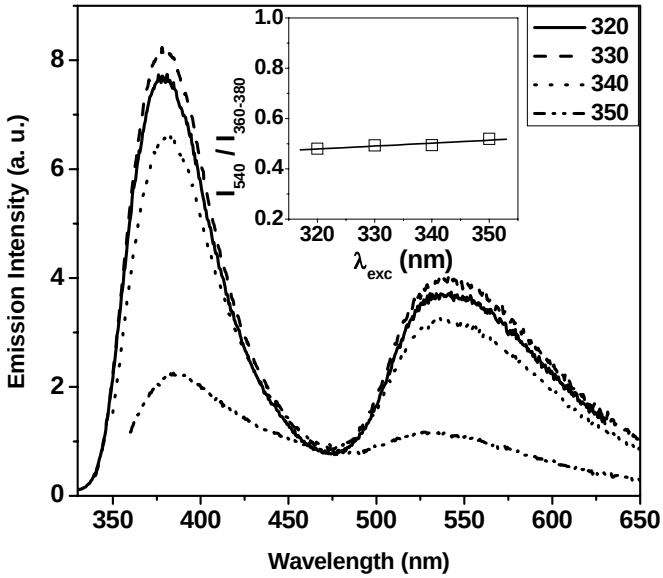

Fig 5.3. Emission spectra of 7-HQ in [bmim][PF_6] with 3.6 M methanol for different excitation wavelengths. Insert shows I_{540} / $I_{360-380}$ variance with excitation wavelength.

5.2.2. Time-resolved behavior

In order to obtain information on the dynamics of the ESPT process, the fluorescence decay behavior of the system has been studied monitoring the short wavelength (360 - 380 nm region) and long wavelength (540 nm) emission bands. Representative decay profiles are shown in Fig. 5.4. The various decay parameters corresponding to the two emission bands for different concentrations of methanol in two RTILs are collected in Tables 5.1-5.2. The decay profiles are found to be biexponential for both the bands. However, while at 360-380 nm region, both the components decay with time, the time-profile of the 540 nm band is characterized by a negative pre-exponential factor (i.e a rise component). It can be seen that the lifetime components associated with the two monitoring wavelengths are not identical. The rise component at

540 nm however is similar to one of the decay components of the short wavelength band. The lifetime values associated with the rise time and the corresponding time constant at 360 nm generally decrease with increase in the concentration of methanol. This is evident from the fact that in [bmim][Tf_2N], the short component at 360 nm decreases from 1.25 ns to 450 ps, while the long component decreases only slightly from 3.8 ns to 2.9 ns. At 540 nm, the rise time decreases from 1.35 ns to 370 ps, whereas the long component remains constant at around 2.7 ns. In [bmim][PF_6], similar changes are apparent from the data shown in Table 5.2. At 360-380 nm, the short decay time varies from 1.01 ns to 580 ps, while the longer one remains more of less constant around 2.5 ns. The rise time observed at 540 nm decreases from 1.22 ns to 350 ps with increase in concentration of methanol while the second decay time remains constant at ~2.5 ns (Table 5.2).

5.3. Discussion

5.3.1. Steady state spectral studies

The structured absorption band of 7-HQ in neat RTILs suggests that the molecule experiences an environment similar to that in polar aprotic solvent such as in acetonitrile.[11] The enhanced absorption in the longer wavelength region in presence of methanol is consistent with the literature, and is commonly attributed to the formation of H-bonded complexes of 7-HQ with methanol.[8,10] The absence of any isosbestic point in the absorption spectra in the presence of methanol indicates that 7-HQ and methanol form complexes of different stoichiometries. This conclusion is in agreement with the literature, which clearly suggests that 7-HQ forms 1:1 and 1:2 (bridged and unbridged) complexes with monohydroxy alcohols.[8-10,12] In this context, we note that there are reports[11,13,14] that in viscous condition 1:2 bridged H-bonded complex of 7-HQ often forms the tautomer in the ground state, which also contributes to the absorption in the long wavelength region. The absorption maximum of the tautomer is reported to be

around 420 – 430 nm. However, in RTILs, such tautomer formation in the ground state could not be detected from the UV-vis absorption measurements.

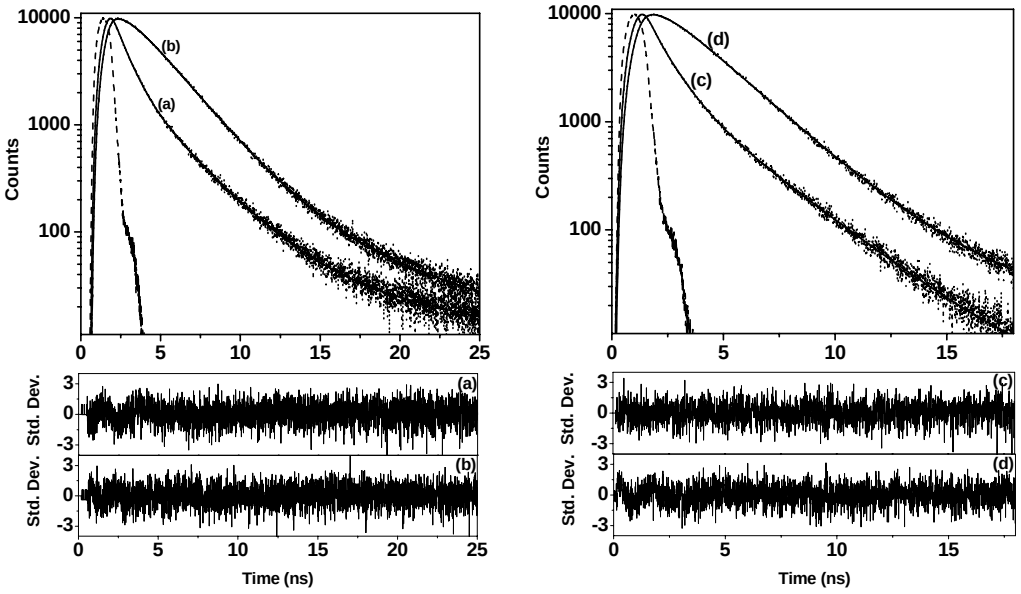

Fig. 5.4. Fluorescence decay profiles of 7-HQ at 360 and 540 nm in [bmim][Tf_2N] (a) and (b) and in [bmim][PF_6] (c) and (d) respectively for MeOH concentration of 1.8 M. The experimental decay profiles are indicated by the dots and and the instrument profile as dashs. The solid lines represent the best-fit to the decay curves. The residuals are indicated below for the respective decay profiles.

Table 5.1. Time resolved fluorescence data of 7-HQ in [bmim][Tf_2N]. λ_{exc} = 331 nm.

[MeOH] (M)	Decay Parameters[a] at 360 nm		at 540 nm		χ^2 360, 540
	τ_1 (a_1)	τ_2 (a_2)	τ_1 (a_1)	τ_2 (a_2)	
0 (49 cP)[b]	1.02 (98.8)	4.91 (1.1)			1.2
0.6	1.25 (94.9)	3.82 (5.0)	1.36 (-31.3)	2.75 (65.6)	1.3, 1.1
1.0	1.23 (92.5)	3.81 (7.5)	1.18 (-36.5)	2.55 (62.3)	1.3, 1.0
1.4	1.12 (88.7)	3.51 (11.2)	1.00 (-37.6)	2.45 (61.5)	1.3, 1.1
1.8	0.79 (79.5)	2.69 (20.1)	0.85 (-37.5)	2.39 (61.7)	1.1, 1.0
2.2	0.73 (77.8)	2.76 (21.8)	0.72 (-36.2)	2.43 (63.1)	1.1, 1.1
2.5	0.64 (76.8)	2.82 (22.8)	0.60 (-35.2)	2.49 (64.2)	1.1, 1.1
3.0	0.58 (63.6)	2.92 (36.1)	0.48 (-35.9)	2.53 (63.5)	1.1, 1.1
3.6	0.53 (62.5)	3.00 (37.2)	0.42 (-36.2)	2.73 (63.7)	1.1, 1.3
4.1 (16.6 cP)[b]	0.45 (61.7)	2.88 (38.0)	0.37 (-44.8)	2.70 (55.1)	1.1, 1.1

[a]The small percentage of the 2nd lifetime component for [Methanol] = 0 is probably due to the RTIL. The amplitudes associated with the two lifetime components in the presence of methanol add to 96.9-99.9 indicating the presence of a very small percentage (0.1-3.1 %) of another component with a long lifetime component, which is probably due to RTIL. [b]Viscosity measured[16] for 0 M and 4.1 M MeOH at 25°C.

Table 5.2. Time resolved fluorescence data of 7-HQ [bmim][PF_6]. λ_{exc} = 331 nm.

[MeOH] (M)	Decay Parameters[c] at 360 nm		at 540 nm		χ^2 360, 540
	τ_1 (a_1)	τ_2 (a_2)	τ_1 (a_1)	τ_2 (a_2)	
0 (260 cP)[d]	0.88 (96.7)	2.45 (3.3)			1.3
0.5	1.01 (86.9)	2.23 (13.1)	1.22 (-31.8)	2.57 (62.5)	1.2, 1.1
0.8	1.03 (87.4)	2.45 (12.6)	1.12 (-39.7)	2.31 (58.5)	1.2, 1.1
1.4	0.93 (83.2)	2.55 (16.8)	0.90 (-40.0)	2.24 (59.5)	1.2, 1.0
1.8	0.86 (81.6)	2.80 (18.4)	0.75 (-38.0)	2.30 (62.0)	1.1, 1.0
2.4	0.77 (66.6)	2.80 (32.5)	0.60 (-36.0)	2.35 (63.3)	1.2, 1.0
4.1 (94 cP)[d]	0.58 (51.5)	2.83 (48.5)	0.35 (-34.5)	2.51 (62.8)	1.2, 1.0

[c]The small percentage of the 2nd lifetime component for [Methanol] = 0 is probably due to the RTIL. The amplitudes associated with the two lifetime components in the presence of methanol add to 94.3-99.5 indicating the presence of a small percentage (0.5-5.7 %) of another component with a long lifetime component, which is probably due to RTIL. [d]Viscosity measured[16] for 0 M and 4.1 M MeOH at 25°C.

As far as fluorescence behaviour is concerned, the emission around 360-380 nm region is attributed to the enolic form of 7-HQ in aprotic media and to the free and various H-bonded enol forms of the molecule in protic media.[4,5,8-10,12] The green emission of 7-HQ, which is observed only in protic media, is attributed to the tautomer.[4,5,8-10,12] Since the 540 nm emission could not be observed in neat RTILs, it can be concluded that the imidazolium cations, which serves as an H-bond donor through the C-2 hydrogen, cannot form a H-bonded network with 7-HQ that allows ESPT in the system in the absence of methanol.

As stated previously, extensive studies have indicated that free enol and various H-bonded forms of 7-HQ emit around 360-380 nm region and that these species could not be distinguished by their emission spectra. Hence, the changes observed around this region in the presence of methanol are to be attributed to the formation of the species, which include free enol and its 1:1, 1:2 bridged and 1:2 unbridged complexes. While the blue emission at 360-380 is assigned to the various uncomplexed and complexed enol forms of 7-HQ, the green fluorescence is attributed to the tautomer.[7] The observation of the 540 nm emission in the presence of methanol indicates that ESPT of 7-HQ does occur in RTILs when methanol is present. This implies that methanol molecules can break the existing network of the RTILs and also form the bridged configuration, which eventually gives rise to the formation of the tautomer. The excitation wavelength dependent emission studies confirm lack of formation of the 7-HQ tautomer in the ground state in RTILs. This may not be surprising as the microviscosity around 7-HQ is significantly lower than that necessary for the formation of tautomer even in the presence of small quantity of methanol. The dependence of the intensity of the 540 nm emission band on methanol concentration may appear surprising as it is reported that methanol concentration does not affect the dynamics of the ESPT reaction in this system. However, it is shown in the following section that dependence of the tautomer emission intensity in RTILs is the result of a large change in viscosity of the medium and consequent change in the ESPT kinetics on methanol addition.

5.3.2. Time-resolved spectral studies

Fluorescence decays monitored at different emission wavelengths give a clear picture of the excited state dynamics. If the mechanism of ESPT in RTILs is governed by Scheme 5.1, which involves an equilibrium between $\mathbf{N_C}^*$ and $\mathbf{T}^*$ in the excited state, the time profiles of the two species are then given by equations (5.1) and (5.2) implying that the two decay times associated with $\mathbf{N_C}^*$ and $\mathbf{T}^*$ are identical.

Scheme 5.1.

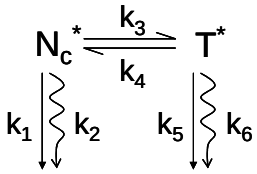

$$\left[N_c{}^*\right] = \frac{\left[N_c{}^*\right]_0}{\lambda_2 - \lambda_1}\left[(\lambda_2 - X)e^{-\lambda_1 t} + (X - \lambda_1)e^{-\lambda_2 t}\right] \tag{5.1}$$

$$\left[T^*\right] = \frac{k_3\left[N_c{}^*\right]_0}{\lambda_2 - \lambda_1}\left[e^{-\lambda_1 t} - e^{-\lambda_2 t}\right] \tag{5.2}$$

where, $X = k_1+k_2+k_3$, $Y = k_4+k_5+k_6$,

$$\lambda_1 = \frac{1}{2}\left\{(X+Y) - \left[(X-Y)^2 + 4k_3k_4\right]^{1/2}\right\}$$

$$\lambda_2 = \frac{1}{2}\left\{(X+Y) + \left[(X-Y)^2 + 4k_3k_4\right]^{1/2}\right\}$$

However, if the equilibrium between the two species is not established in the excited state and the formation of **T*** from $\mathbf{N_C}$* is represented by Scheme 5.2, the time dependence of $\mathbf{N_C}$* and **T*** are given by equations (5.3) and (5.4), according to which $\mathbf{N_C}$* should show a single exponential decay and **T*** exhibit a rise time identical with the decay time of $\mathbf{N_C}$* and a decay time that represents the lifetime of **T*** under the experimental condition.

Scheme 5.2.

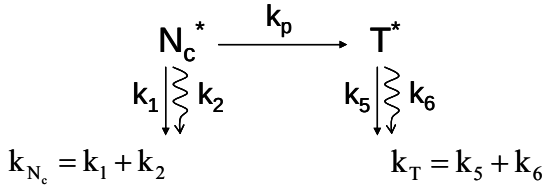

$$\left[N_c^*\right] = \left[N_c^*\right]_0 e^{-\left(k_{N_c} + k_p\right)t} \tag{5.3}$$

$$\left[T^*\right] = \left(\frac{\left[N_c^*\right]_0 k_p}{k_{N_c} + k_p - k_T}\right)\left[e^{-k_T t} - e^{-\left(k_{N_c} + k_p\right)t}\right] \tag{5.4}$$

It appears that the present kinetic data in RTILs (Tables 5.1 and 5.2) is not consistent with either of the mechanisms. However, the data can be easily be interpreted in terms of the 2nd mechanism when one also considers the fact that various enol forms (**N**, $\mathbf{N_a}$, $\mathbf{N_b}$ and $\mathbf{N_c}$) of 7-HQ contribute to emission around the same wavelength region (360 – 380 nm),[9,11] but only one of them, specifically $\mathbf{N_c}$*, is responsible for the formation of **T***. This implies that the second decay time (the long component) associated with the 360 - 380 nm emission arises from the free and H-bonded enol forms of 7-HQ, which do not contribute to ESPT, i.e. **N**, $\mathbf{N_a}$ and $\mathbf{N_b}$. In fact, a similar mechanism is used to account for the time-resolved data of 7-HQ in conventional solvents. The short time-constant, which decreases with increasing amount of methanol, is due to $\mathbf{N_c}$* from which the tautomer is produced. This decay time matches reasonably well with the rise time of the tautomer emission at 540 nm. The rise time, which is the reciprocal of the rate constant of the ESPT reaction, decreases with increasing amount of methanol. It should be noted in this context that Jang and coworkers did not observe any variation of the rise time of the tautomer emission of 7-HQ in alkanes with methanol concentration. However, this result

is not surprising when one considers the change in viscosity of the media on addition of methanol in the two cases and its influence on the ESPT kinetics. It is well known that ESPT in $\mathbf{N_c^*}$ requires readjustment or fluctuation of the solvent nuclear coordinates prior to complete transfer of proton. Therefore, the rate determining step of ESPT in 7-HQ is determined by the rate at which solvent molecules readjust to facilitate ESPT. Since the viscosity of the medium is lowered on addition of methanol (from 260 to 94 cP in [bmim][PF_6] and from 49 to 16.6 cP in [bmim][Tf_2N] in the presence of 4.1 M methanol) the solvent reorganization becomes faster and so is the risetime for the ESPT process. However, when the ESPT process is studied in less viscous alkanes, the change of viscosity on addition of methanol is not so appreciable and hence, the influence of the effect of methanol on the rise time is not evident.

ESPT of 7-HQ in RTILs is expected to be slow because of viscous nature of the media and the requirement of conformational readjustments prior to the proton transfer process. The influence of high viscosity of the RTILs is evident from the long rise time of the tautomer fluorescence observed for small concentrations of methanol. In the presence of 0.49 – 0.59 M methanol, the rise times are in the range of 1.2 – 1.4 ns. These values are considerably higher than those in conventional solvents clearly due to the viscous nature of the RTILs. However, a close look into these values reveals that the viscosity dependence is not so straightforward and the rise times are not solely determined by the bulk viscosities of the media. Even though [bmim][PF_6] is more than 5 times viscous than [bmim][Tf_2N], the risetimes in [bmim][PF_6] are slightly lower than those in [bmim][Tf_2N] for similar quantity of methanol. For example, in the presence of 0.49 M methanol, the rise time in [bmim][PF_6] is 1.2 ns, whereas in less viscous [bmim][Tf_2N] in the presence of 0.59 M methanol the value is higher at 1.4 ns. One can also compare the rise times listed in the last row of the two Tables. In the presence of 4.1 M methanol, when the bulk viscosity of [bmim][PF_6] is 94 cP, the rise time is measured to be 346 ps.

On the other hand, under similar condition, the bulk viscosity of [bmim][Tf_2N] is much lower (16.6 cP) and yet, the rise time is very similar (367 ps). These results can only be explained when the viscosity around 7-HQ is quite different from the measured bulk viscosity of the RTILs. Considering the microheterogeneous nature of the RTILs, which has been indicated in recent studies,[17-20] the existence of small domains/pockets in these media having viscosity quite different from the bulk viscosity is indeed consistent with literature.[21]

5.4. Conclusion

Solvent mediated excited state proton transfer reaction has been studied in RTILs employing 7-HQ, wherein the proton donor and acceptor groups are at some distance away and the proton transfer requires participation of the protic solvent molecules in an orderly manner. The results suggest that it is possible for the methanol molecules to form a bridged hydrogen-bonded architecture with 7-HQ in RTILs that is necessary for the proton relay in the system. The change in the kinetics of the ESPT process with methanol concentration has been attributed to a change of the viscosity of the medium. The lack of any proper correlation between the bulk viscosity and ESPT kinetics is attributed to the presence of micro/nano domains in RTILs having viscosity significantly different from the bulk viscosity.

References and notes

1. (a) Tanner, C.; Manca, C.; Leutwyler, S. *Science* **2003**, *302*, 1736. (b) Rini, M.; Magnes, B.-Z.; Pines, E.; Nibbering, E. T. J. *Science* **2003**, *301*, 349. (c) Gutman, M.; Nachliel, E. *Annu. Rev. Phys. Chem*. **1997**, *48*, 329. (d) Douhal, A.; Kim, S. K.; Zewail, A. H. *Nature* **1995**, *378*, 260. (e) Lill, M. A.; Helms, V. *Proc. Natl. Acad. Sci. USA* **2002**, *99*, 2778.
2. (a) Sengupta, P. K; Kasha, M. *Chem. Phys. Lett*. **1979**, *68*, 382. (b) MaMorrow, D.; Kasha, M. *J. Phys. Chem*. **1984**, *88*, 2235.
3. Mason, S. F.; Philip, J.; Smith, B. E. *J. Chem. Soc*. **1968**, 3051.
4. Thistlethwaite, P. J.; Corkill, P. J. *Chem. Phys. Lett*. **1982**, *85*, 317.
5. Thistlethwaite, P. J. *Chem. Phys. Lett*. **1983**, *96*, 509.
6. Itoh, M.; Adachi, T.; Tokumara, K. *J. Am. Chem. Soc*. **1983**, *105*, 4828.
7. Tokumara, K.; Itoh, M. *J. Phys. Chem*. **1984**, *88*, 3921.
8. Itoh, M.; Adachi, T.; Tokumara, K. *J. Am. Chem. Soc*. **1984**, *106*, 850.
9. Kwon, O-H.; Lee, Y-S.; Yoo, B. K.; Jang, D-J. *Angew. Chem. Int. Ed*. **2006**, *45*, 415.
10. Nakagawa, T.; Kohtani, S.; Itoh, M. *J. Am. Chem. Soc*. **1995**, *117*, 7952.
11. Ochoa-G.; Bisht, P. B.; Sanchez, F.; Martinez-Ataz, E.; Santos, L.; Tripathi, H. B.; Douhal, A. *J. Phys. Chem. A* **1998**, *102*, 8871.
12. Kohtani, S.; Tagami, A.; Nakagaki, R. *Chem. Phys. Lett*. **2000**, *316*, 88.
13. Lavin, A.; Collins, S. *Chem. Phys. Lett*. **1993**, *207*, 513.
14. (a) Douhal, A.; Sastre, R. *Chem. Phys. Lett*. **1994**, *219*, 91. (b) Douhal, A.; Dabrio, J.; Sastre, R. *J. Phys. Chem*. **1996**, *100*, 149. (c) Kwon, O-H.; Doo, H.; Lee, Y-S., Jang, D-J. *Chem. Phys. Chem*. **2003**, *4*, 1079.
15. Paul, A.; Mandal, P. K.; Samanta, A. *J. Phys. Chem. B* **2005**, *109*, 9148.
16. The viscosity of the ionic liquid was measured by a LVDV-III Ultra Brookfield Cone and Plate viscometer (1% accuracy and 0.2% repeatability).
17. Samanta, A. *J. Phys. Chem. B* **2006**, *110*, 13704.
18. Mandal, P. K.; Sarkar, M.; Samanta, A. *J. Phys. Chem. A* **2004**, *108*, 9048.
19. Mandal, P. K.; Paul, A.; Samanta, A. *J. Photochem. Photobiol. A: Chem*. **2006**, *182*, 113.
20. (a) Padua, A. A. H.; Costa Gomes, M. F.; Lopes, J. N. A. C. *Acc. Chem. Res*. **2007**, *40*, 1087. (b) Lopes, J. N. A. C.; Padua, A. A. H. *J. Phys. Chem. B* **2006**, *110*, 3330. (c) Triolo, A.; Russina, O.; Bleif, H.-J.; Di Cola, E. *J. Phys. Chem. B* **2007**, *111*, 4641. (d) Shigeto, S.; Hamaguchi, H. *Chem. Phys. Lett*. **2006**, *427*, 329. (e) Iwata, K.; Okazima, H.; Saha, S.; Hamaguchi, H. *Acc. Chem. Res*. **2007**, *40*, 1174. (f) Xiao, D.; Rajian, J. R.; Cady, A.; Li, S.; Bartsch, R. A.; Quitevis, E. L. *J. Phys. Chem. B* **2007**, *111*, 4669. (g) Jin, H.; Li, X.; Maroncelli, M. *J. Phys. Chem. B* **2007**, *111*, 13473. (h) Hu, Z.; Margulis, C. J. *Acc. Chem. Res*. **2007**, *40*, 1097. (i) Hu, Z.; Margulis, C. J. *Proc. Natl. Acad. Sci*. **2006**, *103*, 831. (j) Wang, Y.; Jiang, W.; Yan, T.; Voth, G. A. *Acc. Chem. Res*. **2007**, *40*, 1193. (k) Wang, Y.; Voth, G. A. *J. Am. Chem. Soc*. **2005**, *127*, 12192. (l) Adhikari, A.; Sahu, K.; Dey, S.; Ghosh, S.; Mandal, U.; Bhattacharyya, K. *J. Phys. Chem. B* **2007**, *111*, 12809.
21. (a) Gutowski, K. I.; Japas, M. L.; Aramendia, P. F. *Chem. Phys. Lett*. **2006**, *426*, 329. (b) Lu, J.; Liotta, C. L.; Eckert, C. A. *J. Phys. Chem. A* **2003**, *107*, 3995.

Chapter 6

Interaction of Bovine Serum Albumin and Human Serum Albumin with Dipolar Molecules: Fluorescence and Molecular Docking Studies

Interaction of bovine serum albumin (BSA) and human serum albumin (HSA) with two series of dipolar molecules having both rigid and flexible structures has been studied by monitoring the spectral and temporal behavior of the intramolecular charge transfer (ICT) fluorescence of the systems. The binding sites of the molecular systems in BSA have been located with the help of docking studies. Binding in the hydrophobic domains of BSA/HSA leads to blue shift of the fluorescence spectra and enhancement of fluorescence intensity and lifetime. This enhancement is found to be the largest for flexible systems in which internal motion serves as a nonradiative decay route. In BSA/HSA-bound condition, some of the dipolar molecules exhibit not-so-common 'dip-rise-dip' time-resolved fluorescence anisotropy profiles. It is shown that a large difference of the fluorescence lifetimes of the protein-bound and free molecules is one of the factors that contribute to this kind of anisotropy profiles. As internal motion is often responsible for the short fluorescence lifetime of the flexible dipolar molecules, a large increase in the fluorescence lifetime of these systems occurs if binding to BSA/HSA leads to disruption/prevention of this motion. It thus appears that it might be possible to obtain information on the prevention/disruption of nonradiative pathway on protein binding from the anisotropy profiles of the kind discussed above. However, since the present study reveals cases where a large change in fluorescence lifetime also occurs due to other reasons, one needs to be careful prior to making any conclusion.

6.1. Introduction

Dipolar molecules are routinely used as fluorescence probes for the study of various complex chemical and biological systems.[1-4] Photoexcitation of these molecules, often termed as electron donor-acceptor (EDA) molecules, results in enhanced separation of charge and these systems commonly emit from an intramolecular charge transfer state. Consequently, the fluorescence parameters of these systems are sensitive to the environment. The wavelength or wavenumber corresponding to the fluorescence

maximum, fluorescence quantum yield, nature of the fluorescence decay profile and fluorescence lifetime are the most commonly monitored fluorescence properties for obtaining information such as the location of the probe in organized assembly, polarity or viscosity of the microenvironment, etc.[3,4] Time-resolved fluorescence anisotropy is also studied to obtain information on the rotational dynamics of the probes.[5] In homogeneous medium, the fluorescence anisotropy usually decreases exponentially with time and the associated time constant provides a measure of the rotational dynamics of the molecule. However, when a probe is distributed in two distinct regions of an organized assembly and when the molecular motion in the two regions occurs in significantly different time scales, the time-resolved anisotropy commonly decays biexponentially with the time constants representing two different time scales of the rotation motion in two regions.[5] A complex multiexponential fluorescence anisotropy decay is expected in the case of a more heterogeneous probe distribution. Studies of time-dependence of the anisotropy profiles of molecular systems in various organized assemblies have revealed more complex and somewhat peculiar anisotropy profiles in some cases.[6] During the course of our studies on the fluorescence response of some common fluorescence probes in various organized assemblies, we found some instances where the fluorescence anisotropy profiles are characterized by a rise component. In this work, we report on the interaction of several commonly used fluorescence probes with bovine serum albumin (BSA) and human serum albumin (HSA) whose presence gives rise to complex time-resolved anisotropy profiles of the kind just described for some of the systems.

Probe molecules belonging to two classes, aminocoumarins and aminonitrobenzoxadiazoles, have been chosen for this purpose (Chart 6.1). Both rigid and flexible aminocoumarins have been selected. While C153 is perhaps the most extensively used probe for the study of solvation dynamics in different media,[7] other coumarin derivatives are also frequently used as fluorescent probes for studying the interaction with

macromolecules like, surfactants[8] and proteins.[9] Twisting (internal rotation) of the amino group is known to play an important role in dictating the fluorescence efficiency and lifetime of aminocoumarins bearing flexible amino groups.[10] A low-lying non-fluorescent twisted intramolecular charge transfer (TICT) state has been speculated in the case of flexible aminocoumarins.[10] The twisting motion of the dialkylamino moiety is severely restricted in environments of cyclodextrins, and micelles.[3b] Literature suggests that constrained environment of protein suppresses the formation of the TICT state in these systems.[9b,11] 4-amino-7-nitrobenz-oxa-1,3-diazoles (NBD) are also extensively used as EDA fluorophores for the study of biological and model membranes.[12] NBD chloride has often been used for labeling proteins, in exploring the protein structure and conformational changes.[13] Fluorescence sensory behavior of NBD-labeled supramolecular systems toward the transition metal ions has also been studied.[14] While early studies indicated the involvement of a nonemissive TICT state in the photophysics of NBD derivatives,[15] a more detailed and recent study on several structurally related NBD derivatives has indicated that nonradiative deactivation in these systems is better described by nitrogen inversion than twisting of the amino functionality.[16] Nevertheless, it is expected that internal rotation or nitrogen inversion will be significantly retarded in protein-bound condition. The rigid probes that we have selected here are expected to serve as reference systems in which no increase in fluorescence intensity or lifetime is expected due to suppression of the internal motion.

As stated, this work is primarily triggered by our observation of complex time-dependent anisotropy profiles of some commonly used fluorescence probes in the presence of BSA and HSA. Our primary objective is not only to understand the nature of the anisotropy profiles, but also to find out whether the nature of anisotropy profile has any connection to the internal rotation in flexible aminocoumarins or nitrogen inversion in the NBD derivatives. If one can indeed establish such a connection, it might be

possible to extract information relating to the internal motion in the molecule from the anisotropy profiles, which is something that has not been explored previously. In addition to the steady state and time-resolved fluorescence behavior of the molecules in the presence of different quantity of BSA and HSA we have investigated the local environment of the probes in BSA-bound condition through molecular docking studies.

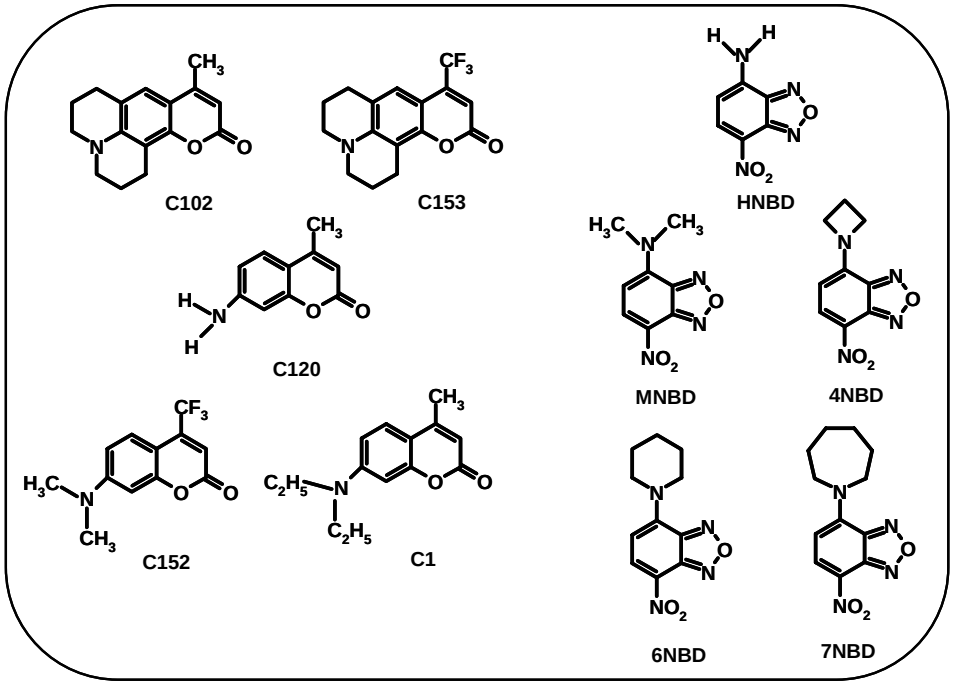

Chart 6.1. Aminocoumarins and 4-amino-7-nitrobenz-oxa-1,3-diazoles (NBD) derivatives used in the study.

6.2. Steady-state behavior

Addition of BSA and/or HSA results in small changes in the absorption spectra of the systems, which is evident from the representative spectra shown in Fig. 6.1. Interestingly, BSA/HSA induced changes in the fluorescence spectra of the systems

(spectral shift or intensity distribution) are much more pronounced. This is evident from some of the representative set of spectra (Fig. 6.2).

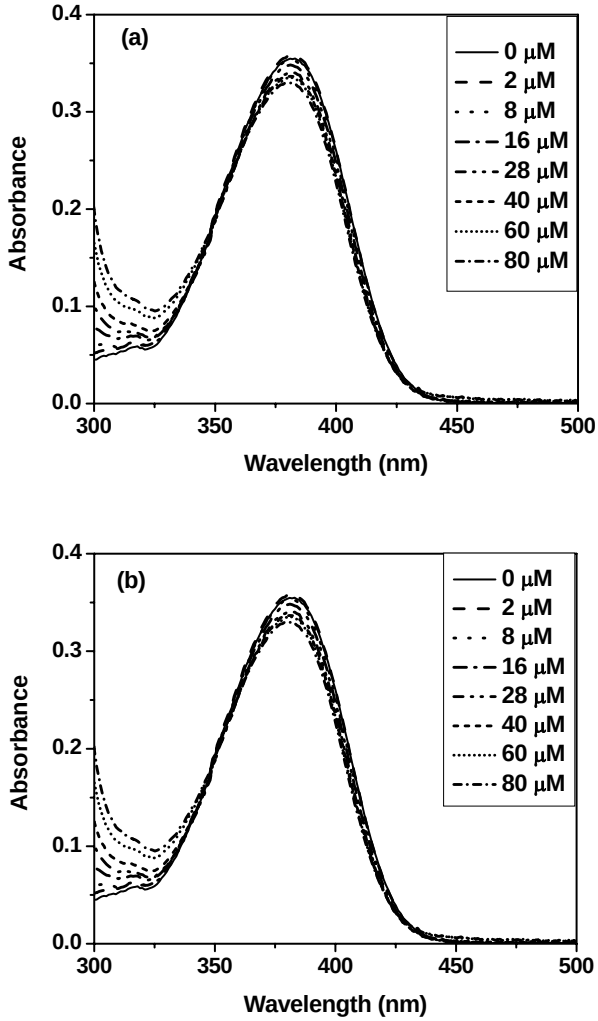

Fig. 6.1. Absorption spectra of C1 for various concentrations of BSA (a) and HSA (b).

With the exception of C120, all systems show significant blue shift of the emission maximum in presence of BSA and/or HSA. On the basis of the spectral data of the

systems in different solvents one can attribute this blue shift to the entry of these molecules from aqueous solution to the hydrophobic domains of BSA and HSA. Fig. 6.3 shows how the spectral shift of different systems varies with concentration of BSA. Lack of spectral shift for C120 is consistent with its hydrophilic nature.[17] That the spectral shift of most of the other systems is accompanied by enhancement of fluorescence intensity is consistent with a higher fluorescence yield of these systems in relatively less polar environment. The extent of fluorescence enhancement (FE) varies for system to system. The variation of fluorescence intensity of the systems as a function of the concentration of BSA is shown in Fig. 6.4. C102, which shows blue shift comparable to other systems (indicating its binding in the hydrophobic pocket of BSA/HSA) however displays small FE. This may not be surprising as ϕ_f of C102 is quite high in aqueous environment (Table 6.1). Very similar is the case of C120 for which no FE, but slight quenching is observed. Interesting are the cases of 6NBD and 7NBD among the NBD derivatives, and C1 and C152 among the coumarins. These systems show higher enhancement compared to the remaining systems of each class. For C1, C152, 6NBD and 7NBD, a higher FE can be rationalized taking into consideration the fact that FE in these systems not only arises due to binding of these molecular systems in the hydrophobic domain of BSA or HSA, but also due to prevention/restriction of internal motion in these systems which is known to be responsible for low fluorescence efficiency of these systems compared to the remaining ones (Table 6.1) in polar media.[3b,10,16]

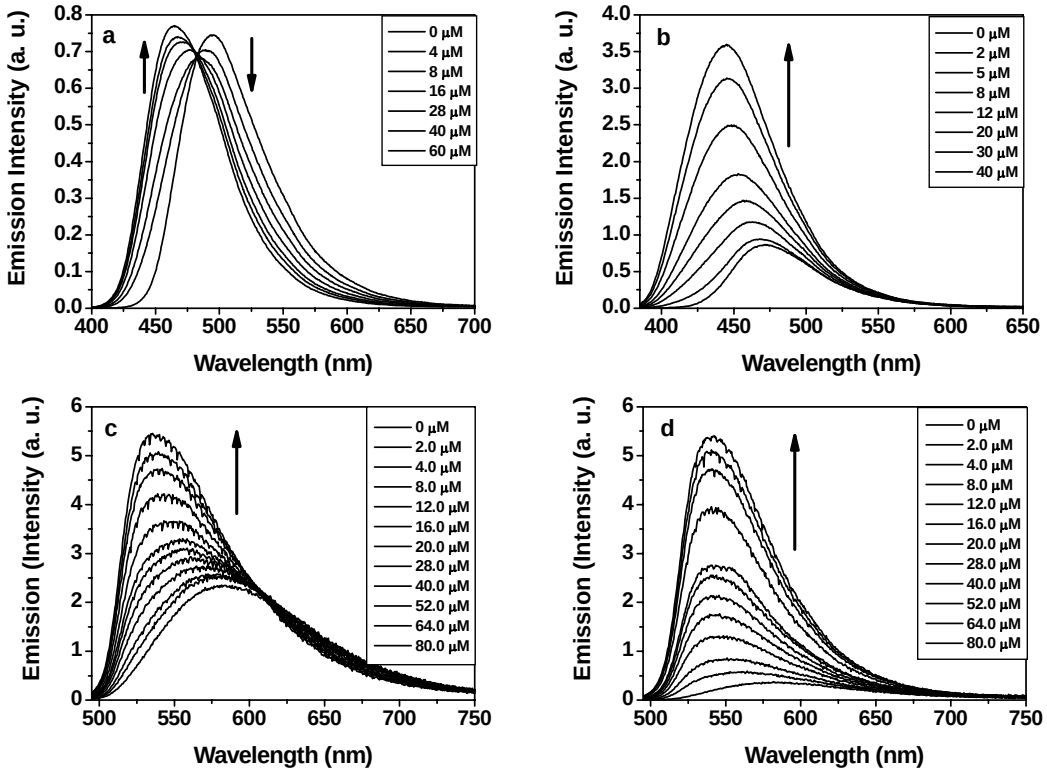

Fig. 6.2.A. Emission spectra of C102 (a), C1 (b), 4NBD (c) and 6NBD (d) for various concentrations of BSA. Fluorescence measurements are carried out in 1cm cuvettes, with the concentration of the dyes in the range of (1-3) x 10^{-5} M^{-1}.

It is interesting to note that for 6NBD and 7NBD, the saturation of the spectral shift occurs at a lower concentration of BSA when compared with the saturation of fluorescence intensity. This difference must be related to the fact that while the spectral shift depends only on the polarity of the medium and it saturates as soon as the molecule reaches the most hydrophobic region, the fluorescence intensity of these flexible systems also depends on the constraint provided by the media. A more constrained environment at higher concentrations of BSA can contribute to the observation. Again, some difference in the fluorescence response of the systems could however be observed when it is compared in two protein environments. For example, on addition of HSA the fluorescence of HNBD is slightly quenched unlike negligible enhancement observed with BSA (Table 6.1). For C1 and C152, HSA induced fluorescence enhancement (FE) is found to be somewhat less compared to BSA. Again, FE induced by HSA is much higher for 6NBD and 7NBD when compared to BSA. It appears that the restriction of internal motion in 6NBD and 7NBD is more in HSA environment than in BSA while the effect of HSA is less for the flexible coumarins.

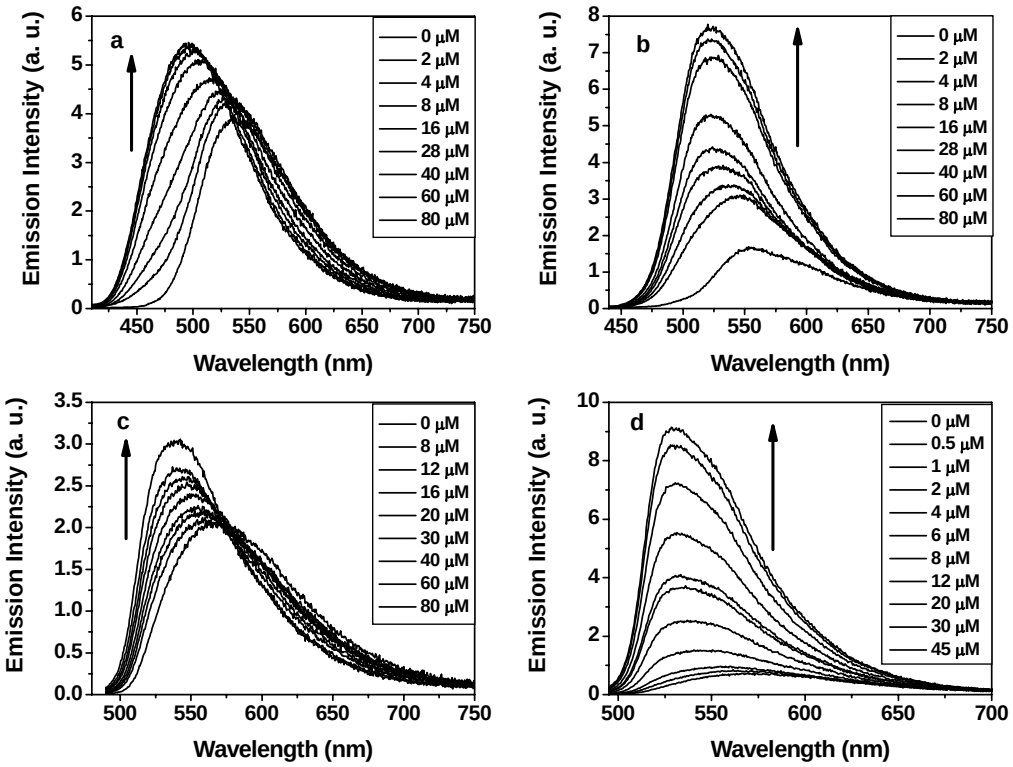

Fig. 6.2.B. Emission spectra of C152 (a), C153 (b), MNBD (c) and 7NBD (d) for various concentrations of HSA. Fluorescence measurements are carried out in 1cm cuvettes, with the concentration of the dyes in the range of (1-3) x 10^{-5} M^{-1}.

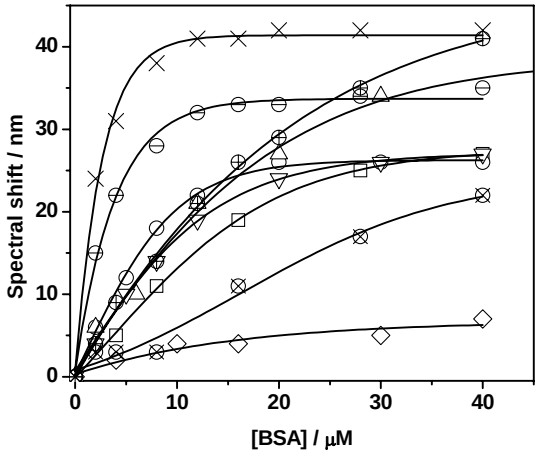

Fig. 6.3. Plot of shift of the spectral maximum for the systems (C102: □; C153: O; C152: Δ; C1: ∇; HNBD: ◊; MNBD: ⊗; 4NBD: ⊕; 6NBD: ×; 7NBD: Θ) versus concentration of BSA.

Table 6.1. Steady-state fluorescence parameters and the measured binding constants for the systems.

System	Φ_f [a]	Blue-shift[c] /nm		FE[d]	
		BSA	HSA	BSA	HSA
C102	0.66	27	32	1.8	2.0
C153	0.12	26	30	7.5	7.9
C120	0.94	nil	nil	0.9	0.9
C152	0.06	37	38	5.4	2.7
C1	0.055	27	25	8.7	6.9
HNBD	0.028[b]	7	11	1.1	0.8
MNBD	0.01	22	23	1.6	1.5
4NBD	0.02	41	48	3.0	4.6
6NBD	0.002	42	47	18.7	56.1
7NBD	0.004	35	41	9.3	24.4

[a]For [protein] = 0, collected from refs. 10b, 16, 17, 18. [b]Fluorescence quantum yield of HNBD was determined using MNBD as reference (ϕ_f = 0.01 in water).[16] [c]Shift of the fluorescence maximum observed for [BSA] = 40 μM. [d]Measured at the fluorescence maximum for [BSA] = 40 μM.

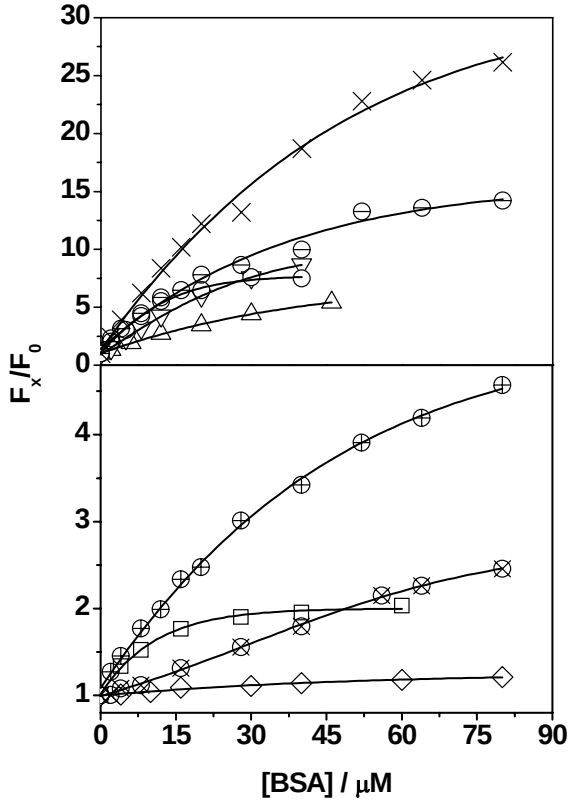

Fig. 6.4. Plot of enhancement of fluorescence intensity (measured at a wavelength where the fluorescence intensity is maximum in presence of BSA) for the systems (C102: □; C153: ○; C152: Δ; C1: ∇; HNBD: ◊; MNBD: ⊗; 4NBD: ⊕; 6NBD: ×; 7NBD: ϴ) versus the concentration of BSA.

Assuming 1:1 interaction between the two, one can evaluate the binding constants of the probes with BSA and HSA by monitoring the changes in the fluorescence intensity using frequently used equation:[19]

$$1/(F_x-F_0) = 1/(F_\infty-F_0) + 1/(F_\infty-F_0)K[L]$$

where, F_0, F_x and F_∞ are the fluorescence intensities of the probes in absence of BSA/HSA, at an intermediate BSA/HSA concentration, and at a concentration corresponding to complete interaction, respectively, and [L] is the BSA/HSA concentration. While estimates of the binding constants can be made using this method, precise estimation of the K values from the intensity measurements may not be practical (and hence, not attempted) as for some systems FE is solely due to binding in the hydrophobic domain, while for some other systems FE is also due to disruption of the internal motion. For rigid coumarins, the K values are estimated to be around 95×10^3 M^{-1} with BSA and (150-200) $\times 10^3$ M^{-1} with HSA.

6.3. Time-resolved behavior

Fluorescence lifetimes of the coumarins vary between 0.4 and 5.9 ns in the aqueous solution. Rigid system C102 has the highest lifetime (Table 6.2). The other rigid system C153 has a lifetime of 1.7 ns. C1 and C152, for which a low-lying nonfluorescent TICT state has been proposed, are characterized by fluorescence lifetime of 0.4 and 0.5 ns. The fluorescent state of the NBD derivatives is much short-lived. In fact, the fluorescent lifetimes of 6NBD and 7NBD are found comparable to the pulse width (98 ps) of the exciting pulse and hence, could not be determined precisely in the absence of BSA/HSA. The short fluorescence lifetime is a reflection of efficient nonradiative deactivation associated with the inversion of the amino nitrogen in these systems.[16] On the other hand, HNBD or 4NBD, for which radiationless process is shown to be unimportant,[16] possess lifetime of 0.9 to 1.0 ns (Table 6.3).

Table 6.2. Time-resolved fluorescence parameters of the coumarins in presence of different quantities of BSA and HSA.

System	BSA				HSA			
	Conc. /(μM)	τ_1 (a_1) / ns	τ_2 (a_2) / ns	τ_2/τ_1	Conc. /(μM)	τ_1 (a_1) / ns	τ_2 (a_2) / ns	τ_2/τ_1
C102	0	5.9			0	5.9		
	4	5.9			8	5.9		
	16	5.8			16	6.0		
	40	5.7			40	6.0		
C153	0	1.7			0	1.7		
	2	1.7 (0.81)	5.1 (0.19)	3.0	2	1.5 (0.8)	5.3 (0.19)	3.5
	8	1.8 (0.59)	5.1 (0.41)	2.8	8	0.9 (0.66)	5.2 (0.33)	5.8
	20	1.8 (0.48)	5.3 (0.52)	2.9	28	0.8 (0.59)	5.5 (0.41)	6.9
	40	1.7 (0.41)	5.2 (0.59)	3.0	40	1.2 (0.49)	5.7 (0.51)	4.7
C152	0	0.5		0	0.5			
	6	0.5 (0.93)	4.4 (0.07)	8.8	8	0.5 (0.92)	4.5 (0.08)	9.0
	12	0.5 (0.85)	4.6 (0.15)	9.2	16	0.6 (0.83)	4.8 (0.17)	8.0
	20	0.6 (0.7)	4.7 (0.29)	7.8	28	0.7 (0.68)	5.0 (0.32)	7.1
	30	0.7 (0.62)	4.8 (0.38)	6.8	40	0.8 (0.57)	5.1 (0.43)	6.4
C1	0	0.4			0	0.4		
	2	0.3 (0.98)	3.6 (0.02)	12.0	2	0.4 (0.96)	4.0 (0.04)	10.0
	8	0.4 (0.84)	4.0 (0.16)	10.0	8	0.5 (0.81)	4.2 (0.19)	8.4
	20	0.5 (0.52)	4.1 (0.48)	8.2	16	0.6 (0.64)	4.2 (0.36)	7.0
	40	0.6 (0.36)	4.1 (0.64)	6.8	40	0.8 (0.44)	4.3 (0.56)	5.4

Table 6.3. Time-resolved fluorescence parameters of the NBD derivatives in presence of different quantities of BSA and HSA.

System	BSA				HSA			
	Conc. /(μM)	τ_1 (a_1) / ns	τ_2 (a_2) / ns	τ_2/τ_1	Conc. /(μM)	τ_1 (a_1) / ns	τ_2 (a_2) / ns	τ_2/τ_1
HNBD	0	0.9			0	0.9		
	8	0.9 (0.98)	6.5 (0.02)	7.2	8	0.9 (0.99)	8.2 (0.01)	9.1
	60	1.0 (0.91)	7.5 (0.09)	7.5	30	1.0 (0.96)	8.2 (0.04)	8.2
	80	1.1 (0.89)	7.7 (0.11)	7.0	80	1.0 (0.9)	8.0 (0.1)	8.0
MNBD	0	0.2						
	20	0.3 (0.88)	3.4 (0.12)	11.3				
	40	0.5 (0.77)	3.4 (0.23)	6.8				
	80	0.6 (0.71)	3.8 (0.29)	6.3				
4NBD	0	0.99			0	1.0		
	8	1.0 (0.94)	6.4 (0.06)	6.4	5	1.0 (0.95)	6.0 (0.05)	6.0
	40	1.2 (0.68)	6.2 (0.32)	5.2	20	1.3 (0.66)	6.5 (0.34)	5.0
	80	1.5 (0.57)	6.9 (0.43)	4.6	30	1.5 (0.57)	6.5 (0.43)	4.3
6NBD	0				0			
	2	0.1 (0.96)	3.8 (0.04)	38.0	1	0.3 (0.91)	3.3 (0.09)	11.0
	8	0.8 (0.75)	5.3 (0.25)	6.6	1.5	0.4 (0.81)	3.4 (0.19)	8.5
	16	1.1 (0.7)	5.4 (0.3)	4.9	2	0.5 (0.71)	3.8 (0.29)	7.6
	40	1.2 (0.66)	5.4 (0.34)	4.5	3	1.0 (0.61)	4.4 (0.39)	4.4
	80	1.4 (0.62)	6.0 (0.38)	4.3	5	1.3 (0.6)	4.8 (0.4)	3.7
					20	1.8 (0.51)	5.1 (0.49)	2.8

In the presence of BSA/HSA no change in fluorescence lifetime of C120 is observed. This observation is consistent with its hydrophilic nature and its location,

where it is exposed to water. For C102, no increase of fluorescence lifetime is observed on its binding in the hydrophobic domain of BSA or HSA as the lifetime in aqueous solution is quite long. The decay profiles for the remaining systems are double-exponential (Table 6.2 and Table 6.3) in presence of BSA/HSA. Typical decay profiles of a given system in the absence and presence of BSA are shown in Fig. 6.5. The biexponential nature of the decay profiles of the systems in presence of BSA/HSA can be interpreted as follows. The short component, whose lifetime is similar/comparable to the lifetime of the probe in aqueous solution, is due to the free (unbound) probe and the long component to the protein-bound probe. The change in amplitude of the two components with gradual addition of BSA/HSA is in accordance with the increased population of bound molecules. For some of the systems, in addition to the change in amplitude of the two components, slight change in the lifetime of the short component is also observed. This is perhaps a reflection of the change of the microenvironment (e.g. viscosity) around the free molecules with increasing concentration of BSA/HSA. It can be seen that the lifetimes of protein-bound C152, C1, MNBD, 6NBD and 7NBD are significantly larger than those for the remaining systems. This is a reflection of the restriction of the internal motion in these systems on binding. For the other systems, C153, HNBD and 4NBD, the increase in fluorescence lifetime on binding to BSA/HSA is presumably due to an increase of the radiative transition probability.

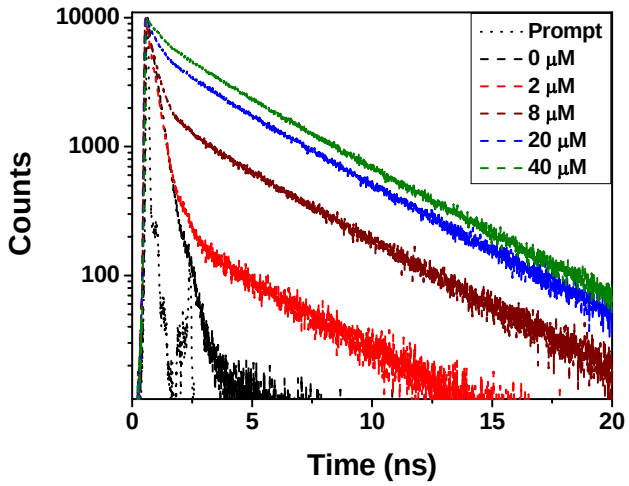

Fig. 6.5. Time-resolved fluorescence profile of C1 monitored at the emission maximum at different concentrations of BSA.

Time-resolved fluorescence anisotropy profiles of the systems are found to be quite interesting in the presence of protein. In the absence of BSA and/or HSA, single-exponential anisotropy decay with a rotational correlation time of ~ 110 – 120 ps is observed for most of the systems. This not only suggests that the probe molecules experience a homogeneous environment, but this data is also consistent with the fact that the sizes of the molecular systems used in this work are comparable. In the presence of BSA/HSA, the anisotropy decay is expected to be bi-exponential because of distinctly different rotational times of the free and protein-bound molecules. This is indeed the case of the rigid system, C102 (Fig. 6.6). Even for flexible system such as C1, a similar time-resolved anisotropy profile is observed in other organized assemblies such as in micelles and Room Temperature Ionic Liquids (RTILs) shown in Fig. 6.7. In all these cases, the short anisotropy decay represents the rotational time of unbound probe molecule, whereas the long component represents the rotational time of protein-bound probe. Interestingly, for most of the systems, in addition to the decaying short and long anisotropy

components, a growth component at intermediate time is also observed (Fig. 6.8) in presence of BSA/HSA giving 'dip-rise-dip' kind of profiles.

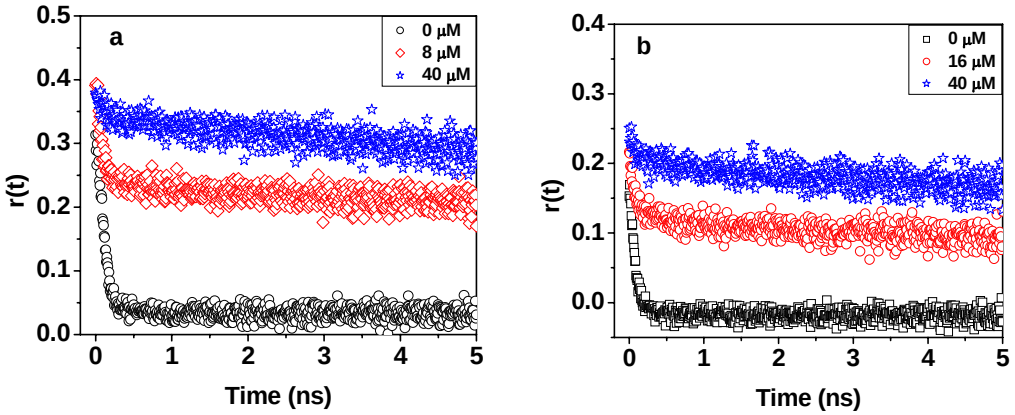

Fig. 6.6. Time-resolved anisotropy profile of C102 for different concentrations of BSA (a) and HSA (b) showing bi-exponential decay.

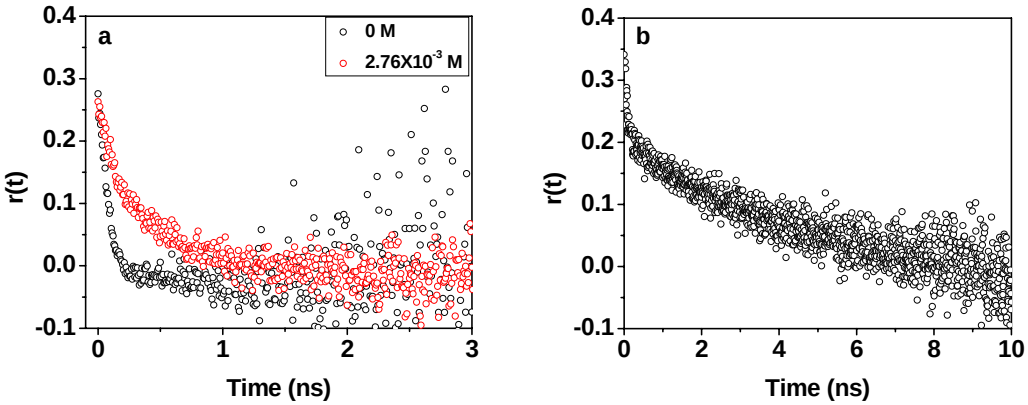

Fig. 6.7. Time-resolved fluorescence anisotropy profiles of C1 (flexible probe) in CTAB (a) and in bmim[PF_6] (b).

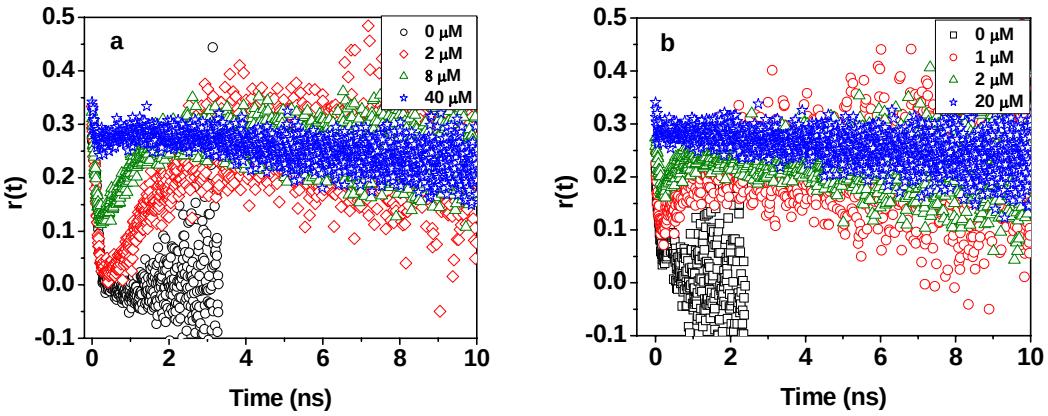

Fig. 6.8. Time-resolved anisotropy profile of C1 for various concentrations of BSA (a) and 6NBD for different concentrations of HSA (b) depicting the dip-rise-dip nature of the profile.

In order to explain the results we should consider the time-resolved fluorescence anisotropy of a heterogeneous system r(t), which is a linear combination of anisotropy decays of all species. For n number of distinct environments, the equation stands as:[20]

$$r(t) = r(0)\left[\sum_{i=1}^{n} g_i(t) \times \left\{\beta_i \exp(-t/\theta_i) + (1-\beta_i) \times \exp(-t/\theta_p)\right\}\right] \quad (1)$$

$$\text{where, } g_i(t) = \frac{\alpha_i I_i(t)}{I(t)} \text{ , } \sum_i \alpha_i = 1 \quad (2)$$

$$\text{and } I(t) = \sum_{i=1}^{n} \alpha_i I_i(t)$$

θ_i is the rotational correlation time of the rotational motion of species i, β_i is the pre-exponential term and θ_p is the rotational correlation time of overall tumbling of the protein to which the dye is bound. β_i is a measure of the extent to which the emission is depolarized by each rotational component, more precisely it gives the residual anisotropy, as $r_0(1-\beta_i) = r_{i\infty}$, the residual anisotropy of the i th component.

This kind of not-so-common time-resolved anisotropy behavior observed in the present case can be explained with the help of a two-component anisotropy equation

(equation 3), suggested by Ludescher et. al[20] which is a simplified version of equation (1) and is applicable to one of the simplest of various possible scenarios[6] assuming the presence of two distinct species, each characterized by its own lifetime and anisotropy decay.

$$r(t) = r(0)[g_1(t)\exp(-t/\theta_1) + g_2(t)\exp(-t/\theta_2)] \quad (3)$$

The above equation is obtained under consideration that the rotational correlation time of overall tumbling of the protein is much larger than the rotational correlation time of the species, i.e, $\theta_p \gg \theta_i$, and also putting $\beta_i = 1$ in equation (1). According to equation (3), the nature of the plot of r(t) vs t is governed by initial anisotropy, r(0), rotational times of the free and bound probes, θ_1 and θ_2 respectively, fluorescence lifetimes of the free and bound probes, τ_1 and τ_2 respectively and the associated amplitudes, a_1 and a_2. It can be shown that if the free and BSA/HSA-bound probes are characterized by widely different rotational correlation times, one obtains anisotropy profiles of the kind shown in Fig. 6.8 when the lifetime and/or amplitudes associated with them are varied (with change of BSA/HSA concentration). We simulated the anisotropy curves (Fig. 6.9) using some of the lifetime data from our experiments to illustrate the point. The effect of widely different rotational times and lifetime ratio (τ_2/τ_1) on the anisotropy profiles are depicted in Fig. 6.10 and Fig. 6.11 respectively.

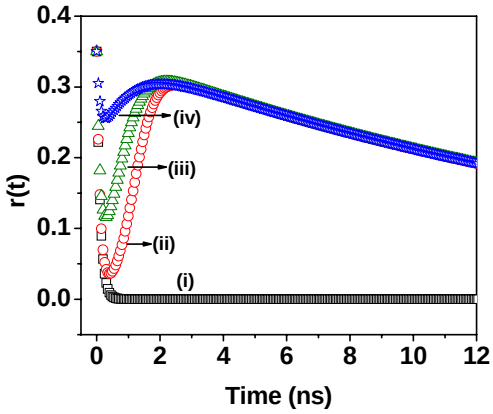

Fig. 6.9. The curves constructed using equation (3) with an initial anisotropy (r_0) of 0.35 and other parameters as follows. Used for (i) θ = 0.11 ns, τ = 0.4 ns; (ii) θ_1 = 0.11 ns, θ_2 = 20 ns, τ_1 = 0.3 ns, a_1 = 0.975, τ_2 = 3.6 ns, a_2 = 0.025; (iii) θ_1 = 0.11 ns, θ_2 = 20 ns, τ_1 = 0.36 ns, a_1 = 0.84, τ_2 = 4 ns, a_2 = 0.16, and (iv) θ_1 = 0.11 ns, θ_2 = 20 ns, τ_1 = 0.65 ns, a_1 = 0.36, τ_2 = 4.1 ns, a_2 = 0.64).

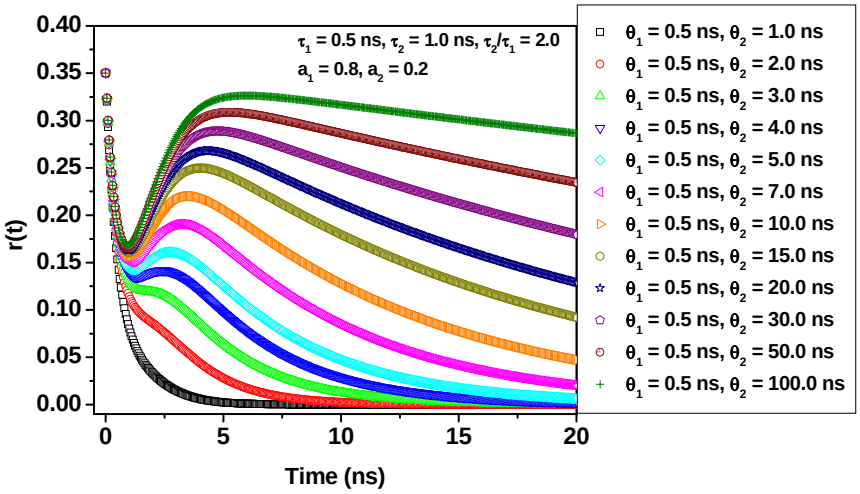

Fig. 6.10. The curves are constructed using equation (3) with an initial anisotropy (r_0) of 0.35 and other parameters as indicated in the graph. The effect of rotational times of the two components on the anisotropy profiles are shown in this figure.

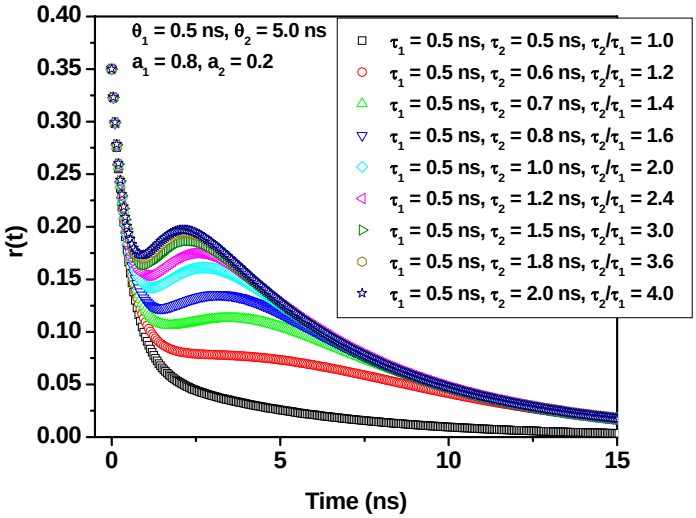

Fig. 6.11. The curves are constructed using equation (3) with an initial anisotropy (r_0) of 0.35 and other parameters as indicated in the graph. The effect of fluorescence lifetimes, precisely the variation of τ_2/τ_1 on the anisotropy curves are illustrated in this figure.

However, even though the interpretation of the time-resolved anisotropy data in terms of two fluorescing components was found physically meaningful, the quality of the fits to the time-resolved anisotropy data was not the best in some cases. We found that the fluorescence decay profiles of the systems with BSA/HSA can satisfactorily be analyzed in terms of two lifetime components except in cases where fluorescence lifetime is short, such as 6NBD, 7NBD for instance. For these systems, we tried a tri-exponential fit to analyze the data obtained with HSA. This necessitated analysis of the time-resolved anisotropy data for 6NBD, 7NBD and similar systems C1 and C152 (similar in the sense that the internal motion of the systems make the fluorescence lifetime quite short) in terms of more than two anisotropy components even though we realized that it might not be possible to attach physical significance to all the components. It is however a common practice to attribute the short lifetime to the free probes and the two long components to the bound probes in different regions.[6f] Considering the distribution of the probe

molecule in three distinct environments in these cases, one obtains (using n = 3 in equation 1) fits that are not particularly great. For higher concentrations of HSA, the quality of the fits further detoriates. Moreover, the rotational time constants obtained from this analysis neither show any particular trend nor are they found physically meaningful. As the analysis involving three different components did not improve the situation, we returned to two-component system, but incorporating this time the residual anisotropy factors into equation (3).

$$r(t) = r(0)[g_1(t)\{\beta_1 \exp(-t/\theta_1) + (1-\beta_1)\}] + g_2(t)\{\beta_2 \exp(-t/\theta_2) + (1-\beta_2)\} \quad (4)$$

Unfortunately, the fits to the anisotropy data using equation (4) were no better. Moreover, it yielded unrealistic values of rotational time constants. Finally, we analyzed the anisotropy profiles using equation (1) but placing $\beta_1 = 1$. This implies that the free probe component does not contribute to the residual anisotropy, as proposed by Das and Mazumdar.[6f] This leads to the following equation.

$$r(t) = r(0)[g_1(t)\exp(-t/\theta_1) + g_2(t)\{\beta_2 \exp(-t/\theta_2) + (1-\beta_2)\} + g_3(t)\{\beta_3 \exp(-t/\theta_3) + (1-\beta_3)\}] \quad (5)$$

The results of this analysis were discarded as negative rotational time constants were obtained.

As, not much improvement of the quality of the fits to the anisotropy data could be achieved with the three-component or two-component equations, discussed in equations (4) and (5), we found it most appropriate to understand the anisotropy data in presence of BSA/HSA using the simple two-component system (equation 3).

Let us now attempt to understand why some systems like C1 shows ‘dip-rise-dip’ anisotropy profile, while rigid probe like C102 does not show a similar behavior. It may be noted that irrespective of whether a system is rigid or flexible, the two rotational times, θ_1 (fast component) and θ_2 (slow component) are expected to be similar for all the systems because of their similar size and similar BSA/HSA-binding property (except C120). The quantities that are different for various systems are the two lifetime

components and amplitudes associated with them. The combined effect of the two is represented by g_1 and g_2. While earlier studies[6f] have rightly stressed on the importance of the time-dependent weighing factor, $g_i(t)$ in giving rise to the 'dip and rise' nature of the anisotropy profile, we find that a 'dip-rise-dip' profile of the kind reported here is best obtained when the two lifetime values are very different. Clearly, the 'dip-rise-dip' anisotropy profile condition is best realized for systems where internal motion is responsible for rapid nonradiative deactivation of the fluorescent state. This is because, these systems are characterized by short fluorescence lifetime and in protein-bound condition when the internal motion is severly restricted, there occurs a large enhancement of lifetime. Hence, systems such as C1, C152, 6NBD, 7NBD are more likely to show this kind of anisotropy profiles. Therefore, it may be possible to obtain information on prevention/disruption of internal motion in flexible molecular system of the kind studied here from the anisotropy profiles. However, since system like HNBD for which a large change of fluorescence lifetime occurs on binding to BSA/HSA for other reason, it is evident that the internal motion in the system cannot be considered as the sole criterion for generating 'dip-rise-dip' anisotropy profiles and hence, one needs to be careful before interpreting this kind of anisotropy profiles.

6.4. Modeling of binding site of BSA

In order to probe the local environment of the molecules in the protein-bound condition, molecular docking studies were carried out in BSA. The amino acid sequence corresponding to BSA was obtained from the website http://www.ncbi.nlm.nih.gov/(NCBI_ID: CAA76847). PDB BLAST (website http://www.ncbi.nlm.nih.-gov/BLAST/) with this sequence as query against the protein structure databank identified several structures of HSA. The 3-D structure of HSA (PDB ID: 1AO6) was used as template structure for homology modeling, using MODELER[21] module available in Insight II, Accelrys. The structure was validated using

PROCHECK[22] that measures the stereochemical quality of the protein structure, and Profiles-3D[23] that measures the compatibility of protein sequence with its model structure.

The structures of the molecular systems were refined using ChemSketch [http://www.acdlabs.com/]. Later these compounds were docked using AutoDock (3.05) into the 3-D structure of BSA. AutoDock[24] uses Lamarckian genetic algorithm to search for the optimum binding site of small molecules to the protein. In order to recognize the binding sites in BSA, blind docking was carried out, the grid size set to 100, 100 and 100 along X-, Y- and Z- axis with 0.603 Å grid spacing. The centre of grid was set to 31.130, 31.715 and 26.672 Å. The AutoDocking parameters used were, GA Population size: 150; maximum number of energy evaluations: 250000. During docking, a maximum number of 10 conformers was considered for each molecule and the RMS (root mean square) cluster tolerance was set to 0.5 Å. The conformation with the lowest binding free energy was used for further analysis. The sequences of BSA and HSA share 88% homology[25] shown in Fig. 6.12. The N-terminal 24 amino acid residues in the bovine sequence that did not have an equivalent in the human template crystal structure (PDB code: 1AO6) were not included in the model.

Fig. 6.12. The sequence alignment of 1A06 (HSA) and BSA is shown depicting 88% homology.

The crystal structure of HSA comprises three domains. The three domains (I, II, III) have similar 3-D structures and highly asymmetric in assembly with 17 disulfide bridges.[26,27] Each domain can be further divided into subdomains ‘a’ and ‘b’, which are composed of six and four α-helices, respectively. A long extended loop traverses the two subdomains to link them together. The pocket of subdomain IIa corresponds to the drug site I, which is known to be warfarin binding site and several other drugs.[28-30] The subdomain IIIa is known to be drug site II, which is similar to drug site I. Thyroxin, octanoate and some other drugs binds to this site.[31,32] For long chain fatty acids, three binding sites with entirely different structural environments have been reported.[33] Our model of the BSA shows that the three domains are identical to those in HSA and the binding sites for the various compounds analyzed in this work have an equivalent binding

site in HSA. The RMS deviation corresponding to equivalent C-alpha atoms in BSA model and HSA structure (PDB code: 1AO6) is 0.303 Å shown in Fig. 6.13. The analysis of protein structure using Profiles-3D reported a 254/264 score and the PROCHECK analysis reported that 99.6% amino acid residues are within the allowed regions of Ramachandran plot depicted in Fig. 6.14.

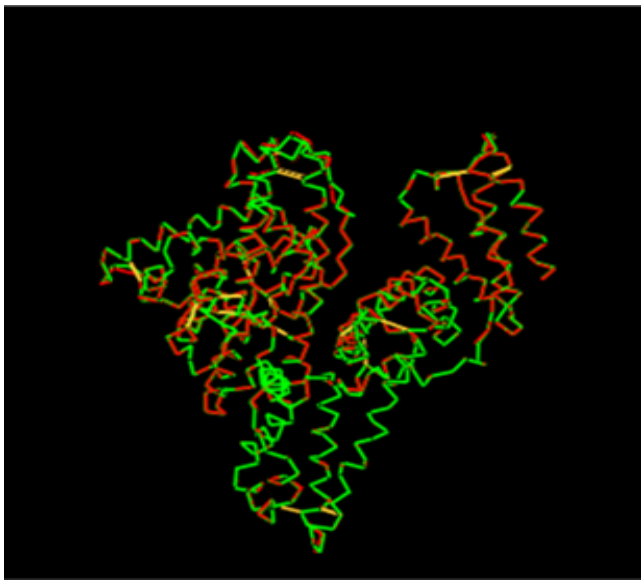

Fig. 6.13. The structural overlay depicting RMS deviation corresponding to equivalent C-alpha atoms in BSA (red) model and HSA (green) structure (PDB code: 1AO6) is 0.303 Å.

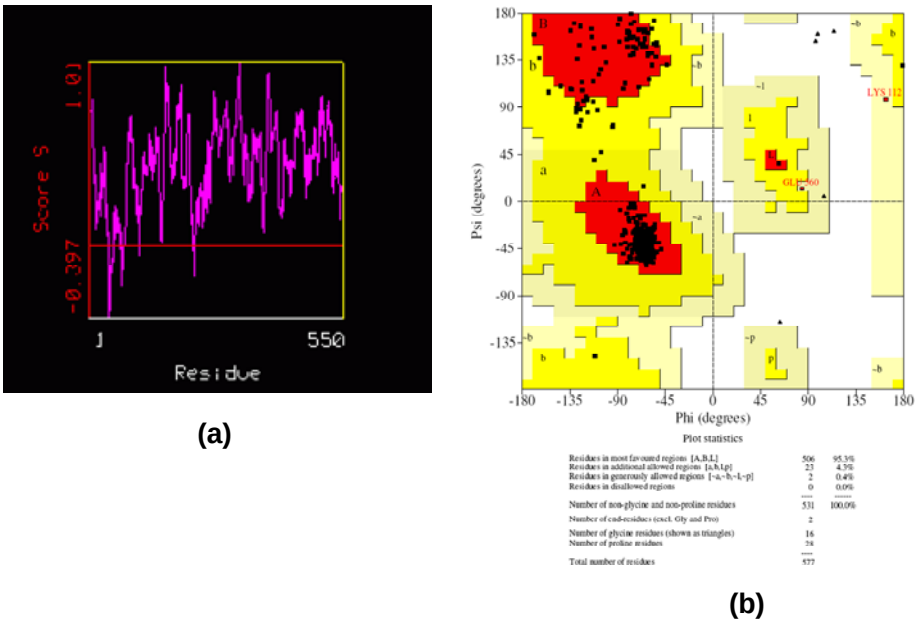

Fig. 6.14. Structure validation of BSA model (a) profiles-3D and (b) Ramachandran plot.

We have docked ten systems into the 3-D structure of BSA using AutoDock Tools. These molecules occupy three different binding sites in BSA. The docking energies of the molecules (in kcal/mol) obtained from AutoDock are -8.02 (C102), -8.25 (C153), -7.26 (C120), -7.04 (C152), -6.83 (C1), -7.70 (HNBD), -7.99 (MNBD), -8.24 (4NBD), -9.13 (6NBD), and -8.51 (7NBD). The molecules in the 1st binding site are: C1, C102, C152, C153, 7NBD. The molecules in the 2nd binding site are: MNBD, 4NBD, 6NBD. The molecules in the 3rd binding site are: HNBD, C120. The location of these sites in the 3-D structure of BSA is shown in Fig. 6.15. It is encouraging to note that the binding sites in bovine are similar to some of the known binding sites in HSA, although no bias was introduced in defining the binding sites in bovine using the AutoDock program.

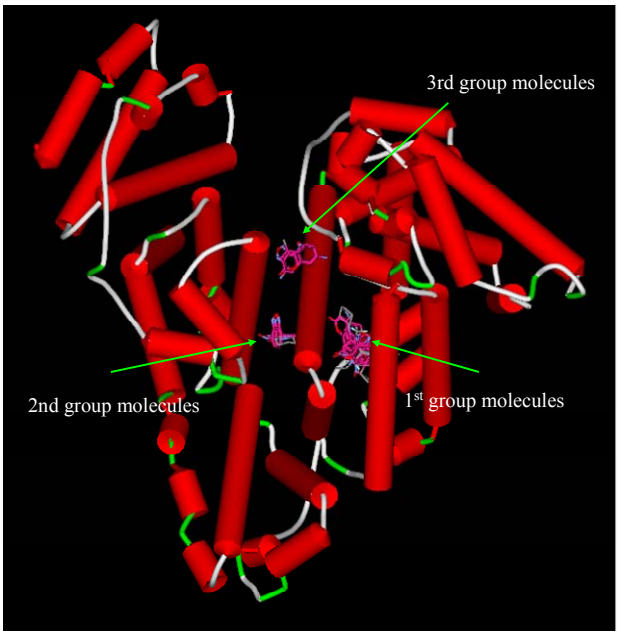

Fig. 6.15. Pictorial representation of BSA model structure indicating the binding pockets and bound molecules.

The 1st group molecules are bound at the subdomain IIa which is known to be drug site I[34-36] (Fig. 6.16). The amino acid residues lining this binding site comprise: Trp213, His237, Leu241, Tyr149, Arg198, Gln195, Arg194, Ala290, Glu291 and Arg217. These molecules bind to the site essentially via hydrophobic and van der Waals forces. In some cases, hydrogen bonding interactions have been observed. C1 makes one hydrogen bond with the Arg194 side chain through its carbonyl group. The CH_3 group of C1 makes CH…π interactions with the aromatic side chain of Tyr149. The side chain $C^{\beta}H$ of Ala290 makes CH….π interactions with the coumarin ring. This coumarin ring also makes Pi…Pi interactions with the guanidinium group of Arg198. Likewise, C102 and C153 make hydrogen bonding interactions with Arg198 side chain through their carbonyl groups. The CH_3 group of C102 makes makes CH…π interactions with the aromatic side

chain of Tyr149. The side chain $C^{\beta}H$ of Ala290 makes CH….π interactions with the coumarin ring. The side chain $C^{\beta}H$ of Ala290 makes CH….π interactions with the coumarin ring in C153. C152 makes four hydrogen bonding interactions with Tyr149 and Arg256 side chains through coumarin ring oxygen and carbonyl oxygen. The side chain $C^{\beta}H$ of Ala290 makes CH….π interactions with the coumarin ring of C152. The side chain $C^{\beta}H$ of Ala290 makes CH….π interactions with the coumarin ring. The 7-membered cyclic ring in 7NBD makes CH…π interactions with the guanidinuim group of Arg198. These molecules are present within (3.6-3.9) Å distance from Trp213 and the side chains of neighboring hydrophobic residues are located close by. Therefore, it is understandable why these molecular systems display significant blue shift of the fluorescence maxima and how internal rotation in some of the flexible systems is retarded giving rise to high FE.

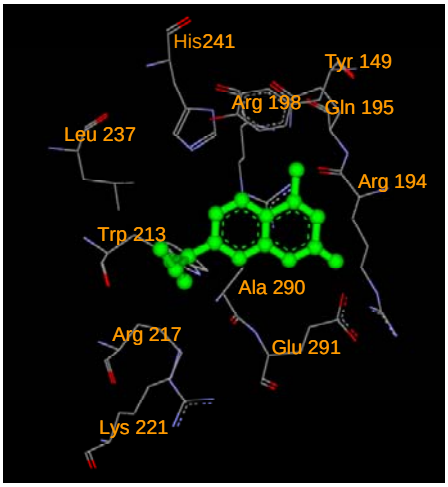

Fig. 6.16. Binding pocket for 1st group molecules (showing C1) within 4 Å distance.

The 2nd group molecules are bound at the interface between subdomains IIa and IIIa (Fig. 6.17). This is located at the bottom of the entrance of the binding pocket of IIa.[34]

This binding site unlike the binding site discussed above is perhaps selective in the type of compounds that bind. The amino acid residues lining this binding site comprises: Arg194, Leu197, Trp213, Arg435, Cys447, Asp450 and Tyr451. The nitro group present in 4NBD, 6NBD and MNBD make two hydrogen bonding interactions with the Arg435 side chain. In the case of MNBD $C^{\alpha}H$ of Tyr451 makes CH…π interactions with the aromatic ring of MNBD. In this case there is enough room around the methyl groups that allow them to be flexible and hence binding is comparatively weak. The 4-membered cyclic group in 4NBD experiences hydrophobic interactions with the side chains of Leu197 and Leu454. The $C^{\alpha}H$ of Tyr451 makes CH…π interactions with the aromatic ring of 4NBD. The six membered ring in 6NBD is close to Trp213 (3.6 Å) and to Leu197 (2.8 Å). $C^{\alpha}H$ of Tyr451 makes CH….π interactions with the aromatic ring of 6NBD. It is possible that these hydrophobic interactions hold 6NBD in a rigid manner within the binding site possibly explaining the greater blue shift and FE when bound to protein.

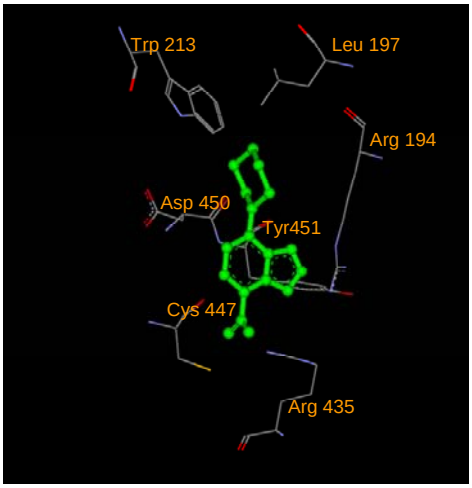

Fig. 6.17. Binding pocket for 2nd group molecules (showing 6NBD) within 4 Å distance.

The 3rd group molecules are bound at the interface between two sub domains IIa and IIIa, which is located just above the entrance of the binding pocket of IIa (Fig. 6.18). The amino acid residues lining this binding site comprises: Arg196, Arg458, Asp108, His145, Asn457, Val461, Leu462, Ala193, Ser192, Leu189 and Arg144. This site is relatively more exposed to the solvent. The molecules C120 and HNBD are bound to this site. HNBD forms two hydrogen bonding interactions with Arg458 and His145 side chains. The guanidinium group of Arg458 makes π…π interactions with the aromatic ring of HNBD and C120. That these compounds prefer a binding site that is highly polar and exposed to the solvent environment explains why HNBD and C120 show less blue shift of the fluorescence maximum compared to the 1st and 2nd group of molecules.

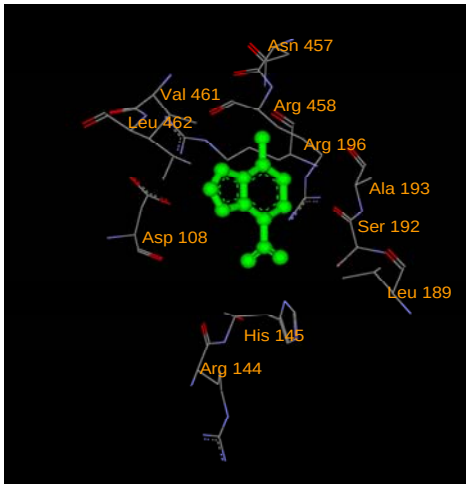

Fig.6.18. Binding pocket for 3rd group molecules (showing HNBD) within 4 Å distance.

6.5. Conclusion

In summary, the results of fluorescence measurements show that coumarins and NBD derivatives bind to both BSA and HSA. It is demonstrated that two well separated fluorescence lifetimes and widely different rotational times of the molecules in presence

of BSA/HSA give rise to the unusual ‘dip-rise-dip’ kind of time-resolved anisotropy profiles. The disruption of internal motion in the flexible molecules on binding to BSA/HSA gives a larger separation of fluorescence lifetimes and hence, a more pronounced ‘dip-rise-dip’ anisotropy profile. It is evident that the environment of BSA or HSA can more effectively restrict the internal motions in the EDA systems compared to other constrained environments such as, micelles and cyclodextrins. Molecular docking studies enable us to identify three different binding sites in BSA for these molecules. Hydrogen bond interactions, CH…π interactions, π…π interactions and hydrophobic interactions are the different interactions shown to be responsible for the binding of the systems to BSA.

References

1. (a) Michel-Bewryerle, M. E. *In The Reaction Centre of Photosynthetic Bacteria*, Springer Verlag: Berlin, 1995. (b) Wasielewski, M. R. *Chem. Rev*. **1992**, *92*, 435. (c) Gust, D.; Moore, T. A.; Moore, A. L. *Acc. Chem. Res*. **1993**, *26*, 198. (d) Bard, A.; Fox, M. A. *Acc. Chem. Res*. **1995**, *28*, 141. (e) Meyer, T. J. *Acc. Chem. Res*. **1989**, *22*, 163.
2. (a) Fabrizzi, L.; Poggi, A. *Chem. Soc. Rev*. **1995**, *24*, 197. (b) Shelton, D. B.; Rice, J. E. *Chem. Rev*. **1994**, *94*, 3. (c) Carter, F. L.; Siatoski, R. E.; Woltjen, H. In *Molecular Electronic Devices*, North Holland: Amsterdam, 1988. (d) Barbara, P.F.; Jarzeba, W. *Acc. Chem. Res*. **1988**, *21*, 195.
3. (a) *Photochemistry in Organised and Constrained Media*; Ramamurthy, V., Eds.; VCH, New York, 1991. (b) Bhattacharyya, K.; Chowdhury, M. *Chem. Rev*. **1993**, *93*, 507 and references therein.
4. (a) *Topics in Fluorescence Spectroscopy*; Lakowicz, J. R., Eds.; Plenum Press: New York, 1994; Volume 4. (b) Kalyanasundram, K. In *Photochemistry in Microheterogeneous Systems*; Academic Press Inc.: London, 1987.
5. Lakowicz, J. R. In *Principles of Fluorescence Spectroscopy*; 2nd Ed.; Kluwer Academic/Plenum Press: New York, 1999. (b) *Topics in Fluorescence Spectroscopy*; Lakowicz, J. R., Eds.; Plenum Press: New York, 1994; Volume 2.
6. (a) Jones, B. E.; Beechem, J. M.; Matthews, C. R. *Biochemistry* **1995**, *34*, 1867. (b) Bilsel, O.; Yang, L.; Zitzewitz, J. A.; Beechem, J. M.; Matthews, C. R. *Biochemistry* **1999**, *38*, 4177. (c) Srivastava, A.; Krishnamoorthy, G. *Archives of Biochemistry and Biophysics* **1997**, *340*, 159. (d) Hudson, B.; Harris, D. L.; Ludescher, R. D.; Ruggiero, A.; Cooney-Freed, A.; Cavalier, S. A. In *Fluorescence in the Biological Sciences*; Taylor, D. L., Waggoner, A. S., Lanni, F., Murphy, R. F., Birge, R., Eds.; Alan R. Liss: New York, 1986; p. 159. (e) Wolber, P. K.; Hudson, B. S. *Biophys. J*. **1982**, *37*, 253. (f) Das, T. K.; Mazumdar, S. *Biophysical Chemistry* **2000**, *86*, 15. (g) Sinha, S. S.; Mitra, R. K.; Pal, S. K. *J. Phys. Chem. B* **2008**, *112*, 4884.
7. (a) Paul, A.; Samanta, A. *J. Phys. Chem. B* **2007**, *111*, 4724. (b) Mandal, P. K.; Samanta, A. *J. Phys. Chem. B* **2005**, *109*, 15172. (c) Karmakar, R.; Samanta, A. *J. Phys. Chem. A* **2003**, *107*, 7340. (d) Biswas, R.; Rohman, N.; Pradhan, T.; Buchner, R. *J. Phys. Chem. B* **2008**, *112*, 9379. (e) Rodriguez, J.; Marti, J.; Guardia, E.; Laria, D. *J. Phys. Chem. B* **2008**, *112*, 8990. (f) Seth, D.; Sarkar, S.; Sarkar, N. *Langmuir* **2008**, *24*, 7085. (g) Jin, H.; Li, X.; Maroncelli, M. *J. Phys. Chem. B* **2007**, *111*, 13473. (h) Sahu, K.; Mondal, S. K.; Ghosh, S.; Roy, D.; Sen, P.; Bhattacharyya, K. *J. Phys. Chem. B* **2006**, *110*, 1056.
8. (a) Kunjappu, J. T. *J. Photochem. Photobiol. A: Chem*. **1993**, *71*, 269. (b) Chakraborty, A.; Seth, D.; Setua, P.; Sarkar, N. *J. Chem. Phys*. **2008**, *128*, 204510. (c) Mandal, U.; Ghosh, S. Dey, S.; Adhikari, A.; Bhattacharyya, K. *J. Chem. Phys*. **2008**, *128*, 164505. (d) Ghosh, S.; Mondal, S. K.; Sahu, K.; Bhattacharyya, K. *J. Chem. Phys*. **2007**, *126*, 204708.
9. (a) Chakraborty, A.; Seth, D.; Setua, P.; Sarkar, N. *J. Phys. Chem. B* **2006**, *110*, 16607. (b) Shobini, J.; Mishra, A. K.; Sandhya, K.; Chandra, N. *Spectrochimica Acta Part A* **2001**, *57*, 1133.
10. (a) Jones II, G.; Jackson, W. R.; Kanoktanaporn, S.; Halpern, A. M. *Opt. Commun*. **1980**, *33*, 315. (b) Jones II, G.; Jackson, W. R.; Choi, C.-Y. *J. Phys. Chem*. **1985**, *89*, 294. (c)

Jones II, G.; Jackson, W. R.; Halpern, A. M. *Chem. Phys. Lett*. **1980**, *72*, 391. (d) Hicks, J. M.; Vandersall, M. T.; Babarogic, Z.; Eisenthal, K. B. *Chem. Phys. Lett*. **1985**, *116*, 18. (e) Hicks, J. M.; Vandersall, M. T.; Sitzmann, E. V.; Eisenthal, K. B. *Chem. Phys. Lett*. **1987**, *135*, 413.
11. Nag, A.; Bhattacharyya, K. *Chem. Phys. Lett*. **1990**, *169*, 12.
12. (a) Longmuir, K. J.; Martin, O. C.; Pagano, R. E. *Chem. Phys. Lipids* **1985**, *36*, 197. (b) Schmidt, N.; Gercken, G.; *Chem. Phys. Lipids* **1985**, *38*, 309. (c) Silvius, J. R.; Leventis, R.; Brown, P. M.; Zuckermann, M. *Biochemistry* **1987**, *26*, 4279. (d) Chattopadhyay, A. *Chem. Phys. Lipids* **1990**, *53*, 1. (e) Chattopadhyay, A.; London, E. *Biochim. Biophys. Acta* **1988**, *24*, 938.
13. (a) Ghosh, P. B.; Whitehouse, M. W. *Biochem. J*. **1968**, *108*, 155. (b) Fager, R. S.; Kutina, C. B.; Abrahamson, E. W. *Anal. Biochem*. **1973**, *53*, 290. (c) Ferguson, S. J.; Lloyd, W. J.; Radda, G. K. *Biochem. J*. **1976**, *159*, 347.
14. (a) Ramachandram, B.; Saha, S.; Samanta, A. *Chem. Phys. Lett*. **1998**, *290*, 9. (b) Ramachandram, B.; Samanta, A. *J. Phys. Chem. A* **1998**, *102*, 10579.
15. Fery-Forgues, S.; Fayet, J. P.; Lopez, A. *J. Photochem. Photobiol. A: Chem*. **1993**, *70*, 229.
16. Saha, S.; Samanta, A. *J. Phys. Chem. A* **1998**, *102*, 7903.
17. López Arbeloa, T.; López Arbeloa, F.; Tapia José, M.; López Arbeloa, I. *J. Phys. Chem*. **1993**, *97*, 4704.
18. Novo, M.; Soufi-Al, W. In *Fluorescence Study of the Supramolecular Interactions between Coumarins and Serum Albumins*; Proceedings of the International Electronic Conference on Synthetic Organic Chemistry; MDPI: Basel, Switzerland, 2007.
19. Mallick, A.; Haldar, B.; Chattopadhyay, N. *J. Phys. Chem. B* **2005**, *109*, 14683.
20. Ludescher, R. D.; Peting, L.; Hudson, S.; Hudson, B. *Biophysical Chemistry* **1987**, *28*, 59 and references therein.
21. Sali, A.; Blundell, TL. *J. Mol. Biol*. **1993**, *234*, 779.
22. Laskowski, R. A.; MacArthur, M. W.; Moss, D. S.; Thornton, J. M. *J. Appl. Cryst*. **1993**, *26*, 283.
23. Lüthy, R.; Bowie, J. U.; Eisenberg, D. *Nature* **1992**, *356*, 83.
24. Morris, G. M.; Goodsell, D. S.; Halliday, R. S.; Huey, R.; Hart, W. E.; Belew, R. K.; Olson, A. J. *J. Comput. Chem*. **1998**, *19*, 1639.
25. Peters, T. *Adv. Protein Chem*. **1985**, *37*, 161.
26. He, X. M.; Carter, D. C. *Nature* **1992**, *358*, 209.
27. Sugio, S.; Kashima, A.; Mochizuki, S.; Noda, M.; Kobayashi, K. *Protein Eng*. **1999**, *12*, 439.
28. Petitpas, I.; Bhattacharya, A. A.; Twine, S.; East, M.; Curry, S. *J. Biol. Chem*. **2001**, *276*, 22804.
29. Dockal, M.; Chang, M.; Carter D. C.; Rüker, F. *Protein Sci*. **2000**, *9*, 1455.
30. Maes, V.; Engelborghs, Y.; Hoebeke, J.; Maras, Y.; Vercruysse, A. *Mol. Pharmacol*. **1982**, *21*, 100.
31. Tian, J.; Liu, J.; He, W.; Hu, Z.; Yao, X.; Chen, X. *Biomacromolecules* **2004**, *5*, 1956.
32. Zhang, Q.; Huang, Y.; Zhao, R.; Liu, G.; Chen, Y. *Biosens. Bioelectron*. **2008**, *24*, 48.
33. Curry, S.; Brick, P.; Franks, N. P. *Biochim. Biophys. Acta* **1999**, *1441*, 131.

34. Ghuman J.; Zunszain, P. A.; Petitpas, I.; Bhattacharya, A. A.; Otagiri, M.; Curry S. *J Mol Biol*. **2005**, *353*, 38.
35. Yuan, J. L.; Iv, Z.; Liu, Z. G.; Hu, Z.; Zou, G. L. *J. Photochem. Photobiol. A: Chem*. **2007**, *191*, 104.
36. Tang, K.; Qin, Y. M.; Lin, A. H.; Hu, X.; Zou, G. L. *J. Pharm. Biomed. Anal*. **2005**, *39*, 404.

Chapter 7

Concluding Remarks

This chapter summarizes the results of the investigations delineated in this thesis. The scope of further studies based on the findings of the present work has also been outlined.

7.1. Overview

The work embodied in the thesis has been undertaken with the primary objective of exploring the effect of different environments into some of the fundamental photoinduced processes. The different photoinduced processes handled in this thesis are nonradiative deactivation, photoinduced electron transfer and proton transfer. To achieve our goal we chose several fluorophores suitable for the above studies. It is known that in structurally flexible systems unusually high nonradiative rate is due to their internal motion. We have therefore selected some of the flexible systems to determine the nature of nonradiative deactivation pathway in them and also how the environment (conventional organic solvents and proteins) affect such nonradiative processes. Photoinduced electron transfer (PET) has been studied in molecular systems with *fluorophore-spacer-receptor* architecture to obtain direct evidence of the PET process in those systems. Excited state intramolecular proton transfer reaction (ESIPT) has been studied in room temperature ionic liquids (RTILs) to find out whether or to what extent this process differs from that occurring in conventional solvents, and secondly, to determine the role of other features of RTILs like the hydrogen bonded network, ionic constituents and microheterogeneity of the medium in the above mentioned photoprocess. Several instrumental techniques and methodologies, namely, NMR spectroscopy for characterization, cone and plate viscometer, UV-visible absorption, steady-state and time-resolved fluorescence and laser

flash photolysis techniques and molecular docking have been employed to carry out this work. The results obtained from the investigations are outlined below.

In order to find out the nature of possible nonradiative pathway in aminophthalimide (AP) derivatives, we have monitored the triplet state of three structurally similar AP derivatives comprising cyclic amino functionalities of different ring sizes in less polar (1,4-dioxane), polar aprotic (acetonitrile) and protic (methanol) media. Using flash photolysis technique, it is found that the aminophthalimides are characterized by low triplet yields and moderate values of molar extinction coefficients of the triplet-triplet absorption. Even in protic media, where the systems are very weakly fluorescent, the triplet yield is found to be quite low. The results of this work suggest that an enhanced internal conversion process is responsible for the low fluorescence efficiency of the systems in polar protic and aprotic media.

With a view to obtain some direct evidence of the PET reaction in molecules with *fluorophore-spacer-receptor* architecture, we have carried out transient absorption measurements on some 1,8-naphthalimide derivatives. In the present study, the products of the electron transfer reaction i.e radical ions have been detected which provide the required evidence for PET in these systems. The participation of the triplet state in the PET process is observed. The studies also reveal that polarity of the solvent dictates whether singlet or triplet state will be involved in the PET process. The triplet quantum yield, radical anion yield, triplet state lifetime for these set of derivatives have been determined in solvents of different polarity.

ESIPT reaction of 7HQ mediated by methanol molecules has been studied in two RTILs using steady state and time-resolved fluorescence measurements. No ESIPT is observable in neat RTILs. A rise time associated with the tautomer fluorescence, observed in presence of methanol suggests that proton transfer in 7-HQ is an excited state phenomenon where the methanol molecules form a bridged hydrogen-bonded

architecture with 7-HQ in RTILs for the proton relay in the system. The rise time of the tautomer fluorescence has been found to decrease with increasing methanol concentration and is attributed to the change of viscosity of the medium upon methanol addition. The lack of definite correlation between the bulk viscosity and rise time has been attributed to the microheterogeneity of the media.

The study of spectral and temporal behavior of the intramolecular charge transfer (ICT) fluorescence of aminocoumarins and aminonitrobenzoxadiazoles in presence of bovine serum albumin (BSA) and human serum albumin (HSA) is carried out in order to understand how the environment of protein affects the internal motions in these molecules. The binding sites of the molecular systems in protein (BSA) have been located with the help of docking studies. Binding in the hydrophobic domains of BSA and HSA leads to blue shift of the fluorescence spectra and enhancement of fluorescence intensity and lifetime. The well-separated fluorescence lifetimes and very different rotational time constants of the free and bound probes give rise to unusual ‘dip-rise-dip’ kind of time-resolved fluorescence anisotropy profiles for some of the studied systems. This kind of dip-rise-dip nature of the fluorescence anisotropy profile has been correlated to the disruption of internal motion in the structurally flexible systems. It thus appears that it may be possible to obtain information on the prevention/disruption of nonradiative pathway on protein binding from the anisotropy profiles of the kind discussed in the chapter. It is evident from the studies that the environment of BSA or HSA can more effectively restrict the internal motions of the electron-donor-acceptor (EDA) systems compared to other constrained environments such as, micelles and cyclodextrins.

7.2. Future scope

Considering the fact that AP derivatives are highly fluorescent in aprotic solvents, but very weakly fluorescent in protic media, our finding that internal conversion rate in aprotic and protic media of these systems is responsible for the observed behavior

provides insight into a fundamental issue relating to the molecules. There are however several other EDA molecules where this issue is not yet resolved. Perhaps those systems may be subjected to investigation of this type.

When it comes to the issue of PET in *fluorophore-spacer-receptor* systems, the systems studied here to obtain convincing evidence of PET constitute only very few of this class. There exists a variety of molecular systems comprising different combinations of fluorophore, spacer and receptor components, where the mechanism of communication between the terminal moieties is not ascertained yet and such systems should be studied by laser flash photolysis technique.

Although the use of RTILs as alternative solvent media has increased in recent times, the potential of these liquids as media for photophysical studies has hardly been exploited. This is evident from the fact that the ESIPT reaction that is carried out here is the first of its kind. Obviously, there is a lot that one can do exploiting some of the unique features of these ionic liquids. Photophysical processes influenced by the charged constituents of the ionic liquids are not yet been demonstrated. Spatial heterogeneity of these substances are yet to be exploited to carry out controlled photoreactions that are not otherwise possible in conventional solvents.

Our study of the interaction of dipolar probes with proteins throws some insight into the structural behavior of the molecules under constrained environment. We find that the environment of protein affects the fluorescence parameters of flexible dipolar molecules in such a way that it is possible to observe unusual fluorescence anisotropy profiles, which can be correlated with the disruption of internal motion in the probes. It will be a good idea to introduce more number of molecules into this kind of study such that we can extract information relating to the internal motion in the fluorophore instead of the same on the structure and dynamics of the protein molecule, which stands out as the main objective of studying protein-ligand interactions otherwise.